ANALYSIS OF NUCLEOPROTEIN COMPLEXES FORMED BY E.COLI RecA PROTEIN USING AFFINITY CLEAVAGE

Thesis by

Ramesh Baliga

In Partial Fulfillment of the Requirements

for the Degree of

Doctor of Philosophy

California Institute of Technology

Pasadena, California

1996

(Submitted May 7, 1996)

To Dad

Acknowledgements

I am deeply grateful to my advisor Professor Peter B. Dervan, for his support and patience particularly during the challenging times of the final phase of my thesis work. His boundless enthusiasm and intensity have been and will continue to be a great example. Practically limitless resources, extremely motivated and dedicated coworkers and one of the single most relevant and exciting problems to work on–there is not much more that one could be fortunate enough to get from a mentor in graduate school.

I would like to thank my thesis committee, Professors John H. Richards, Barbara Imperiali and Carl S. Parker for their constructive criticism during the course of my graduate work particularly during candidacy.

In my first year I had the good fortune of sharing a lab with Tom Povsic and Scott Strobel. Tom's impressive work ethic and Scott's "cut-to-the-chase" approach to science have both been great examples to emulate. I also thank Dr. John Josey for taking the time to patiently teach me the rudiments of organic synthesis.

Dr. Karen Draths and George Best gave me some much needed advice on presentation skills–after one of my early long-winded and excruciatingly verbose research seminars! Heartfelt thanks go to Jen Wales for initiating the studies that have helped me write this thesis. Her careful record-keeping gave me a jump-start in my efforts to study what has proved to be a complex problem.

I would like to thank Matt Taylor for his friendship and support throughout graduate school. Long conversations about life and science with Matt were a welcome break when science seemed daunting. Trips to Sushi or Indian food with Matt and Will Greenberg are some of the best memories from my stay at Caltech. I would like to thank Eldon Baird for his friendship and true generosity. Eldon's unique mix of brilliant science and down-to-earth humor makes it a lot of fun to have him around. I have never seen anyone pick up the intensity and productivity of everyone around, the way he has. On a more sombre note, I would like to thank Joe Hacia for providing a great example of professionalism while facing personal loss.

I thank all the members past and present of 320/330 Church who have made the laboratory a friendly and comfortable workplace. In particular I would like to thank David Herman and David Liberles who were extremely accomodating of my need for more space in the last frenetic days of labwork.

I am deeply indebted to my family for their love and support through all these years and particularly through the final phase of graduate work.

Last and probably the *most*, I would like to thank Sensei Tsutomu Ohshima and all my seniors at the Caltech Karate Club. I would most certainly not have lasted through these last few weeks of graduate school without the tools they given me for handling stress and keeping everything in perspective.

Abstract

Homologous recombination, a process ubiquitous to most living cells, involves the exchange of strands between two molecules of double-stranded DNA at sites of sequence homology, resulting in the formation of hybrid products. One of the best studied model systems for *in vitro* studies of homologous recombination is the three-strand reaction catalyzed by the *Escherichia coli* RecA protein. In the presence of appropriate cofactors, RecA protein polymerizes on single-stranded DNA to form nucleoprotein filaments which can then bind to homologous sequences on duplex DNA. This thesis describes the use of affinity cleavage with oligonucleotides carrying an EDTA moiety appended at a single position, to study the binding of RecA• oligonucleotide filaments on duplex DNA. Chapter One provides a general overview of protein-DNA recognition, chemical approaches to molecular recognition of B-form DNA (including oligonucleotide-directed triple helix formation) and what is currently known about the role of RecA protein in homologous recombination and DNA repair. Chapter Two describes the technique of affinity cleavage and its optimization for RecA•oligonucleotide filaments. Chapter Three describes the use of affinity cleavage to observe cooperative binding of nucleoprotein filaments to adjacent sites on duplex DNA and an investigation into the basis for the observed cooperativity. In Chaper Four affinity cleavage with oligonucleotides carrying a single thymidine-EDTA residue at an internal site

is used to determine the groove location of the incoming strand, in the three-stranded complex formed by recognition of a homologous site on duplex DNA. Finally, in Chapter Five the results from various chemically modified substrates of the three-strand reaction are presented in support of a mechanism of homologous recognition that does not involve formation of a pre-exchange triple helical intermediate.

Table of Contents

List of Figures and Tables

CHAPTER ONE

CHAPTER TWO

CHAPTER THREE

CHAPTER FOUR

CHAPTER FIVE

CHAPTER ONE

Introduction

Deoxyribonucleic acid (DNA) molecules are the site at which virtually all the information required for the functioning of living cells is stored. In its simplest and most common form–the B-form, DNA exists as a right-handed antiparallel double-helix of linear polymers of nucleotide subunits, each of which is composed of a heterocyclic base, a deoxyribose sugar and a phosphate moiety. Pairs of bases on opposite strands–adenine(A) and thymine(T), or guanosine(G) and cytosine(C)–are held together by complementary hydrogen bonds in a helical array stabilized by vertical π stacking interactions between adjacent base-pairs. This helical arrangement of base pairs gives rise to two grooves which are distinctive in their dimensions and also in the manner in which functional groups on the bases are displayed (Figure 1 A,B). For example in an AT base-pair, functional groups available for recognition in the wide and shallow "major groove" are the N7 nitrogen and 2-amino group of adenine, and O4 oxygen and the 5-methyl group of thymine. On the other hand, located in the deep and narrow "minor groove" are the N3 nitrogen of adenine and the O2 oxygen of thymine. In the forty years since the structure of B-form DNA was first elucidated by Watson and Crick (1) it has become clear that the regulation of a variety of cellular processes depends critically on molecular recognition of various features of this structure–the sugar phosphate backbone, the functional groups on bases and also the local morphology of the double helix.

Figure 1: CPK model of one turn of the B-form DNA double-helix viewed from the major (**A**) or minor (**B**) groove. Also shown for the central TA and GC base pairs are two-dimensional representations of the functional groups available for hydrogen-bonding with ligands. The lobes represent lone pairs. The 5-methyl group of thymidine recognized by hydrophobic interactions is shown boxed.

A

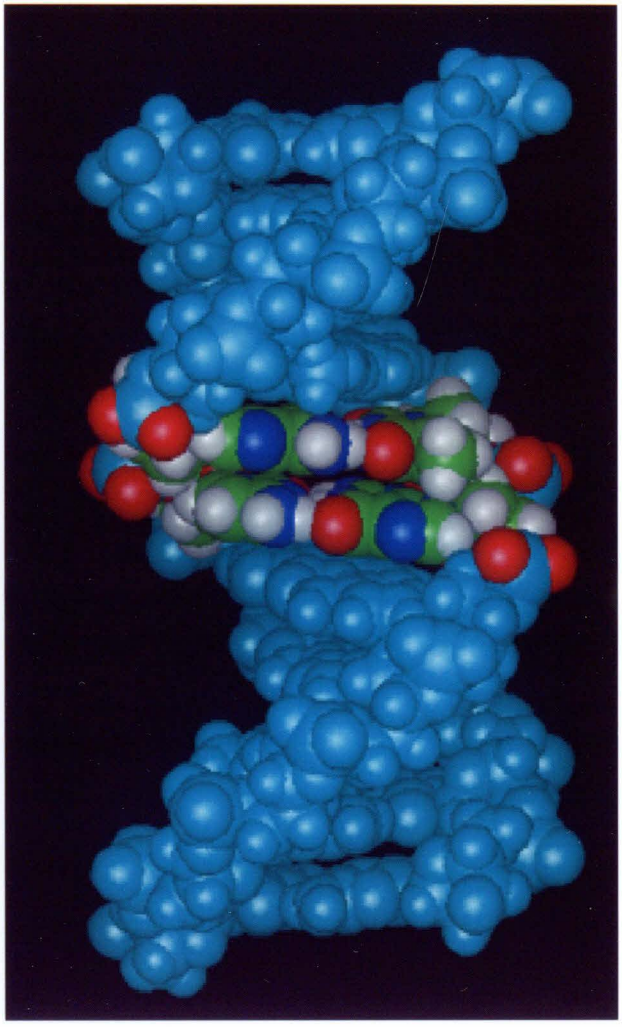

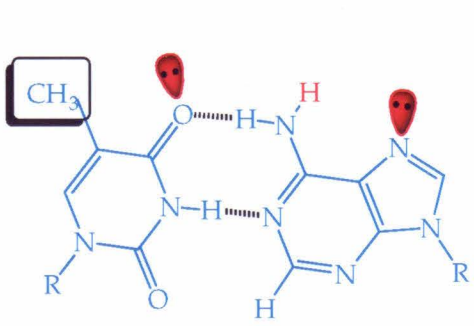

T•A

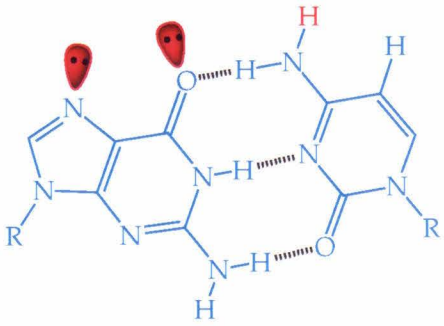

G•C

B

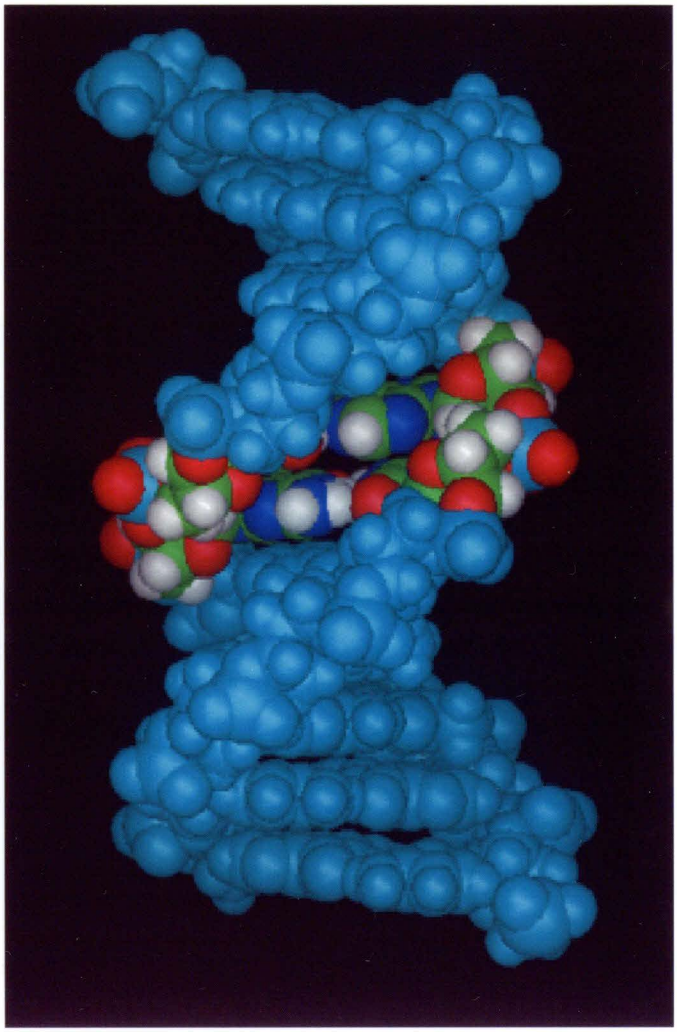

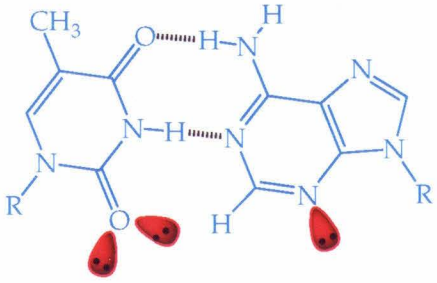

T•A

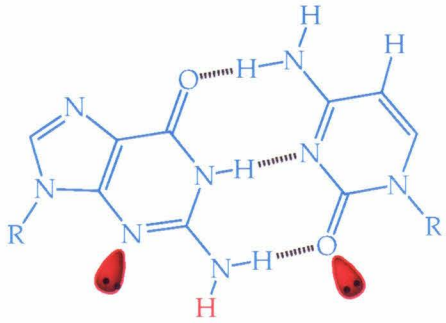

G•C

Recognition of double stranded DNA by proteins

Since excellent detailed reviews in the field of protein-DNA recognition are available (2), the discussion here will be limited to a brief overview of how B-form DNA is recognized in nature. Although the principles governing the sequence-specific binding of proteins to cognate sequences remain incompletely understood, proteins that bind duplex DNA sequence-specifically use a number of common structural motifs. Among these are helix-turn-helix (HTH), leucine zipper, zinc finger, and β-ribbon motifs.

The first class of sequence-specific DNA binding proteins discovered were prokaryotic repressors which use the helix-turn-helix (HTH) motif (3). This motif consists of two α-helices connected by a single turn. The orientation of the two helices and the structure of the turn region is similar in all the members of the HTH family of proteins. The sequence specificity arises from contacts between side-chains on the "recognition helix" which lies in the major groove, and specific bases at the recognition site (Figure 1.2). Additional affinity for the site arises from the favorable alignment of the dipole of the accompanying helix and also from contacts between these helices and the phosphate backbone. Since their identification in prokaryotic repressors, several eukaryotic transcription factors (homeodomain proteins) utilizing the HTH motif for DNA binding have also been identified (4).

The "zinc finger" motif commonly found in eukaryotic transcription factors consists of a characteristic pattern of two cysteine and two histidine

Figure 1.2: (A) Ribbon model of a dimer of the *Drosophila Melanogaster* homeodomain protein *engrailed* bound to its target site.
(B) An enlarged view of residues in the recognition helix of *eng* interacting with bases at the target site.
(Images from the Swiss-3D image database)

A.

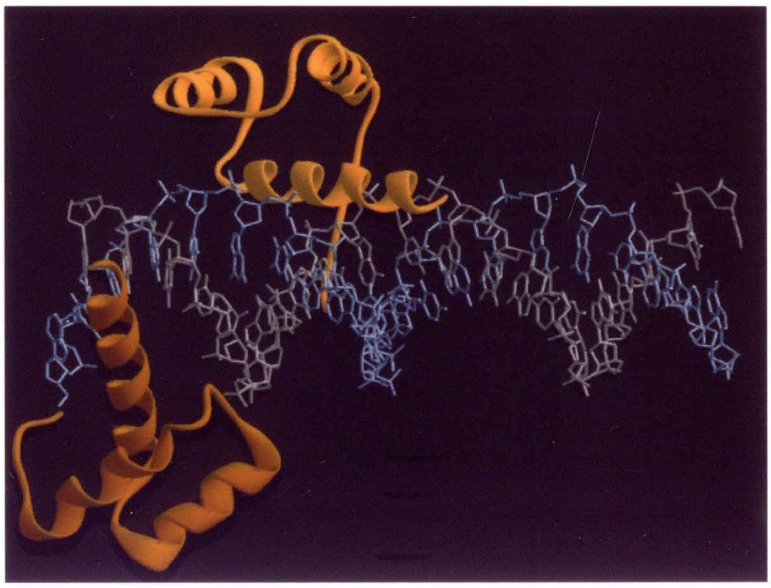

B.

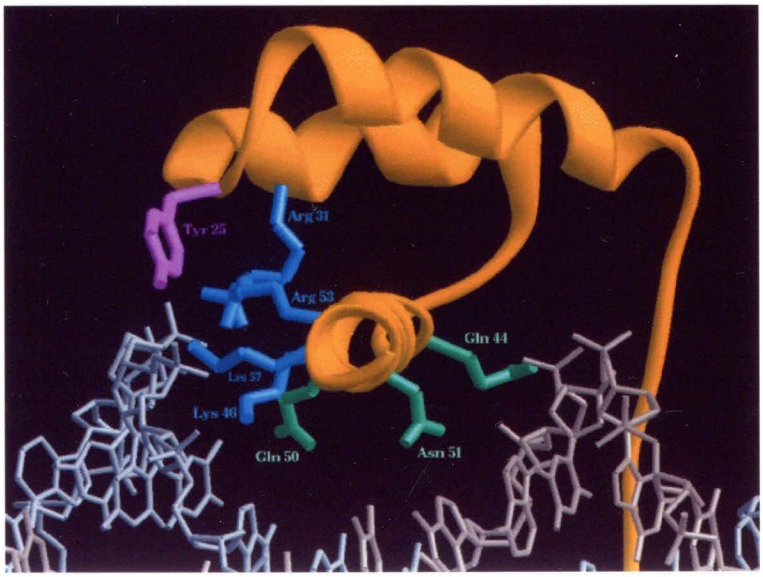

(Cys-Cys-His-His) residues separated by a region of twelve residues containing two invariant hydrophobic side chains (Figure 4). The first structure of this independent folding domain was characterized by Wright and coworkers (5). Since then three different families of zinc fingers have been identified which differ in the residues used to coordinate the zinc atom. Members of the glucocorticoid receptor superfamily have zinc fingers that use four cysteines (Cys-Cys-Cys-Cys), viral *gag* proteins use three cysteines and a histidine (Cys-Cys-His-Cys) and proteins such as the yeast transcription factor Gal 4 contain a binuclear zinc cluster containing six cysteine residues (Cys-X_2-Cys-X_6-Cys-X_6-Cys-X_2-Cys-X_6-Cys) (6). Tetrahedral coordination of the zinc atom is required for proper folding of the zinc finger scaffold which allows sequence specific recognition of the target site primarily through contacts between side chain residues of the α-helix and bases in the major groove.

A third class of motifs the "leucine zippers" are found in DNA binding domains of several eukaryotic transcription factors. This motif was first proposed in the yeast transcription factor GCN4 based on the occurrence of the characteristic leucine heptad repeat. Since then leucine zipper motifs have been identified in eukaryotic transcription factors such as C/EBP as well as oncogene products such as *jun*, *fos* and *myc*.. The cocrystal structure of GCN4 DNA binding domain with its cognate binding site has been solved by Harrison and colleagues (7). It reveals two parallel α-helical regions forming a coiled-coil structure stabilized primarily by hydrophobic packing of

Figure 1.3: (A) Solution structure of the zinc finger domain from human Y - chromosomal protein ZINFY1.

(B) Crystal structure of the *S.Cereviseae* (baker's yeast) transcriptional activator Gal4 showing the binuclear zinc finger.

Figure 1.4: Crystal structure of the leucine zipper DNA binding domain of GCN4 protein from *S.Cereviseae* complexed with its cognate AP-1 site.

(Images from the Swiss-3D image database)

A.

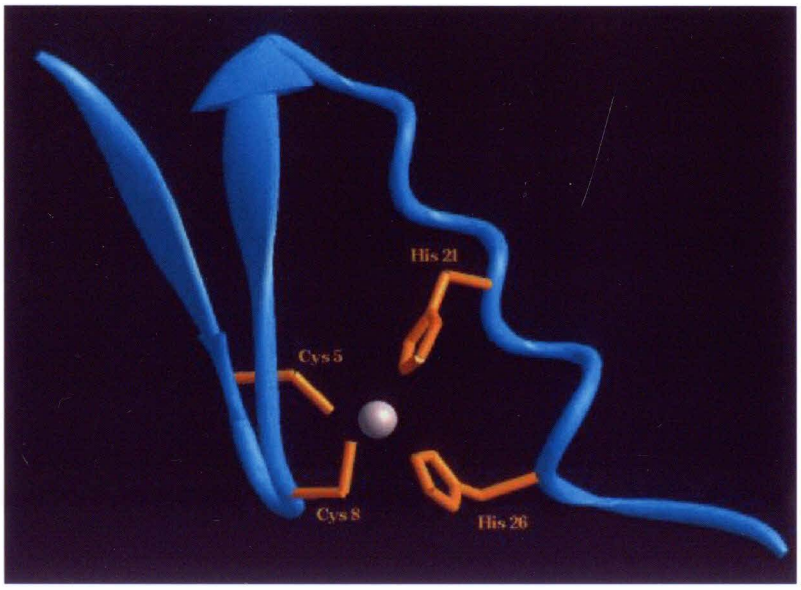

B.

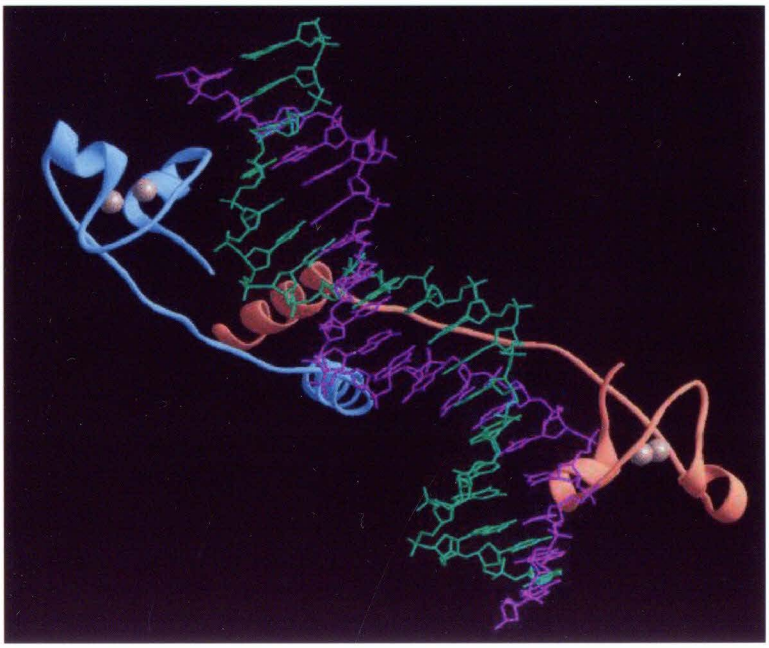

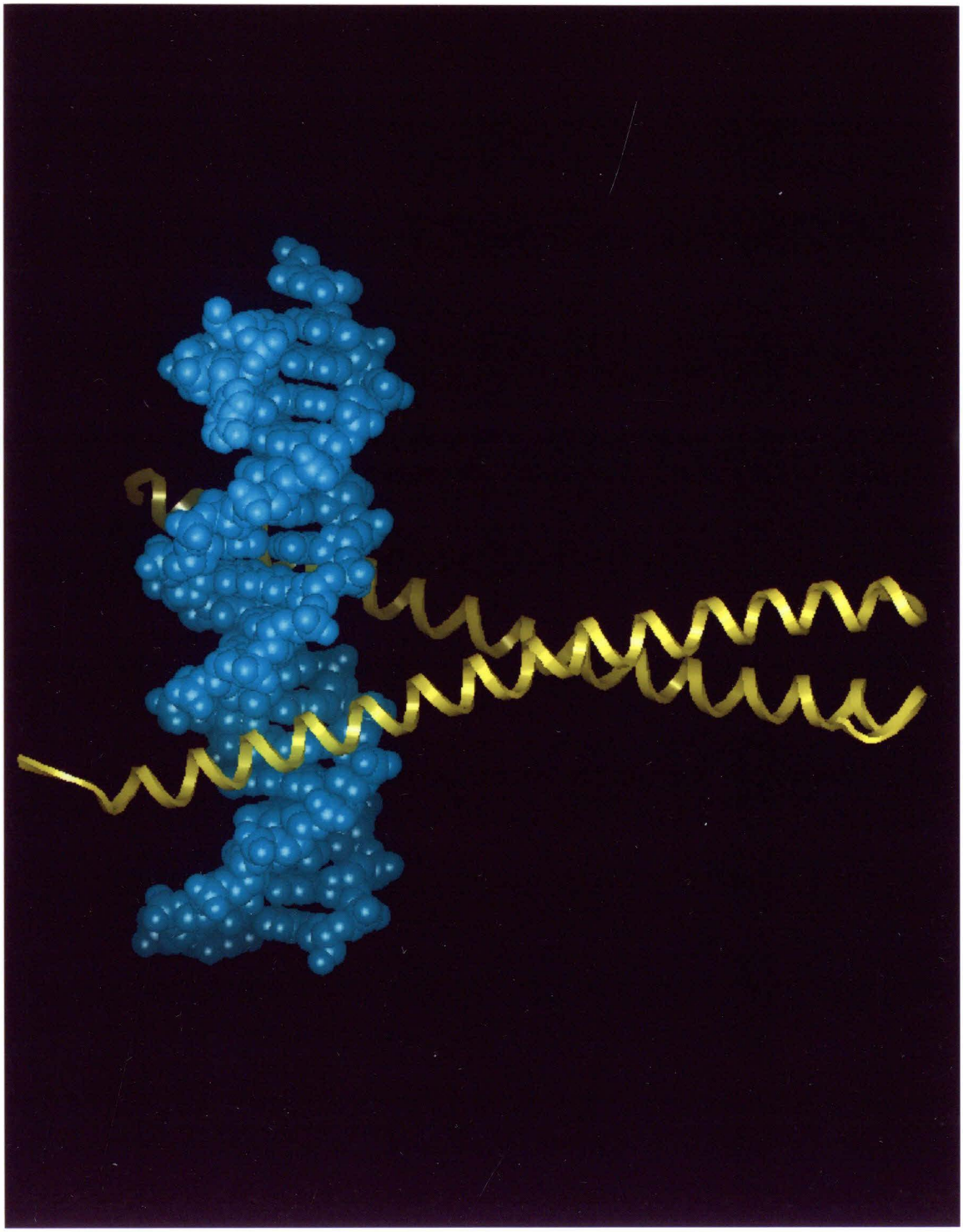

leucine residues at the interface. The two helices diverge slightly at the point of contact with DNA placing the basic region α-helices located at the N termini in the major groove, allowing contacts between specific side chains and bases in the major groove (Figure 5).

A fourth class of DNA binding protein uses a two-stranded antiparallel

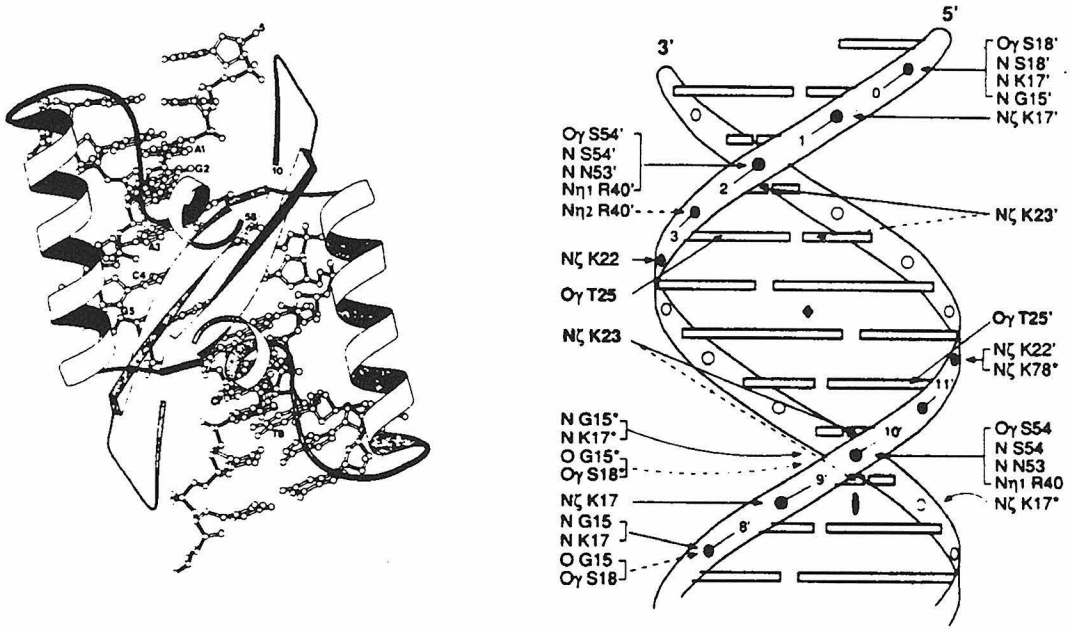

Figure 1.5: Schematic diagram of recognition by the *met* repressor using β-ribbon motif (8).

β-ribbon structure for specific recognition. The β-ribbon motif was first identified in the *met* repressor from *E.Coli* by Phillips and coworkers (8). One β-strand from each monomer of *met* repressor is used to form an antiparallel β-ribbon that packs tightly into the major groove (Figure 1.5). Side chains from the β-ribbon make specific contacts with bases at the recognition site.

The β-ribbon structure has subsequently also been identified in the solution structure of the *arc* repressor by Kaptein and coworkers (9).

It is clear from the above discussion that for recognition of specific sequences by endogenous proteins, there is no single "code". A combination of interactions between the protein side-chains and backbone, with the DNA bases and DNA backbone results in sequence specific binding and in many cases, sequence dependent DNA flexibility is utilized to fine-tune the affinity of related proteins to their cognate sites.

Chemical approaches to recognition of B-form DNA

The design of molecules to bind the regular helical structure of DNA is an important goal for the chemist. The motives for such an endeavor are primarily to control the action of regulatory proteins that interact with DNA or to physically isolate fragments of DNA sequences of interest by directing cleavage chemistry to specific sites on duplex DNA. Perhaps the most extensively studied molecules for recognition of duplex DNA are intercalators, polyamides and triple helix forming oligonucleotides.

Intercalators are some of the earliest studied DNA binding molecules. They are planar aromatic molecules that can insert themselves into duplex DNA by unstacking adjacent base pairs and distorting the sugar phosphate backbone. Examples of intercalating drugs and dyes are ethidium, acridine, proflavine, daunomycin, actinomycin etc. These molecules have little if any sequence specificity and they exert their effects primarily by the extension, unwinding and distortion produced in the regular helical structure

of DNA as a result of their binding. Many of these molecules have found use as antibiotics, cancer therapeutics and also as stains for detecting DNA (10).

Polyamides are small molecules based on the natural products netropsin and distamycin that bind in the minor groove of B-form DNA (11). The affinity and specificity of binding is derived from the formation of hydrogen bonds with specific functional groups in the minor groove as well as from van der Waals contacts with the sides of the minor groove (Figure 1.6). The realization that a "two-letter-code" composed of N-methyl pyrrole and imidazole carboxamide can be used to bind any sequence in the minor groove using 2:1 complexes of polyamides with DNA (12), coupled with recent advances in synthetic methodology for obtaining a variety of polyamides (13) has resulted in a dramatic increase in the ability to target arbitrary sequences with remarkably high affinity and specificity.

Figure 1.6: (A) Two dimensional and space filling representation of 1:1 binding of distamycin in the minor grove of AT rich DNA. (B) Two dimensional and space filling representation of 2:1 binding of the polyamide 2-imidazole netropsin to the sequence 5'-TGTCA-3'.

A

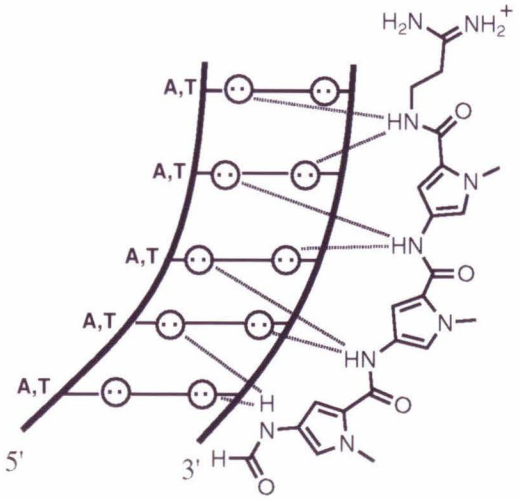

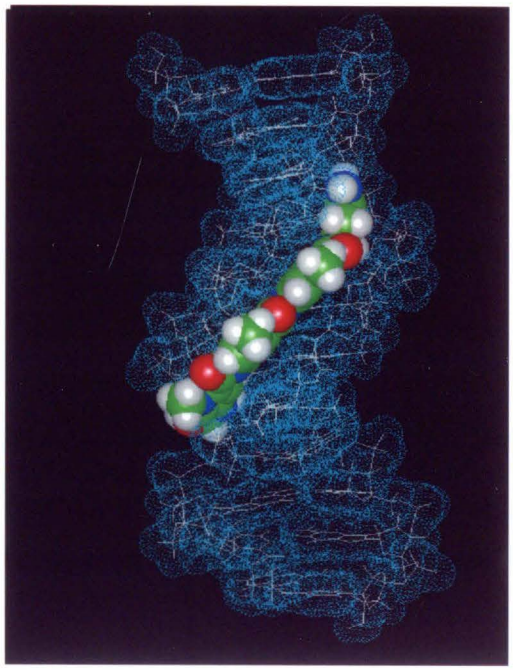

B

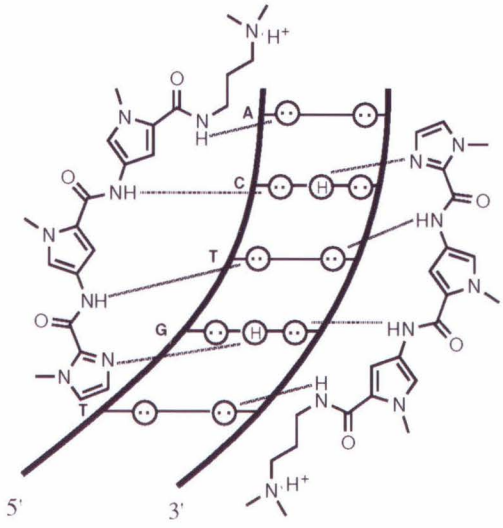

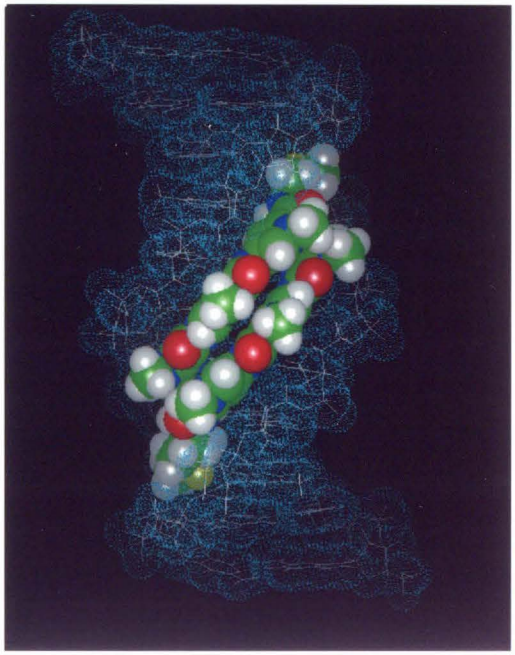

The formation of *triple helical complexes* was first described by Rich and coworkers from fiber diffraction studies on homopolymers of uridine and adenine (14). Soon thereafter, Lipsett and coworkers described the formation of 2:1 complexes of poly(riboC) with poly(ribo G) at acidic pH(15). Interest in triple helical complexes saw a dramatic upsurge since the demonstration by Moser and Dervan in 1987 (16) that a small synthetic oligonucleotide containing both protonated cytidine and thymidine residues can recognize a 15 bp homopurine tract triplets in the so called "pyrimidine motif". The third strand binds parallel to the purine strand and the sequence specificity is derived from T•AT and C^+•GC triplets involving discrete hydrogen bonds with the Hoogsteen face of the major groove (Figure 1.7 A-C). Since then, oligonucleotide mediated triple helix formation has been successfully used to recognize single sites within increasingly longer sequences of DNA (17). Oligonucleotide directed triple helix formation has also been used to recognize G-rich purine tracts in the "purine motif" (18). In this case, specificity is derived from G•GC, T•AT and A•AT triplets, with the third strand binding *anti-parallel* to the purine strand in the major groove (Figure 1.7D). In both motifs, only one strand–the purine strand–of the duplex is contacted by the base in the third strand. Oligonucleotide directed triple helices have sometimes been called "anti-parallel triplexes" to indicate the fact that the third strand binds anti-parallel to the strand of like sequence (19). We note that this is not true in the case of the T•AT triplet in the purine motif. Despite a protracted effort in the direction of synthesis of novel bases to

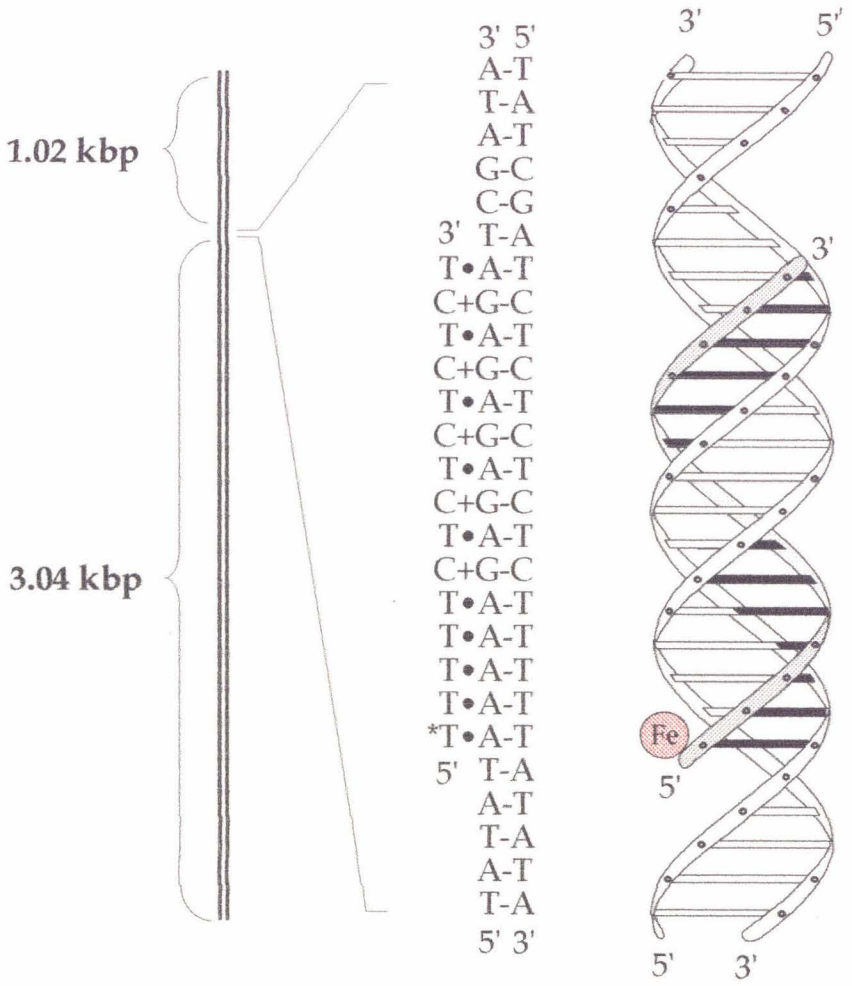

Figure 1.7A: Ribbon model of the triple helix formed 15 base pyrimidine oligonucleotide at a single site in a 4 kbp restriction fragment.

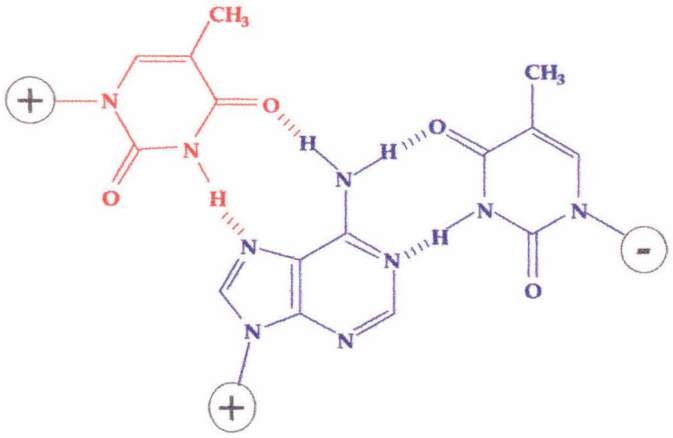

T•AT

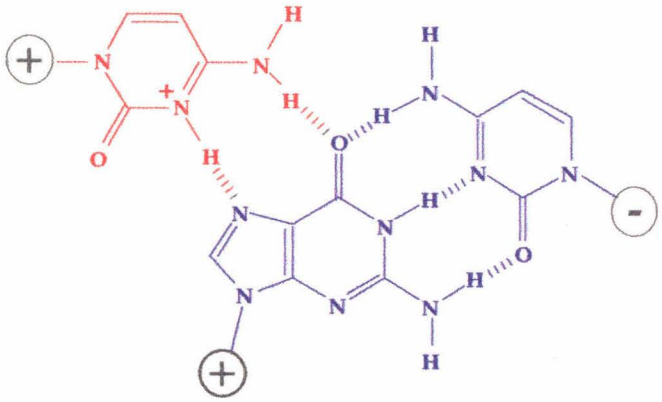

C+GC

Figure 1.7B: Two dimensional representation of T•AT and C+•GC triplets formed in pyrimidine oligonucleotide directed triplex formation. Note that the third strand binds parallel to and makes contacts with only the purine strand.

Figure 1.7 C: Space-filling representation of the NMR structure of the pyrimidine motif triple helix (18).

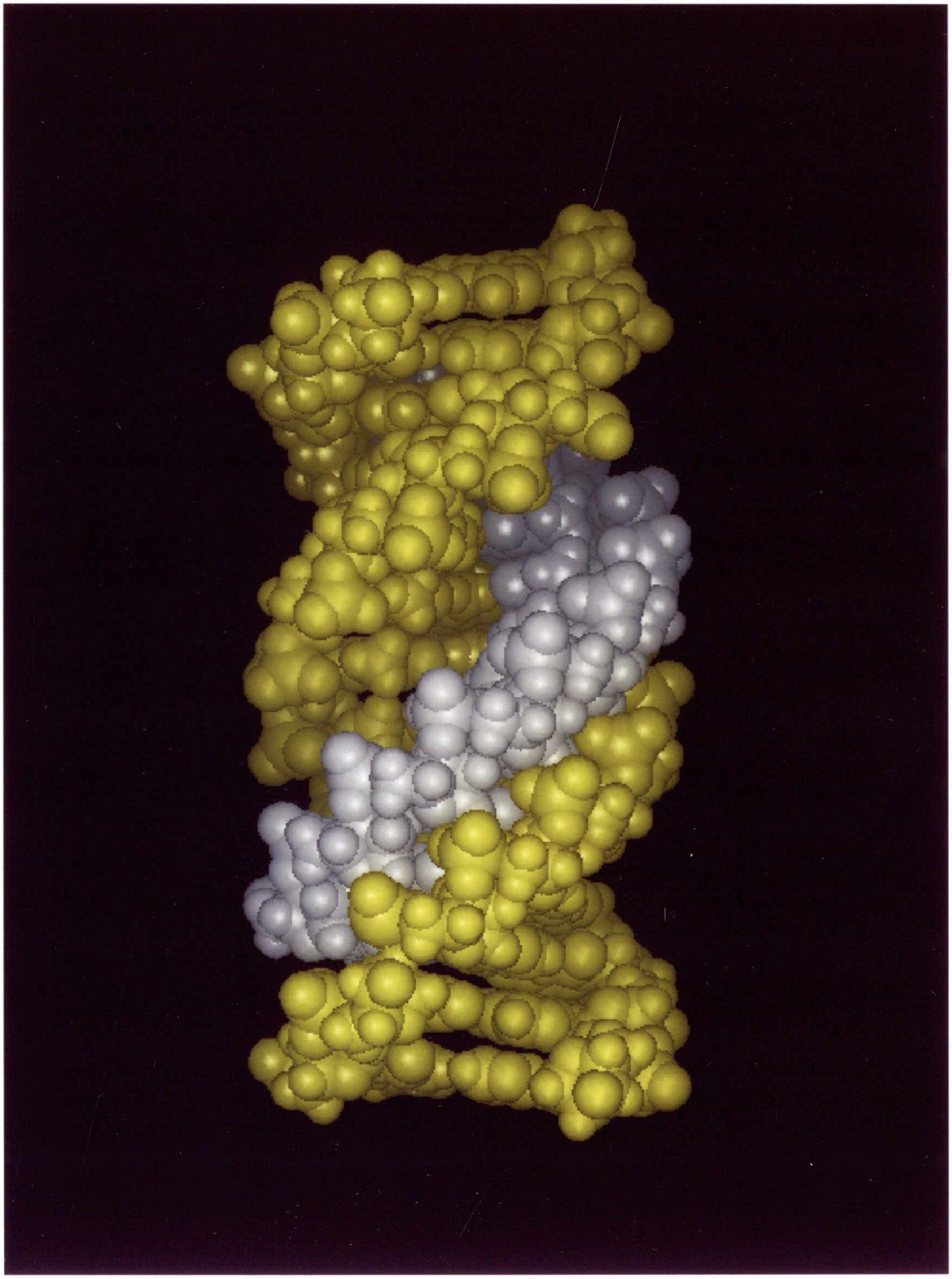

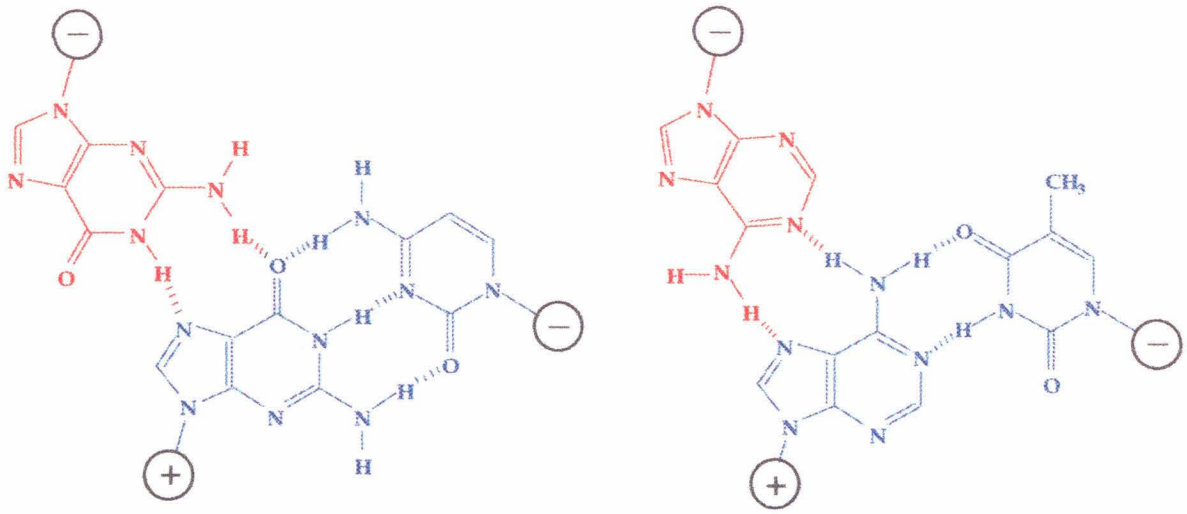

G•GC

A•AT

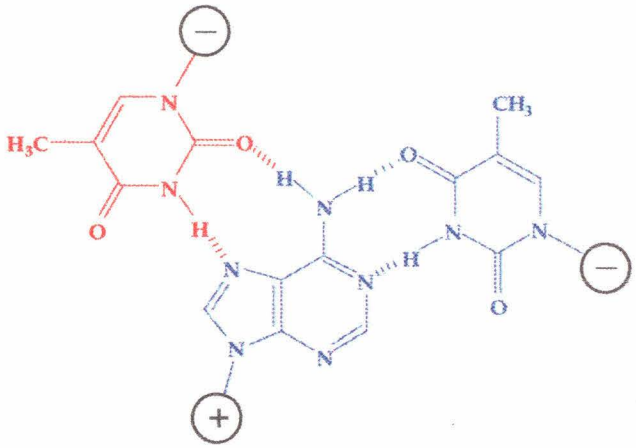

T•AT

Figure 1.7D: Two dimensional representation of G•GC, A•AT and T•AT triplets formed in purine motif triple helices. Note that the third strand (red) binds antiparallel to the purine strand.

generalize oligonucleotide directed triple helix formation to any sequence (20), only a limited number of sequences can be easily targeted due to the inability to recognize CG and TA base pairs, independent of the sequence context, in either motif.

The *E.Coli* RecA protein and its role in homologous recombination

General and site-specific recombination

The process of recombination involves the exchange of genetic information between two molecules of double stranded DNA resulting in the formation of hybrid products. It is a process that is vital for the survival of most organisms because it creates the genetic diversity necessary for evolution and also provides the basis for repair of damaged DNA. At least two distinct types of recombination exist in living cells. *Site specific recombination* involves the recruiting of one or more specific proteins to short (10-20 bp) recognition sites on DNA to bring about close juxtaposition of two recognition sites before affecting chemical cleavage and religation of the strands involved leading to the formation of hybrid products (21). Both the proteins involved and their recognition sites are highly specific to the particular system and recognition of the target site for recombination takes place in much the same way as with other sequence-specific DNA binding proteins. For example in the FLP recombinase from the *S. Cereviseae* 2 μ plasmid, recognition takes place at the so called FLP recognition target (FRT) region–a site containing two inverted 13 bp sites surrounding a core region of 8 bp (22). Other examples of site-specific recombination are integration of

bacteriophage lambda into the E.Coli genome (23), and VDJ recombination in immunoglobulin switch regions (24).

General Recombination on the other hand can, in principle, occur at arbitrary sequences between any two DNA molecules with the only requirement being the presence of homologous sequences. Therefore the proteins involved in general recombination bind DNA non-sequence-specifically. Although families of proteins involved in general recombination have been described in a variety of organisms (25) such as phage T4, E.Coli, yeast and humans, the most extensively studied such protein is the RecA protein from E.Coli.

The RecA protein of *E. Coli* (38 kD) plays a central role in homologous genetic recombination and repair and is involved in the cellular S.O.S. response to gene damage (26). The first evidence for formation of helical nucleoprotein filaments by RecA in presence of single-stranded DNA came from the analysis of electron micrographs of single-stranded M13 viral DNA coated with RecA (27). The binding of RecA resulted in formation of right-handed helical filaments in which approximately eight monomers of RecA protein were bound to 20 nucleotides. The filament had a pitch of 9 nm and a width of 9.3 nm. Similar filaments could also be formed in the presence of duplex DNA (Figure 1.8A). Examination of RecA•dsDNA filaments showed that the duplex was extended to 1.5 times its length and underwound to give ~18.6 bp per turn of the helix, reducing the angular twist between base pairs from 36° to about 20° and increasing the internucleotide spacing from 3.4 Å to approximately 5.1 Å. Ethylation interference studies and dimethyl sulfate

(DMS) footprinting of RecA•ssDNA filaments showed that RecA protein binds to single-stranded oligonucleotides at least 10 bases in length, interacting primarily with the sugar-phosphate backbone and leaving the bases accessible to chemical probes (28). In complexes with double-stranded DNA, binding of RecA results in approximately two-fold more reactivity toward DMS on the major groove side accompanied by a two-fold decrease in reactivity in the minor groove suggesting that RecA coats the minor groove without melting the duplex (29). A conflicting observation comes from Bianchi *et al.* who showed that RecA has an ATP dependent strand separating activity detectable with duplexes shorter that 30 bp (30).

The x-ray crystal structure of the RecA homopolymer as well as the homopolymer bound to the cofactor ADP has been solved (31). Each monomer consists of a major central domain flanked by two smaller subdomains at the N- and C-termini which help to stabilize inter monomer and inter polymer contacts respectively (Figure 1.8 B). The central domain has predominantly anti-parallel β-sheet structure. The monomers are assembled into a 6_1 helix with the a pitch of ~83 Å and width 120 Å. Two disordered loops–Loop1 (residues 157-164) and Loop2 (residues 195-209)–project into the core of the polymer and are known from photochemical crosslinking to be involved in DNA binding (32). The utility of the crystal structure has been limited largely due to the disorder in these DNA binding loops. Low resolution cryo-electron micrographs have been somewhat informative in

Figure 1.8: (A) A comparison of the helix parameters for B-form DNA and the RecA bound "R-form" DNA.

(B) Crystal structure of the RecA protein from *E.Coli* (31).

View from the helical axis of the filament looking outward.

	B-form	**"R-form"**
Pitch	34 Å	95 Å
Base-pairs / turn	10.4	18.6
Internucleotide spacing	3.4 Å	5.1 Å
Angular twist per residue	36°	20°

RecA protein

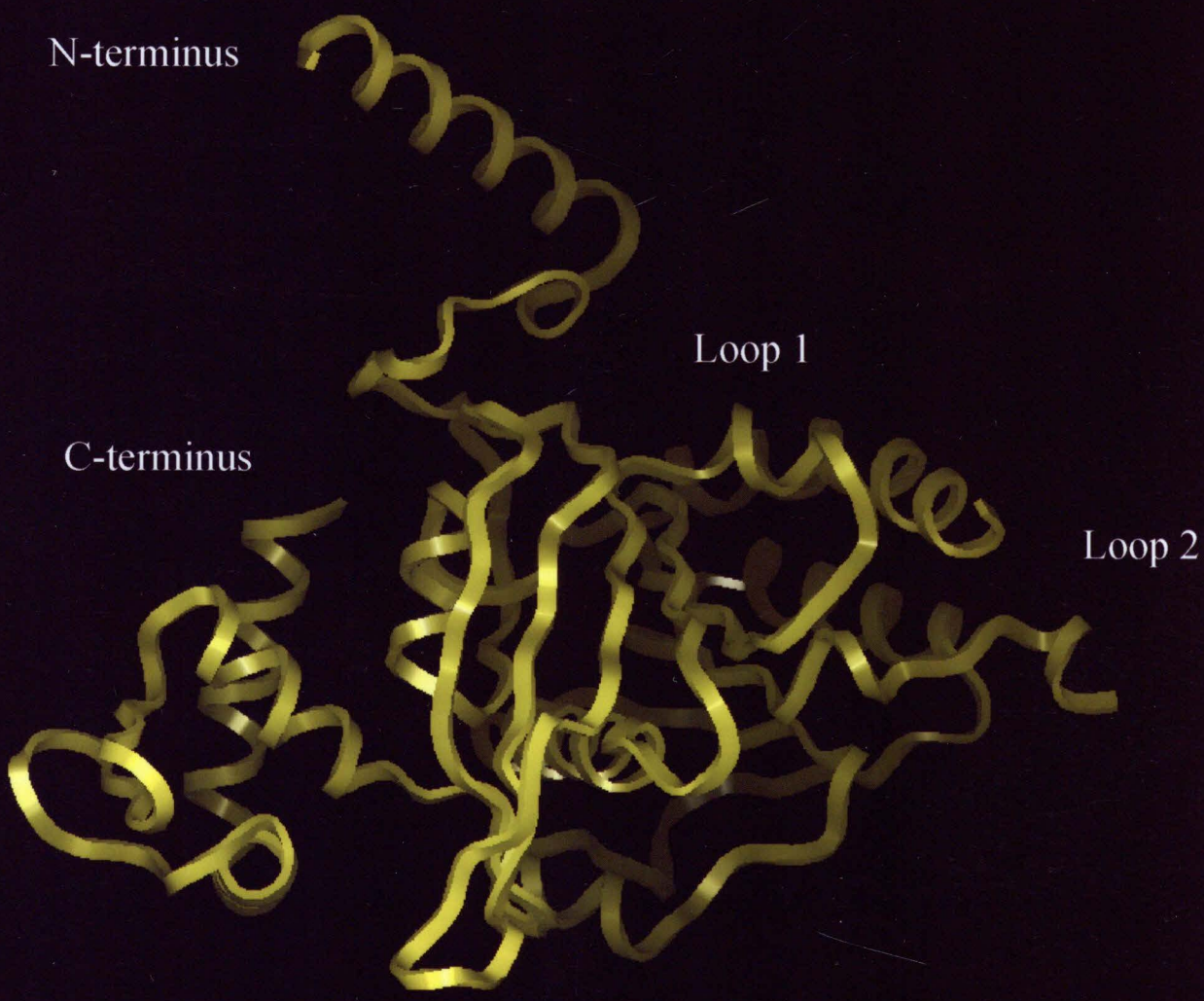

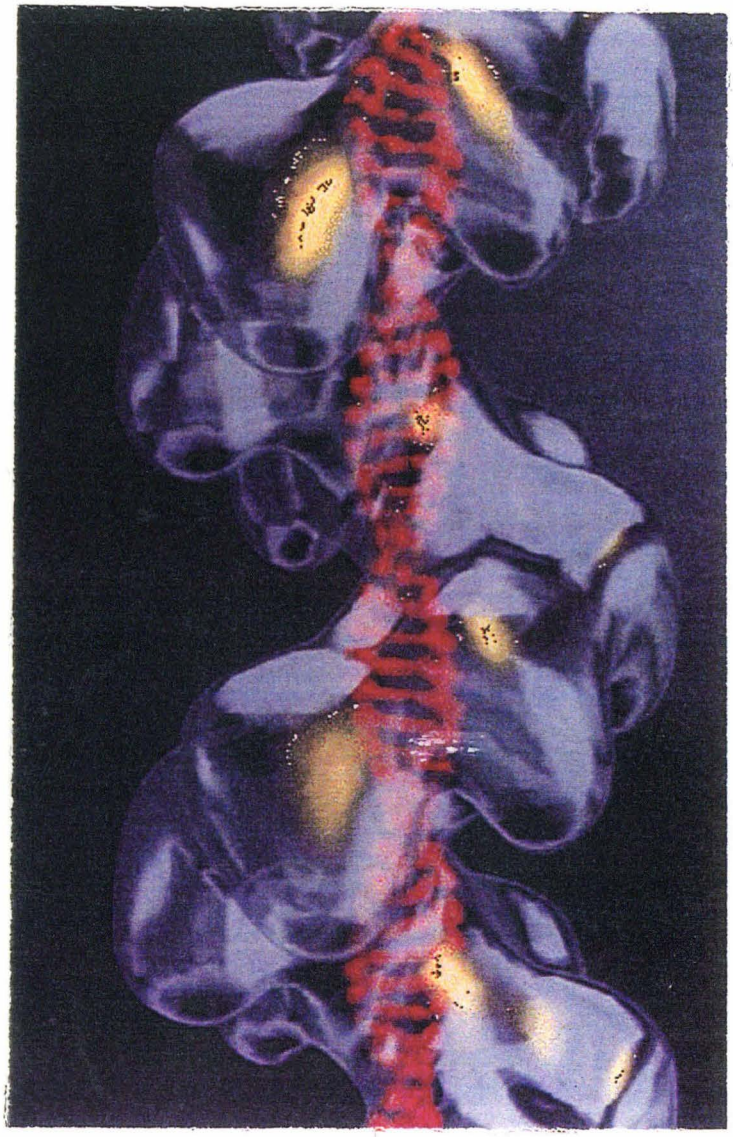

Figure 1.9: Image reconstruction of cryo-electronmicrograph of RecA bound to duplex DNA (32).

determining the approximate location of the DNA within the filament (Figure 1.9).

In vitro, RecA protein mediates a set of DNA strand exchange reactions which have been used as model systems for homologous recombination *in vivo*. In these model studies, RecA-catalyzed strand exchange occurs between two DNA molecules of homologous sequence when one of the molecules of DNA is completely or partially single-stranded. The typical substrates for these studies are linearized plasmid DNA and circular single-stranded DNA from a phage such as M13 (Figure 1.10 A). In the first step, in the presence of an appropriate cofactor such as ATP or its slowly-hydolyzed analog ATP-γ-S, RecA monomers assemble on the single-stranded DNA to form a presynaptic nucleoprotein filament capable of finding it homologous site on the duplex target. Next, a very rapid search for homology leads to the formation of a synaptic complex between the filament and the duplex at sites of homology. Note that unlike site-specific DNA binding proteins, RecA binds DNA non-sequence-specifically and uses the sequence information of the single-strand bound within the filament to achieve sequence specificity. In the synapsis step, a joint molecule is formed which contains all three strands of DNA and numerous RecA monomers. The final step is the release of the strand exchange products–a displaced single strand and a heteroduplex. The process is polar occurring in the 5'- to 3'- direction with respect to the strand being displaced from the duplex. When homology between the two substrates is limited (Figure 1.10 B), the outcome of the

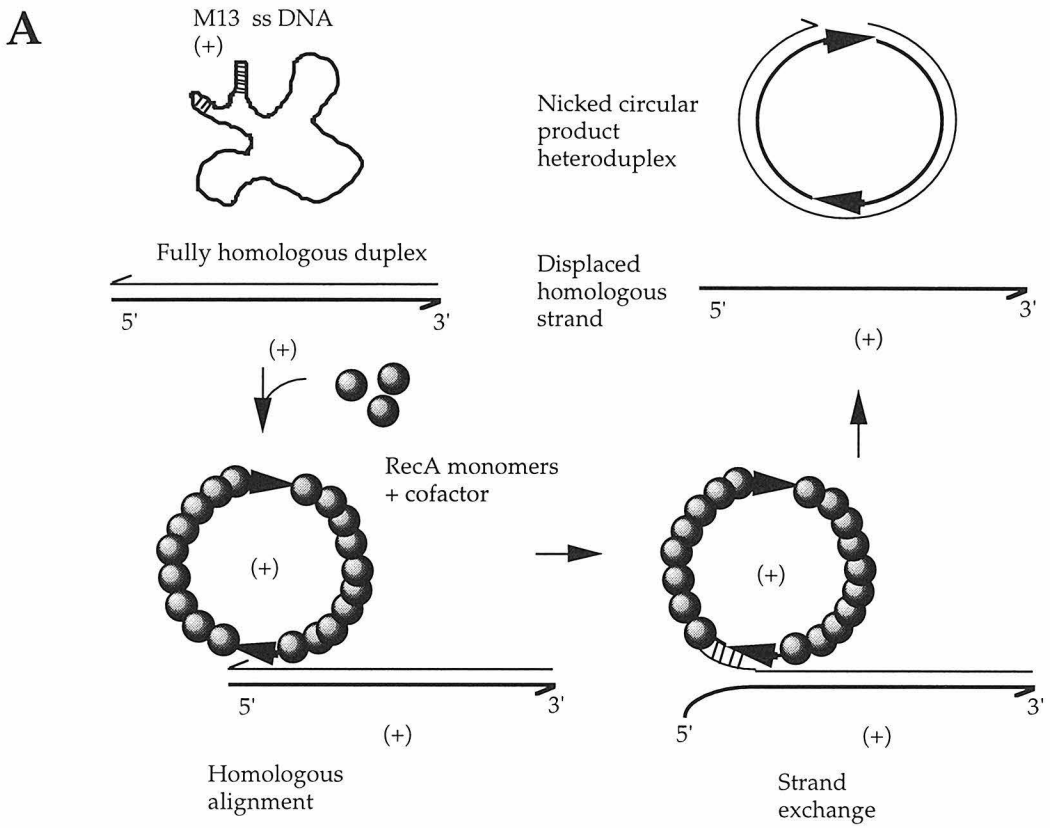

Figure 1.10: **A.** Schematic diagram of substrates commonly used for studying the three-strand reaction. Circular M13 single-stranded DNA and fully homologous linear duplex lead to the formation of a nicked circular duplex product and displaced homologous single strand.

B. Schematic diagram of substrates commonly used for studying intermediates of the RecA mediated three-strand reaction.

C. Example of substrates used for studying *deproteinized* intermediates of the RecA mediated three-strand reaction.

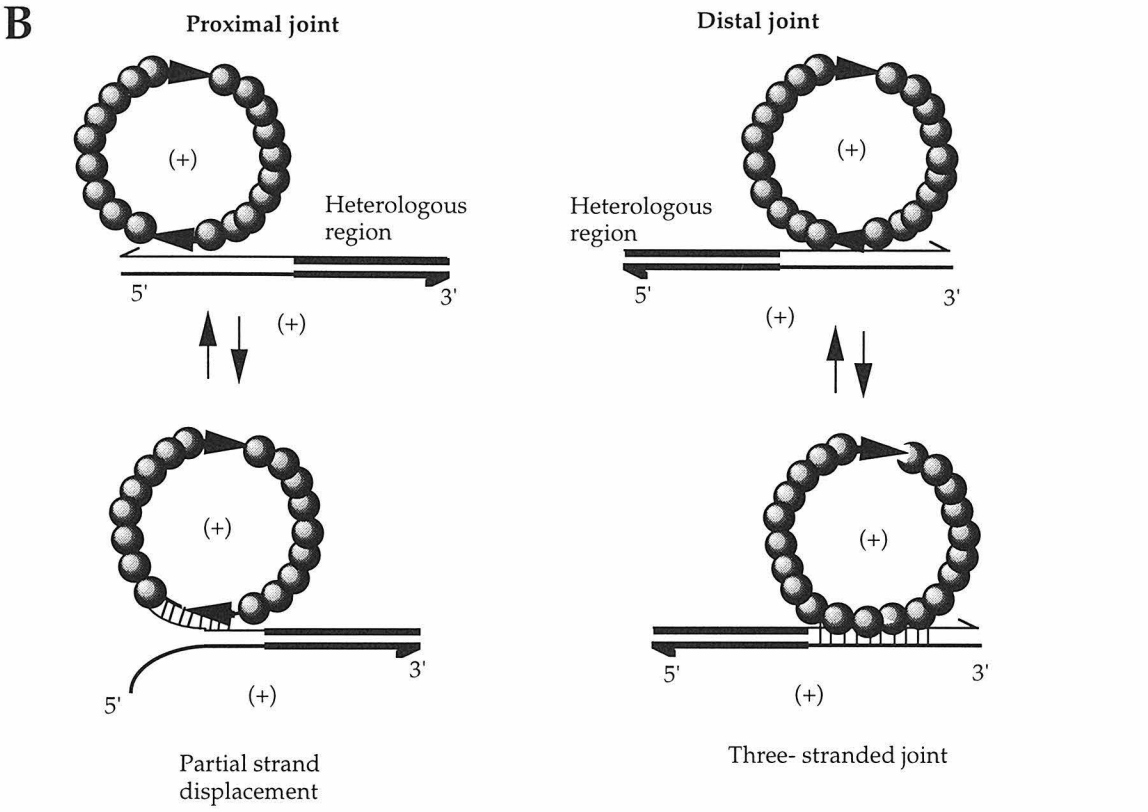
B
Proximal joint
Distal joint
(+)
Heterologous region
5'
3'
(+)
Heterologous region
5'
3'
(+)
(+)
3'
5'
(+)
(+)
5'
3'
(+)
Partial strand displacement
Three- stranded joint

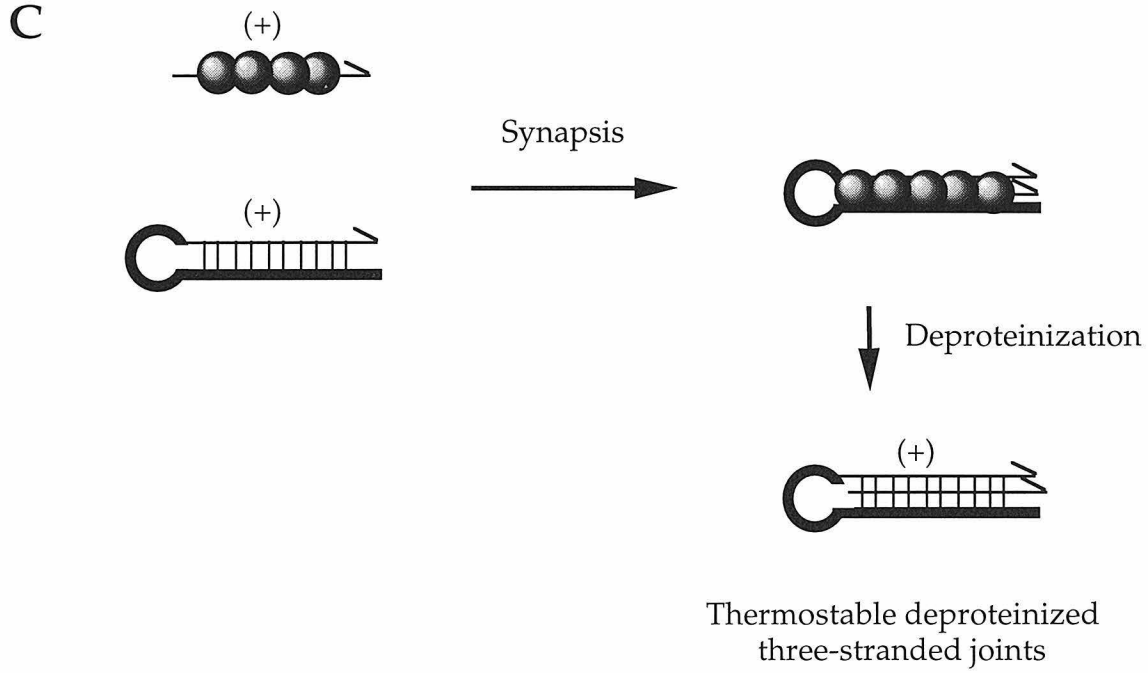
C
(+)
(+)
Synapsis
Deproteinization
(+)
Thermostable deproteinized three-stranded joints

synapsis depends on the location of homology. If the homologous region is located such that the 5'-end of the strand to be displaced is at the end of the linear duplex (proximal homology), strand displacement proceeds to the point where heterologous sequence is located to give a "proximal joint". Branch migration then leads to the slow dissociation of the filament from the target duplex giving back the starting substrates. However, when the 5'-end of the homologous strand is trapped at an internal site within the duplex (distal/medial homology), three-stranded "distal/medial joints" are formed that exist in a dynamic state (34). A number of studies pertaining to the role of the cofactor ATP in the three-strand reaction have helped reach the consensus that while binding of the cofactor is essential for high-affinity binding of RecA to single-stranded DNA in the presynaptic filament, its hydrolysis is required only for the transformation of RecA to a form that has low affinity for the product heteroduplex (35).

Camerini-Otero and coworkers have described the formation of a three-stranded intermediates by the synapsis of RecA•ssDNA filaments with homologous duplexes, which were thermostable even upon deproteinization (36). Radding and coworkers have also described similar thermostable deproteinized intermediates (37). It is unclear if these deproteinized three-stranded complexes (Figure 1.10 C) bear any structural resemblance to the RecA associated complex or are in way representative of an intermediate in the three-strand reaction. Details of biochemical studies conducted on these

three-stranded intermediates and their proposed role in homologous recombination are discussed in Chapter 4.

In summary, although the last two decades have seen a great deal of research into every aspect of the three strand reaction, little is known about (a) the process by which nucleoprotein filaments locate their homologous sites (b) the disposition of the three strands in the protein associated three-stranded joint molecule or (c) the mechanism by which the three-stranded joints are processed to give the products of strand exchange. Since the availability of a good starting structural model is useful for the interpretation of data from any biochemical studies, the protein associated three-stranded joint molecule is an ideal system for study using techniques such as affinity cleavage.

Description of Thesis Work

This thesis work describes the use of affinity cleavage to study the binding of RecA nucleoprotein filaments to homologous sites on duplex DNA. Chapter Two provides an introduction to the technique of affinity cleavage and describes the optimization of affinity cleavage with RecA•oligonucleotide filaments first described by Singleton (38) with respect to length of the oligonucleotide and other solution conditions. Experiments are described that help rationalize the disparity between site occupancy by the RecA•oligonucleotide nucleoprotein filament and the maximum observable amount of cleavage. Chapter Three describes the use of affinity cleavage to observe the cooperative binding of nucleoprotein filaments formed with

short oligonucleotides and an investigation into the basis for the observed cooperativity. Chapter Four provides an introduction to the existing models for the mechanism of the three-strand reaction catalyzed by RecA protein. Experiments are described that use affinity cleavage to determine the groove location of the third strand in the RecA associated three-stranded complex. The results provide strong evidence for *minor groove* binding of the incoming strand. Chapter Five describes the use of "functional group mutagenesis" to reveal the functional groups critical for the process of homologous alignment. Our results are consistent with a model for recognition of target duplexes that involves the melting of the target duplex and testing of homology by simple Watson-Crick complementarity.

References

(1) Watson, J.D., Crick, F.H.C. (1953) *Nature* **171**, 737-738.

(2) Harrison, S.C. (1991)*Nature* **353**, 715-719; Pabo, C.O., Sauer, R.T. (1992)*Ann. Rev. Biochem.*, 1053-1095.

(3) Anderson, W.F. et al. (1981) *Nature* **290**, 754-758.

(4) Ottig, G. et al. (1990) *EMBO J.* **9**, 3085- 3092; Qian, Y. Q. et al. (1989) *Cell* **59**, 573-580; Brennan, R.G., Matthews, B. W. (1989) *J. Biol. Chem.*, **264**, 1903-1906.

(5) Lee, M.S. et al. (1989) *Science* **245**, 635-637.

(6) Summers, M.F. et al. (1990) *Biochemistry* **29**, 329-240; Pan, T., Coleman, J.E. (1990)*Proc. Natl. Acad. Sci. U.S.A.* **87**, 2077-2081.

(7) Ellenberger, T.E., Brandl, C.J. , Harrison, S.C. (1992) *Cell* **71**, 1223-1237.

(8) Rafferty, J. B. et al. (1989) *Nature* **341**, 705-710.

(9) Vershon, A.K. et al. (1985) *J. Bol. Chem.* **260**, 12124-12129.

(10) Saenger, W. (1984) *Principles of Nucleic Acid Structure* Springer Verlag: New York.

(11) Dervan, P.B. (1986) *Science* **232**, 64-71.

(12) Geierstranger, B. H., Mrksich, M.M., Dervan, P.B., Wemmer, D.E. (1994) *Science* **266**, 646-650.

(13) Baird, E.E., Dervan, P.B. *J. Am. Chem. Soc.* (1996) (in press).

(14) Felsenfeld, G., Davies, D.R., Rich, A. (1957) *J.Am. Chem. Soc.* **79**, 2023-2024.

(15) Lipsett, M.N. (1964) *J. Biol. Chem.* **239**, 1256-1260.

(16) Moser, H.E., Dervan, P.B. (1987) *Science* **238**, 645-650.

(17) Strobel, S.A., Moser, H.E., Dervan, P.B. (1988) *J. Am. Chem. Soc.* **110**, 7927-7929; Strobel, S.A., Dervan, P.B. (1990) *Science* **249**, 73-75; Strobel, S.A., Doucette-Stamm, L. A., Riba, L. Housman, D.E., Dervan,P.B. (1991) *Science* **254**, 1639-1642.

(18) Beal, P.A., Dervan, P.B. (1991) *Science* **251**, 1360-1363.

(19) Cameriniotero, R.D., Hsieh, P. (1993) *Cell* **73**, 217-223.

(20) Reviewed in Priestley, E.S., Ph.D. Dissertation, (1996).

(21) For a recent review see Stark, W. M. et al. (1992) *Trends Genet.* **8**, 432-439.

(22) Zhu, X.D. et al. (1995) *J. Biol. Chem.* **270**, 11646-11653.

(23) Craig, N.L (1988) *Ann. Rev. Genet.* **22**, 77-105.

(24) Ferrier et al. (1989) *Cold Spring Harbor Symposia on Quantitative Biology* **54**, 191-202.

(25) For a recent review of proteins in homologus recombination see Camerini-Otero, R.D. , Hsieh, P. (1995) *Ann.Rev.Genet.* **29**, 509-552.

(26) For recent reviews on RecA : Cox, M. M. (1995) *J. Biol. Chem.* **270**, 26021-26024; Kowalczykowski, S. C. & Eggleston, A. K. (1994) *Ann. Rev. Biochem.* **63**, 991-1043.

(27) Satsiak, A. & Egelman, E..H. (1982) *Nature* **229**, 185-186; Flory, J., Tsang, S. S. & Muniyappa, K. (1984) *Proc. Natl. Acad. Sci.*, U.S.A. **81**, 7026-7030.

(28) Leahy, M. C. & Radding, C. M., (1986) *J. Biol. Chem.* **261**, 6954-6960.

(29) Capua, E. D. & Muller, B. (1987) *EMBO J.* **6**, 2492-2498.

(30) Bianchi, M., Riboli, B., Magni, G. (1985) *EMBO J.* **4**, 3025-3030.

(31) Story, R. M., Weber, I. T. & Steitz, T. A. (1992) *Nature* **355**, 318-325; Story, R. M. & Steitz, T. A. (1992) *Nature* **355**, 374-376.

(32) Ogawa, T., Yu, X., Shinohara, A., Egelman, E.H. (1993) *Science* **259**, 1896-1899.

(33) Morimatsu, K., Horii, T. (1995) *Eur. J. Biochem.* **234**, 695-705; Wang, Y. , Adzuma, K. (1996) *Biochemistry* (in press).

(34) Reddy, G., Jwang, B., Rao, B.J. and Radding, C.M. (1994) *Biochemistry* **33**, 11486-11492.

(35) Reviewed in Cox, M.M. (1994) *Trends Biochem. Sci.* **19**, 217-222.

(36) Hsieh, P. & Camerinioteró, R. D. (1990) *Genes Dev.* **4**, 1951-1963.

(37) Rao, B. J., Dutreix, M., Radding, C. M. (1991)*Proc. Natl. Acad. Sci. USA* **88**, 2984-2988.

(38) Singleton, J. W., Master's Dissertation, California Institute of Technology (1994).

CHAPTER TWO

Affinity Cleavage with RecA•oligonucleotide-EDTA•Fe(II) Nucleoprotein Filaments

Introduction

A number of well established techniques exist for detecting and quantitating the binding of ligands to nucleic acid targets. Among them are gel mobility shift analyses, chemical interference footprinting, nuclease sensitivity, restriction enzyme inhibition, photocrosslinking, spectroscopic methods such as circular and linear dichroism, and affinity cleavage (1). Among these affinity cleavage is notable for being exceptionally versatile and informative.

The technique of affinity cleavage involves tethering an agent that can cleave DNA efficiently and non-sequence-specifically to a DNA binding

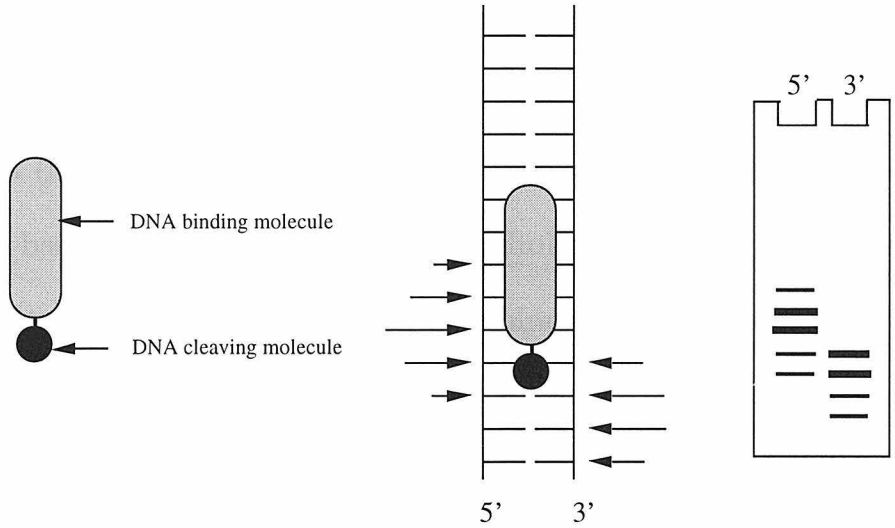

Figure 2.1 : Schematic representation of the concept of affinity cleaving.

molecule, such that the location of the cleavage patterns generated by the conjugate reveals the binding site and orientation of the ligand and the intensity of the cleavage pattern is related to the affinity of the ligand for its target site (Figure 2.1). One of the most common DNA cleaving reagents used for affinity cleavage is chelated iron (Fe(II)) in the presence of molecular

oxygen and a reducing agent such as dithiothreitol (DTT) or ascorbate. Although the details of the cleavage reaction are not completely understood, the mechanism is thought to be the abstraction of a proton from the C4′ position in the minor groove by hydroxyl radical, partitioning of the C 4' radical center between hydroxyl and hydroperoxide formation, followed by a cascade of reactions that result in DNA strand scission (2). Presence of a reducing agent is required for recycling Fe(II) which is oxidized to Fe(III) in the process of activation of molecular oxygen to hydroxyl radical. The technique of affinity cleavage was first described by Hertzberg and Dervan in 1982, when in an effort to mimic the DNA cleaving properties of the natural product bleomycin, EDTA was appended to the intercalator methidium via a short alkyl linker (Figure 2.2A). The resultant conjugate, methidium propyl EDTA (MPE) caused largely non-sequence-specific oxidative cleavage of the DNA backbone (3). In the same year Schultz and Dervan appended EDTA to the naturally occurring minor groove binding polyamide distamycin (Figure 2.2B). The weak specificity of distamycin for AT tracts resulted in cleavage localized to those regions of the target duplex (4). In the following years, EDTA was appended to a variety of longer polyamides leading to the generation of increasingly specific DNA cleaving molecules. The versatility of affinity cleavage was further extended when Dreyer and Dervan (5) described the synthesis of a nucleoside analog Thymidine-EDTA (T*) which had EDTA appended to the 5-position of the thymine heterocycle via a short alkyl linker (Figure 2.2C). Affinity cleavage has since been used to study the binding

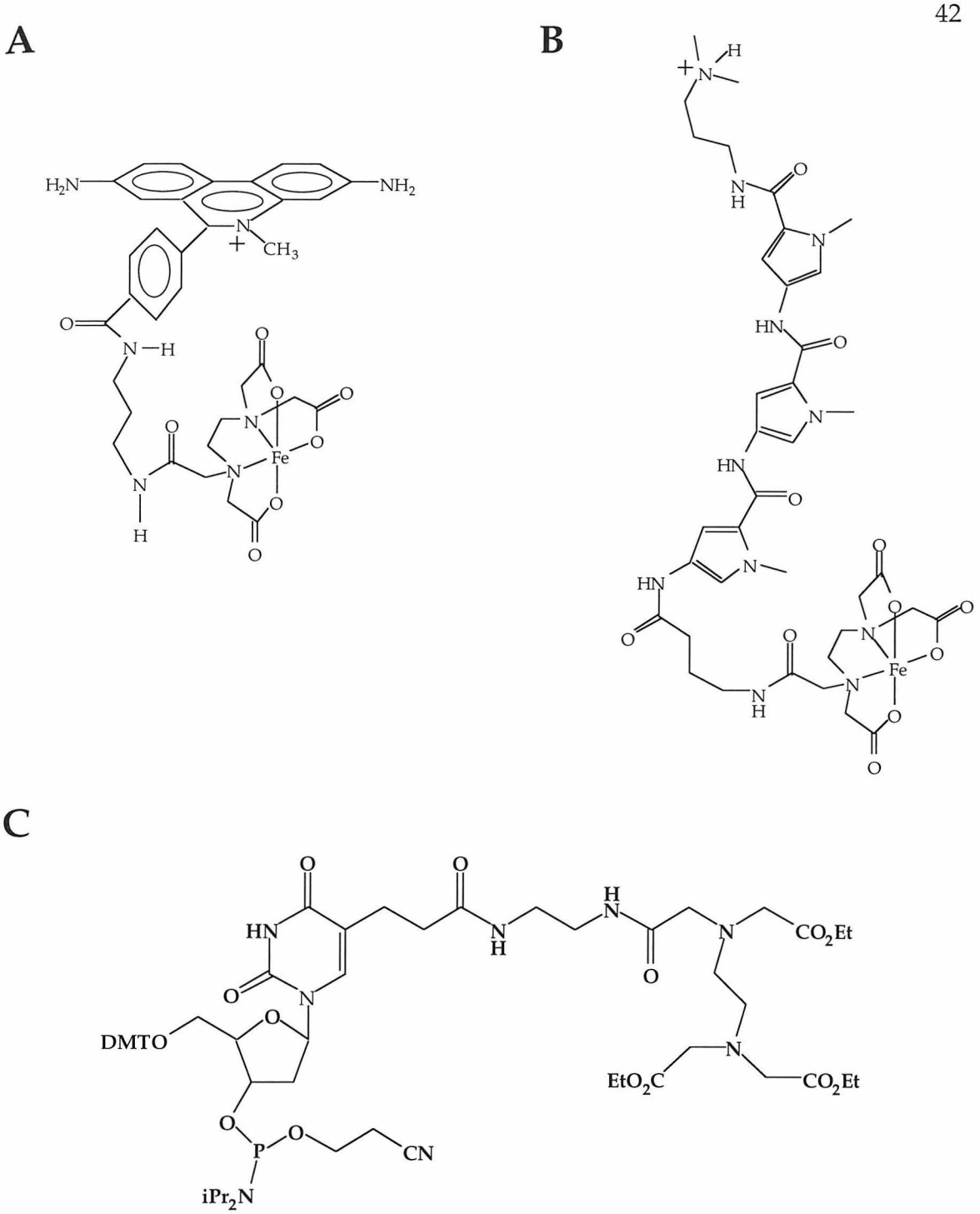

Figure 2.2: Chemical structure of molecules used for affinity cleavage of DNA.
A. Methidium propyl EDTA (MPE) .
B. Distamycin EDTA.
C. β-cyanoethyl phosphoramidite of Thymidine EDTA (T*).

orientation and affinity of oligonucleotides carrying T* in triple helical complexes in two different motifs (6). As mentioned earlier, affinity cleavage using oligonucleotide directed triplex formation has been used to cleave single sites in genomic DNA (7). However this approach suffers from the fact that CG and TA base pairs can not be targeted with high affinity in a generalizable fashion in both motifs of triple helical complexes.

The RecA protein of *E. Coli* (38 kD) is a small, 352 residue protein that plays a central role in both general recombination and SOS DNA repair (8). In the presence of single stranded DNA and an appropriate cofactor such as adenosine triphosphate (ATP), RecA protein forms a right-handed helical nucleoprotein filament with a binding stoichiometry of approximately one RecA monomer for every three bases (9). These single-stranded DNA•RecA filaments can scan duplex DNA for sequences homologous to the strand within the filament. The process of sequence searches is very rapid and has been estimated to be of the order of 6.4 kbp min^{-1} (10). When sequence homology is located, a three-stranded intermediate is formed that contains all three strands and numerous RecA monomers. Displacement of the homologous strand from the three-stranded intermediate begins from the 5'-end of the homologous strand. The outcome of the three-strand exchange reaction is determined by the extent and location of homology on the duplex target. When the 5'-end of the homologous strand can not be displaced either because it is held in the middle of a longer duplex or because it is trapped in the form of a hairpin, strand exchange does not proceed to completion and

the three-stranded intermediate exists in equilibrium with the nucleoprotein filament and target duplex (11). The formation of three stranded complexes has been previously described for systems in which short (20-50 base long) oligonucleotides of mixed sequence were targeted to a single site within a plasmid ~3 Kb long (12). Although a number of different models exist for the interactions between the three strands in this synaptic complex, the precise nature of forces that hold the three strands in close proximity is not understood (13). However, since the three-stranded complexes can, in principle, be formed using oligonucleotides of arbitrary sequences, Singleton and Dervan adapted this chemoenzymatic approach to target a single 31 base site within a duplex of 300 bp using affinity cleavage (14). Nucleoprotein filaments were formed using an oligonucleotide carrying a thymidine-EDTA(T*) moiety at a single terminal position (Figure 2.3). Upon incubation with the duplex target followed by exposure to reductant, affinity cleavage was successfully directed to the site predicted by antiparallel binding of the RecA•oligonucleotide filament to its target site. Major cleavage was observed only on the strand complementary to the oligonucleotide held within the filament, indicating that the homologous strand is either displaced in the form of a D-loop or held in a conformation that is inaccessible to cleavage by the tethered Fe(II) EDTA. The experiments described in this chapter are directed toward determining (a) if the absence of affinity cleavage on the homologous strand is simply a result of differential specific activities resulting form the labeling protocols (b) what if any effect the length and

sequence of the oligonucleotide or the solution conditions used for affinity cleavage might have on the efficiency of cleavage (c) if affinity cleavage by nucleoprotein filaments can be optimized to obtain double-strand cleavage with higher efficiency, with the aim of directing chemical cleavage at arbitrary sites on duplex DNA with high efficiency.

Results and Discussion

Affinity cleavage with complementary oligonucleotide

Affinity cleavage reactions were carried out as previously described (14). The oligonucleotides carrying T* at their termini used in this study are shown in Figure 2.4. Oligonucleotides **1** and **2** carrying T* at the 3'- and 5'-ends respectively, were previously shown to generate cleavage patterns on only one strand–the complementary strand. The procedure used for labeling the two strands involves fill-in using Klenow fragment for 3'-end labeling and the use of calf intestinal phosphatase followed by T4 polynucleotide kinase for 5'-end labeling. Although the efficiency of labeling with polynucleotide kinase can be close to quantitative, compared to the maximum of about 65% achievable by the Klenow fill-in reaction (15), due to the inherent losses in the kinase procedure, typically 2 to 5-fold higher labeling efficiencies are obtained from fill-in reactions. To investigate if this difference in labeling efficiencies is the reason why affinity cleavage patterns are visible only on the complementary strand, oligonucleotide **3** of sequence complementary to **1** and **2** and carrying T* at its 5'-end was synthesized.

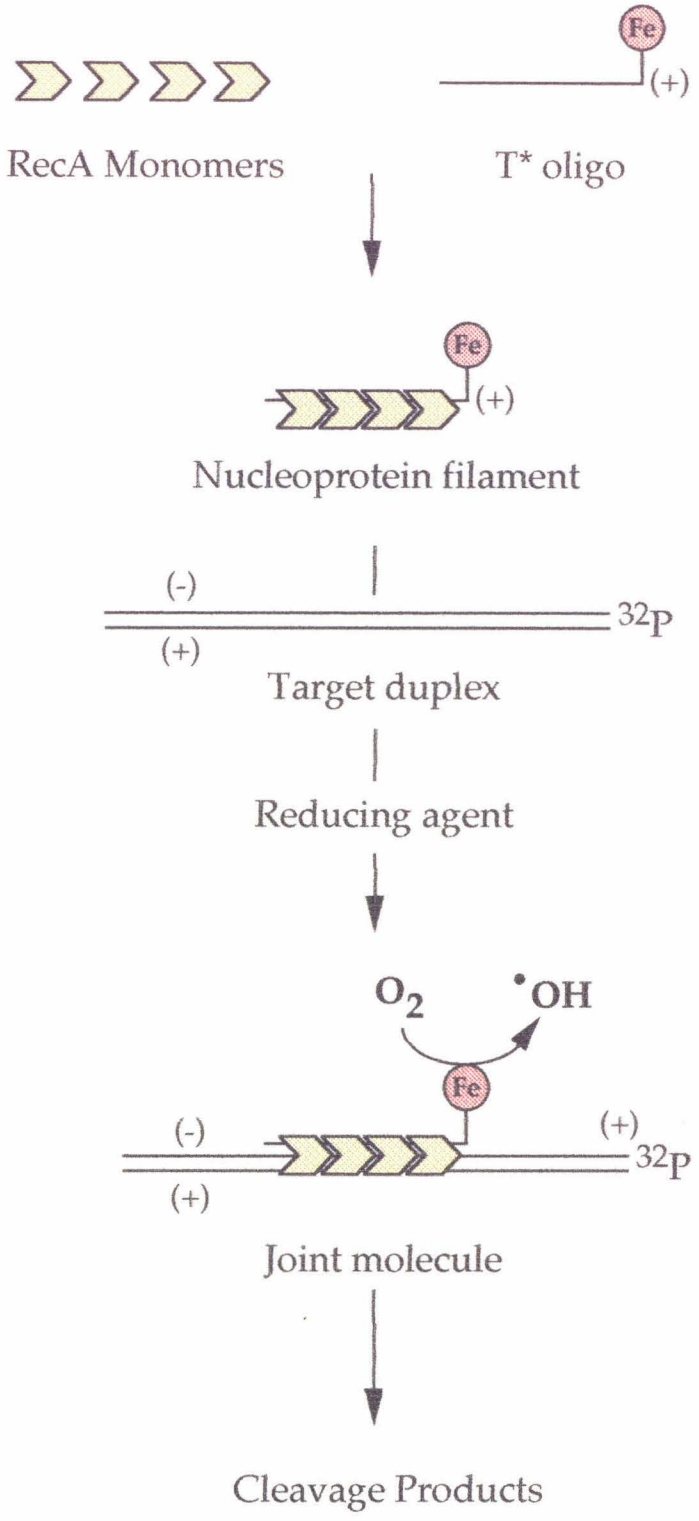

Figure 2.3 : Affinity cleavage with nucleoprotein filaments formed using RecA and oligonucleotide EDTA. Adapted from 14.

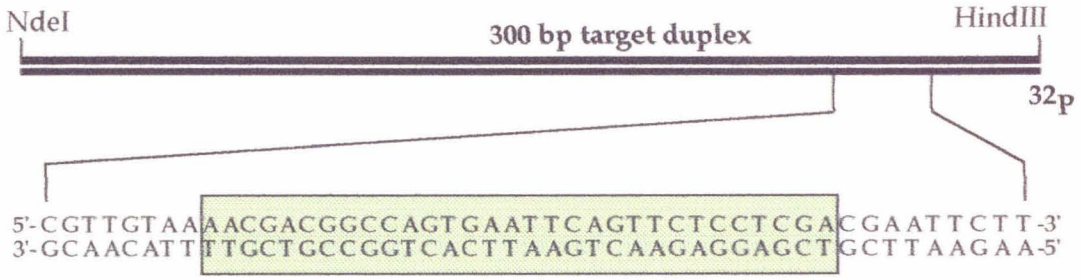

1 3'-TTGCTGCCGGTCACTTAAGTCAAGAGGAGCT*-5'

2 3'-T*TGCTGCCGGTCACTTAAGTCAAGAGGAGCT-5'

3 3'-T*AAAACGACGGCCAGTGAATTCAGTTCTTCT-5'

4 3'-T*TGCTGCCGGTCACTTAAGTCAAGAGGAGCTGCTTAAGAA-5'

5 3'-T*GCTGCAACATTTTGCTGCCGGTCACTTAAGTCAAGAGGAGCTGCTTAAGAA-5'

6 3'-T*TGCTGCCGGTCACTTAAGTCAAG-5'

7 3'-T*TGCTGCCGGTCACTTAAGTC-5'

8 3'-T*TGCTGCCGGTCACTTAA-5'

9 3'-T*TGCTGCCGGTCACT-5'

10 3'-TAAGTCAAGAGGAGCT*-5'

Figure 2.4: Duplex target on pUCJW with sequences of oligonucleotides used for studies in Chapter Two.

The cleavage patterns generated by oligonucleotides **1-3** on both 3'- and 5'-labeled target duplex are shown in Figure 2.5 A and histograms corresponding to each reaction are presented in Figure 2.5 B. The cleavage patterns obtained from oligonucleotides **1** and **2** are essentially the same as observed by Singleton (12). From examination of the cleavage pattern obtained from **3** it is clear that cleavage is visible only on the complementary strand for oligonucleotides homologous to either strand of the target duplex and the effect seen is therefore independent of the labeling efficiency obtainable for either protocol.

Figure 2.5. **(A)** Storage phosphor autoradiogram of an 8% denaturing polyacrylamide gel containing the products of affinity cleavage reactions. Lanes 1-4 contain cleavage products from DNA labeled on the 3′-end at the HindIII site and lanes 5-8 contain products from DNA labeled on the 3′-end at the Hind III site. Lanes 1 and 5 contain the products of adenine-specific reaction (16) on 3'-end labeled duplex and 5'-end-labeled duplex respectively. Reaction components for all lanes were as indicated in the figure under conditions described in the Experimental section.

(B) Histogram representation of the observed cleavage pattern. The lengths of the arrows represent the relative cleavage intensity at each nucleotide position.

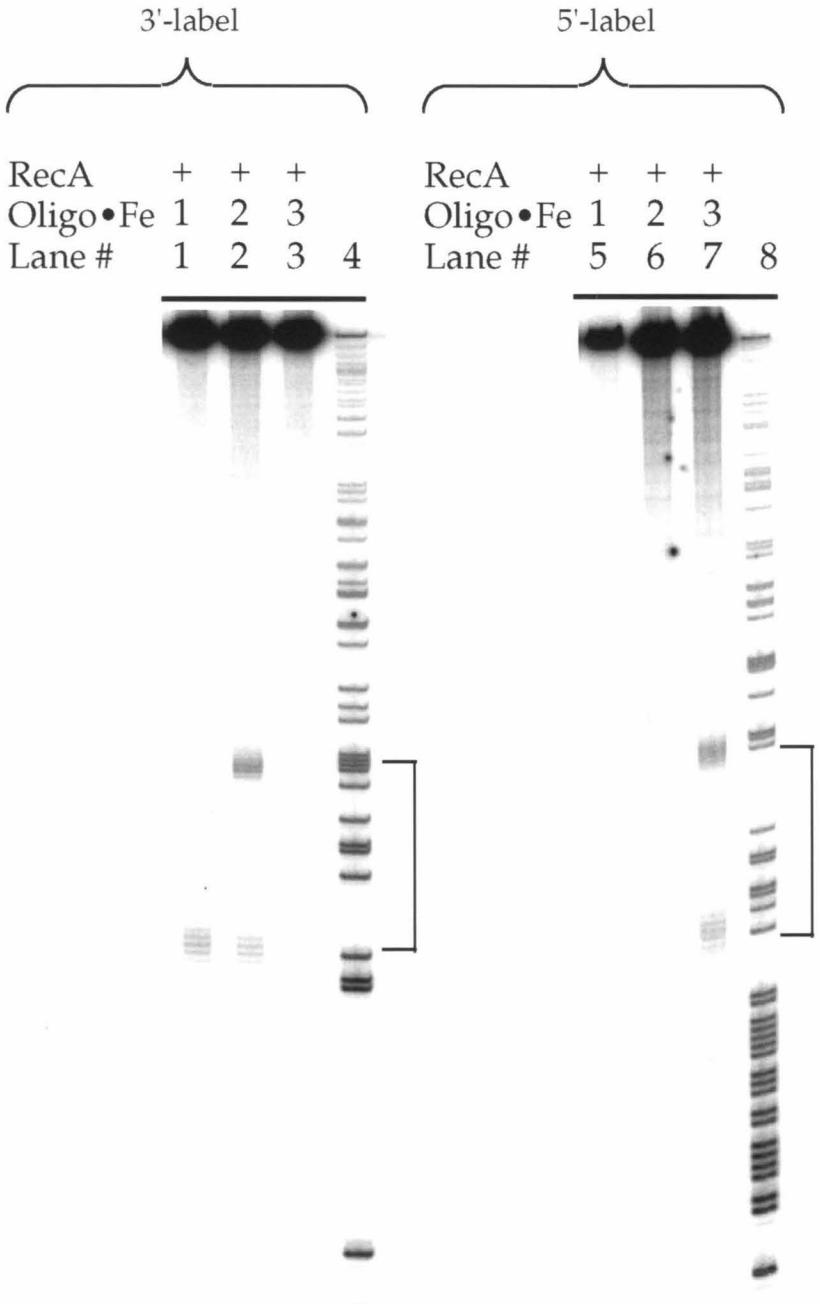
3'-label
5'-label
RecA + + + RecA + + +
Oligo•Fe 1 2 3 Oligo•Fe 1 2 3
Lane # 1 2 3 4 Lane # 5 6 7 8

A.


3'-T T GCT GCCGGTCACTTAAGTCAAGAGGAGCT*-5'
5'- C G T T G T A A A A C G A C G G C C A G T G A A T T C A G T T C T C C T C G A C G A A T T C T T -3'
3'- G C A A C A T T T T G C T G C C G G T C A C T T A A G T C A A G A G G A G C T G C T T A A G A A -5'

B.

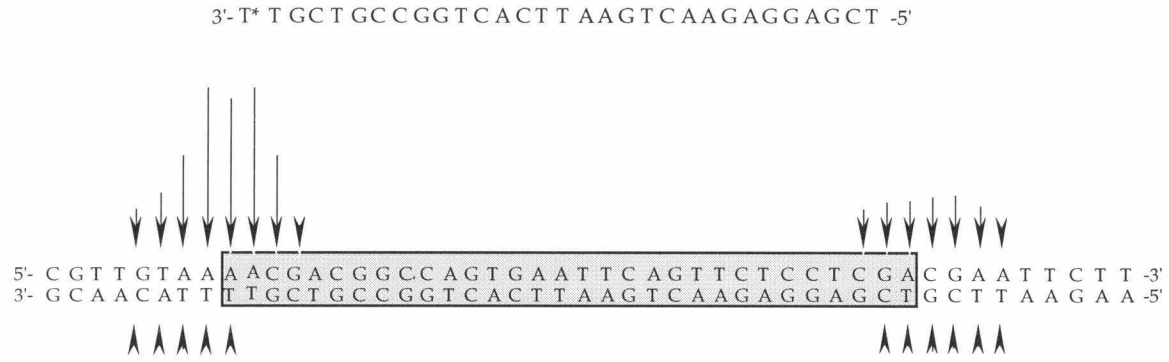
3'-T* T GCT GCCGGTCACTTAAGTCAAGAGGAGCT -5'
5'- C G T T G T A A A A C G A C G G C C A G T G A A T T C A G T T C T C C T C G A C G A A T T C T T -3'
3'- G C A A C A T T T T G C T G C C G G T C A C T T A A G T C A A G A G G A G C T G C T T A A G A A -5'

C.


5'-T* A A A A C G A C G G C C A G T G A A T T C A G T T C T C C T -3'
5'- C G T T G T A A A A C G A C G G C C A G T G A A T T C A G T T C T C C T C G A C G -3'
3'- G C A A C A T T T T G C T G C C G G T C A C T T A A G T C A A G A G G A G C T G C -5'

Effect of nucleotide to RecA monomer ratio

For three-strand reactions involving short oligonucleotides and linearized duplex substrates, the efficiency of complex is known to be dependent on the ratio of nucleotide units or base pairs to RecA monomers (12). To observe the effect of changing the nucleotide to RecA monomer ratio on the efficiency of cleavage, oligonucleotide **1** at 2 μM was incubated with varying concentration of RecA keeping all other solution conditions the same. It is clear from the results shown in Figure 2.7 that the optimal ratio of Nt/RecA monomer is between 2:1 and 3:1. At higher ratios, although the intensity of the major cleavage pattern is enhanced, non-specific cleavage at the opposite end of the bound filament increases considerably.

Figure 2.6. Storage phosphor autoradiogram of an 8% denaturing polyacrylamide gel containing the products of affinity cleavage reactions. All lanes contain cleavage products from DNA labeled on the 3'-end at the Hind III site. Reaction components and Nucleotide:RecA monomer ratios for all lanes were as indicated in the figure under conditions described in the Experimental section. Note that appropriate amount of RecA storage buffer to give the same final concentration of glycerol in each reaction. Lane 1 contains the products of adenine-specific reaction (16).

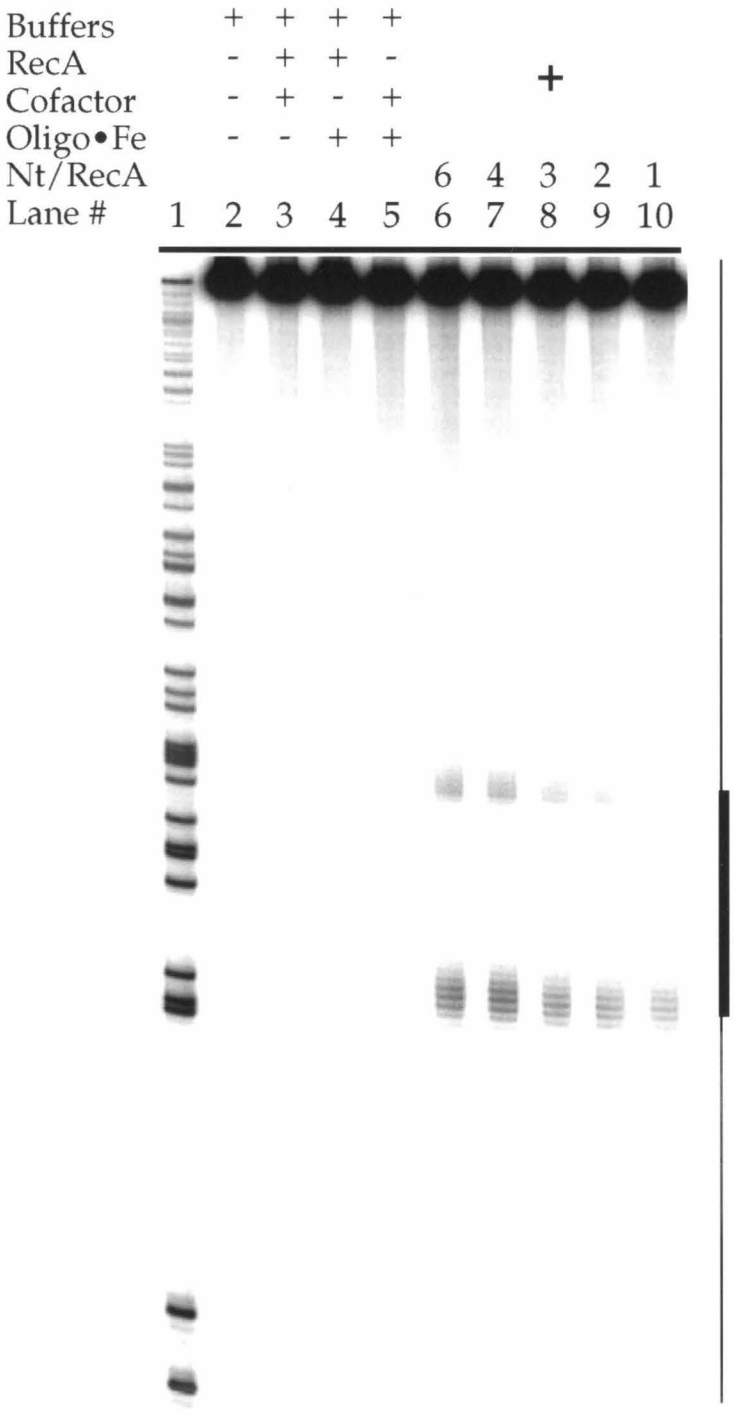
Buffers + + + +
RecA - + + -
Cofactor - + - +
Oligo•Fe - - + +
Nt/RecA 6 4 3 2 1
Lane # 1 2 3 4 5 6 7 8 9 10

Effect of length of oligonucleotides used for filament formation

The initial choice of length for the oligonucleotide–31 bases– was based on the observation by Camerini-Otero and coworkers that RecA nucleoprotein filaments formed with oligonucleotides 26 bases and longer could form three-stranded complexes at homologous sites on supercoiled duplex DNA which were stable after deproteinization (12). To determine the effect of length of the oligonucleotide on the efficiency of affinity cleavage observed, oligonucleotides **4** through **10** varying in length from 50 to 15 nucleotides were synthesized each carrying a single T* residue at its 3'-end (Figure 2.4). Affinity cleavage reactions were performed keeping the filament concentration at 2 μM in each case. The results from this study are shown in Figure 2.7. It is clear that increasing the length of the

---

Figure 2.7. Storage phosphor autoradiogram of an 8% denaturing polyacrylamide gel containing the products of affinity cleavage reactions. All lanes contain cleavage products from DNA labeled on the 3′-end at the Hind III site. Reaction components and Nucleotide:RecA monomer ratios for all lanes were as indicated in the figure, under conditions described in the Experimental section. Note that appropriate amount of RecA storage buffer to give the same final concentration of glycerol in each reaction. Lane 1 contains the products of adenine-specific reaction (16).

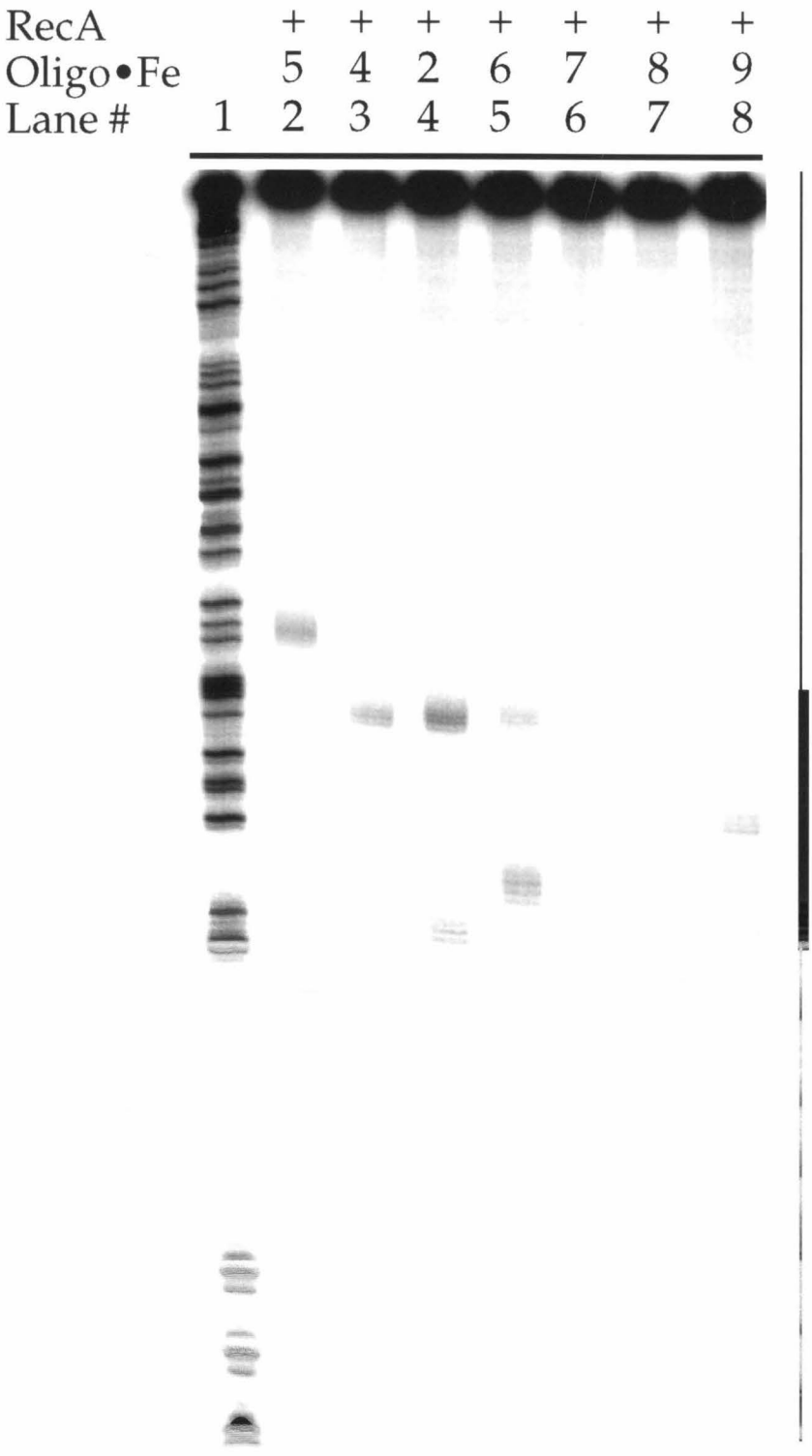
RecA + + + + + + +
Oligo•Fe 5 4 2 6 7 8 9
Lane # 1 2 3 4 5 6 7 8

oligonucleotide beyond 30 causes little increase in cleavage efficiency. A sharp decrease in cleavage efficiency is observed when the length of the oligonucleotide is decreased beyond 24 nucleotides. However, oligonucleotide **10** which is only 15 nucleotides in length is found to bind at least as efficiently as the 24 mer oligonucleotide **6** indicating that the stability of three-stranded joints might not be sequence neutral as is widely believed.

Effect of concentration of nucleoprotein filaments

The technique of quantitative affinity cleavage titration for measuring the binding affinities of triple helix forming oligonucleotides at their homopurine target sites has been described in detail (18). Since the number of equilibria involved in the association of nucleoprotein filaments to their homologous sites on duplex DNA are far more complex than the two state system approximated by binding of oligonucleotides to duplex target in the absence of any protein, the analysis here is limited to a semi-quantitative determination of the filament concentration required for obtaining maximal cleavage.

Nucleoprotein filaments were formed by incubating oligonucleotide **1** with RecA and cofactor. Appropriate volumes were dispensed from a stock solution of preincubated filament into separate reactions to obtain the filament concentrations shown the figure 2.8, followed by addition of the duplex target. From this relatively coarse analysis, it is apparent that for the 31 base long oligonucleotide **1**, a filament concentration of approximately 0.4 μM is sufficient for complete saturation of the duplex target under the conditions

of the experiment (Described in Experimental). The diminution of cleavage seen at high filament concentration is likely a result of inhibition of the cleavage reaction by excess protein and glycerol.

Effect of solution conditions

The reaction conditions used in these studies have many components that are deleterious to the affinity cleavage reaction. For example, Tullius and co-workers have reported that concentrations of glycerol (a radical scavenger) above 0.5%, and to a lesser extent, buffers containing Tris at concentrations above 10 mM, significantly reduce the amount of achievable cleavage (19). Since these components are unavoidable in the three-strand reaction, a possible solution to this problem is the use of stronger reducing agents or longer reaction times. The use of sodium ascorbate as a reducing agent instead of DTT has been shown to give significantly higher yields in affinity cleavage reactions (20). Shown in figure 2.9 are time-courses of the affinity cleavage reaction using either DTT or ascorbate as a reducing agents. Using ascorbate, maximal cleavage can be achieved in as little as 1 hr. whereas cleavage by DTT does not reach its maximal level till much later (~8 hrs.).

Figure 2.8. Storage phosphor autoradiogram of an 8% denaturing polyacrylamide gels containing the products of affinity cleavage reactions with nucleoprotein filaments at the indicated concentrations. Lane 1 contains the products of adenine-specific reaction (16) on 3'-end labeled duplex.

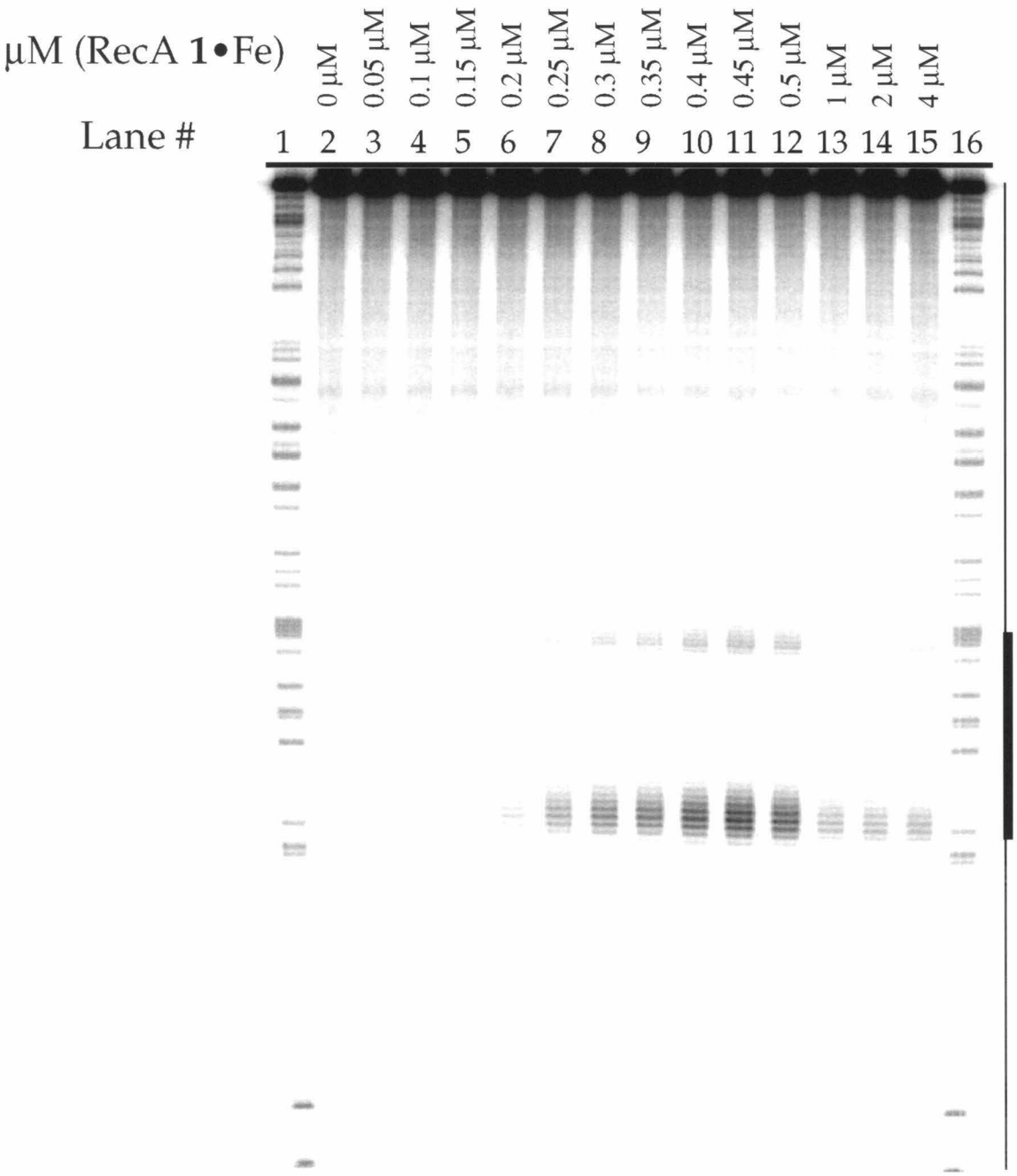
μM (RecA 1•Fe)
0 μM
0.05 μM
0.1 μM
0.15 μM
0.2 μM
0.25 μM
0.3 μM
0.35 μM
0.4 μM
0.45 μM
0.5 μM
1 μM
2 μM
4 μM
Lane #
1 2 3 4 5 6 7 8 9 10 11 12 13 14 15 16

Figure 2.9. Storage phosphor autoradiogram of 8% denaturing polyacrylamide gels containing the products of affinity cleavage reactions carried out for the indicated times using either DTT or sodium ascorbate as reducing agent at a final concentration of 1 mM. Sequencing lanes contain the products of adenine-specific reaction (16) on 3'-end labeled duplex.

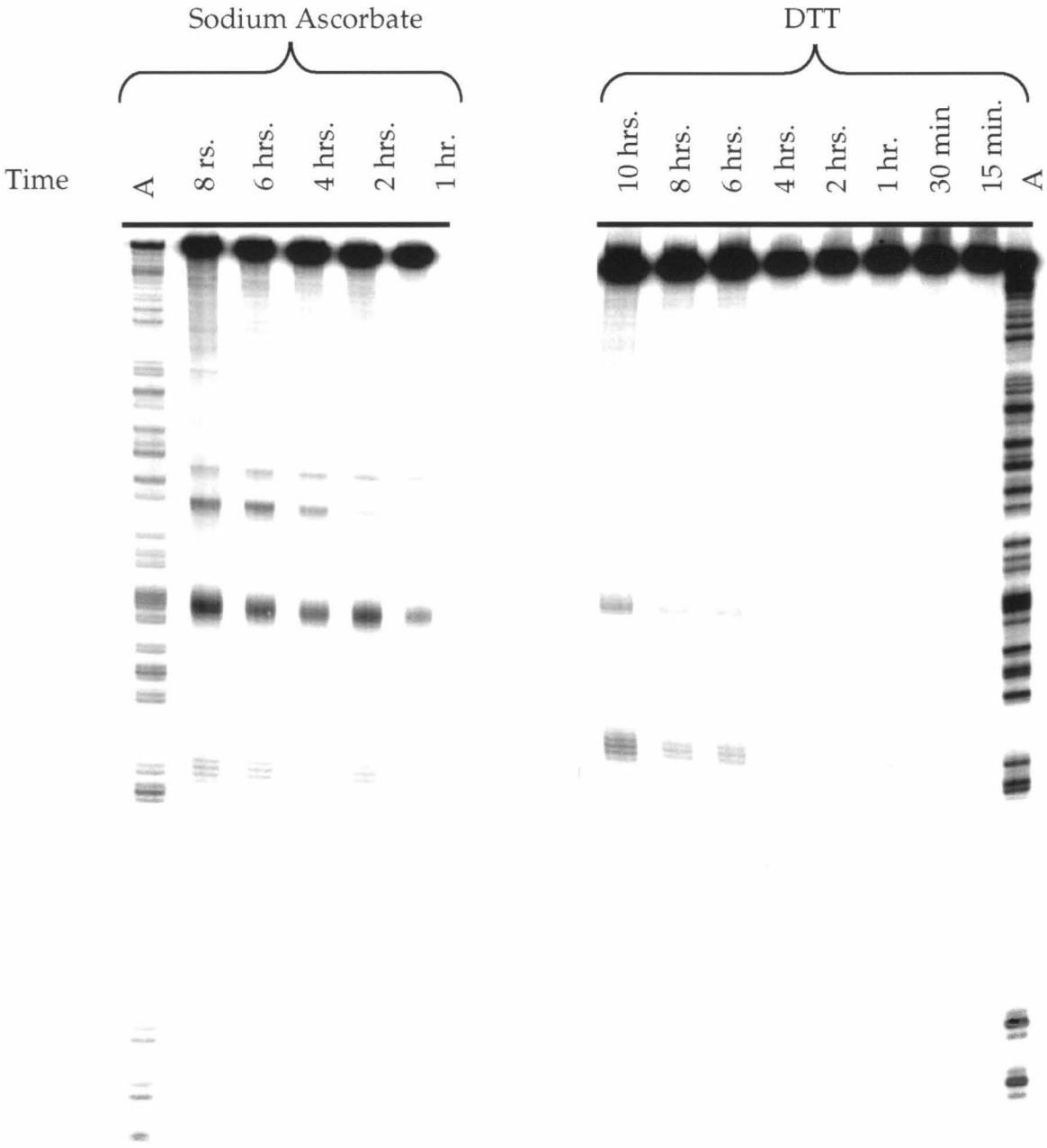
Sodium Ascorbate
DTT
Time
A
8 rs.
6 hrs.
4 hrs.
2 hrs.
1 hr.
10 hrs.
8 hrs.
6 hrs.
4 hrs.
2 hrs.
1 hr.
30 min
15 min.
A

Site occupancy of filaments

Double strand cleavage yields by pyrimidine oligonucleotides carrying T* have been reported to be as high as 25% (21). The maximum single strand cleavage efficiency observed in this system is approximately 15%. To determine the site occupancy of oligonucleotides used in this study, the plasmid pRBNN was constructed in which the 31 mer target site with mixed flanking sequences was inserted into the large NdeI/NarI fragment of pUC 18. The resulting construct has two EcoRI sites ~225 base pairs apart, only one of which is overlapped by the target site of the filament (Figure 2.10 A). Upon incubation with nucleoprotein filaments formed using oligonucleotide **1** this results in protection of the overlapped site from EcoRI cleavage. If pRBNN linearized with Eco0109I is used as a substrate in the three-strand reaction, followed by cleavage with EcoRI, comparison of intensities of the 470 bp partial digest product with the 224 base fragment from complete digestion reveals the site occupancy. Reactions conducted in the absence of oligonucleotide indicate that under the conditions of the experiment, non-specific binding of RecA to the target duplex occurs at a significant level. However in the presence of a random 31 base oligonucleotide **11**, non-specific binding of RecA to the target duplex is reduced to a low level persisting even after extended incubation with EcoRI (Figure 2.10 B). Results from the restriction enzyme cleavage inhibition assay are shown in figure 2.11.

Figure 2.10: A. Schematic diagram of the construct used to determine site-occupancy. The plasmid pRBNN contains the standard 31 base target site and its flanking sequences inserted into the NdeI/NarI large fragment of pUC18. The locations of the sites for EcoO109I used for linearization, and the control EcoRI site are also shown.

B. Storage phosphor autoradiogram of 5% non-denaturing polyacrylamide gel containing the products from control restriction enzyme inhibition experiments carried out using RecA alone or RecA in presence of the random oligonucleotide **11**. The size-markers are 100 bp ladders starting at 100 bp.

A

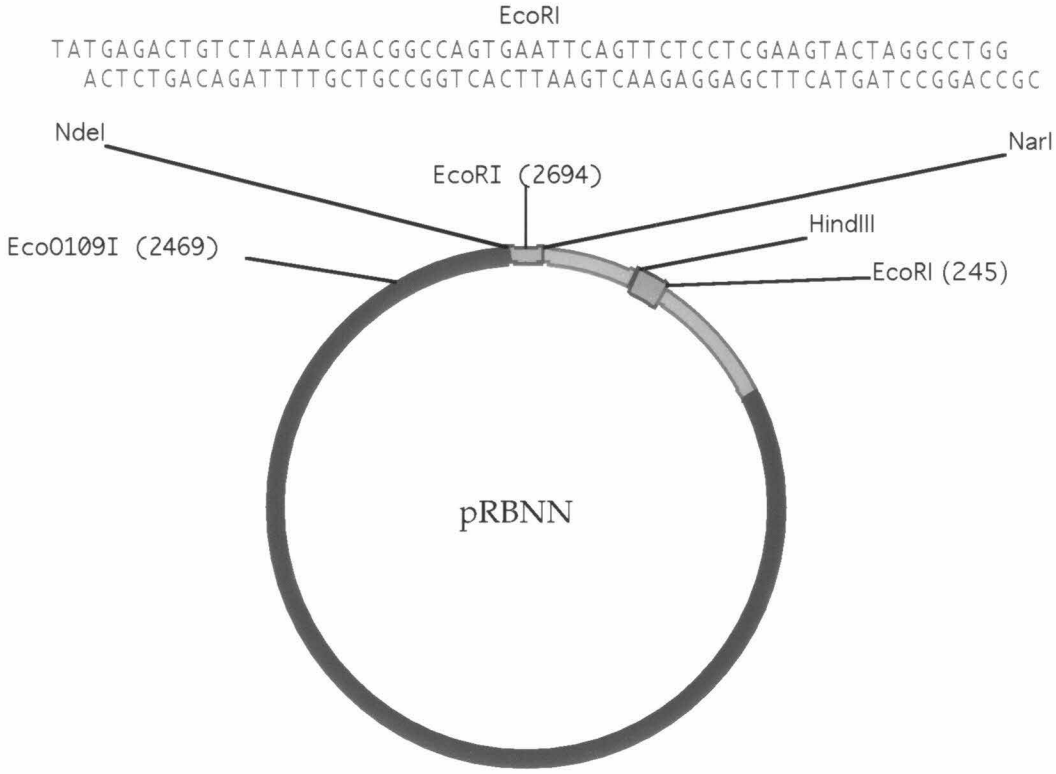

B

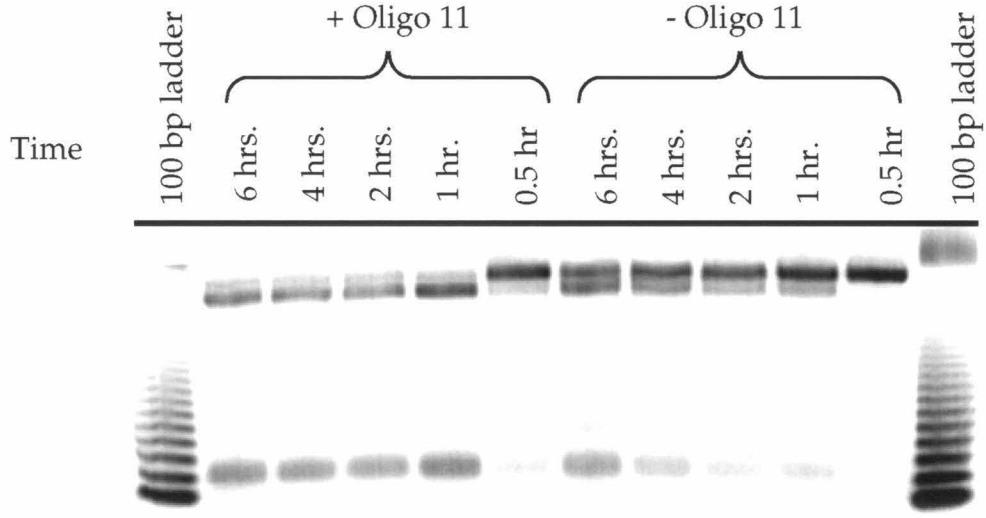

11 3'-T GAACAGT AGTT CGAAAAT CT ATT AT CGAAT -5'

Figure 2.11: Storage phosphor autoradiogram of 5% non-denaturing polyacrylamide gel containing the products from restriction enzyme inhibition experiments carried out using RecA in presence of the indicated oligonucleotides. The size-markers are 100 bp ladders starting at 100 bp. The % protection based on comparison of the intensities of the 225 and 400 bp fragments were: 48% Lane 5, 31% Lane 6, 52% Lane 7, 29% Lane 8, 23% Lane 9, 21% Lane 10.

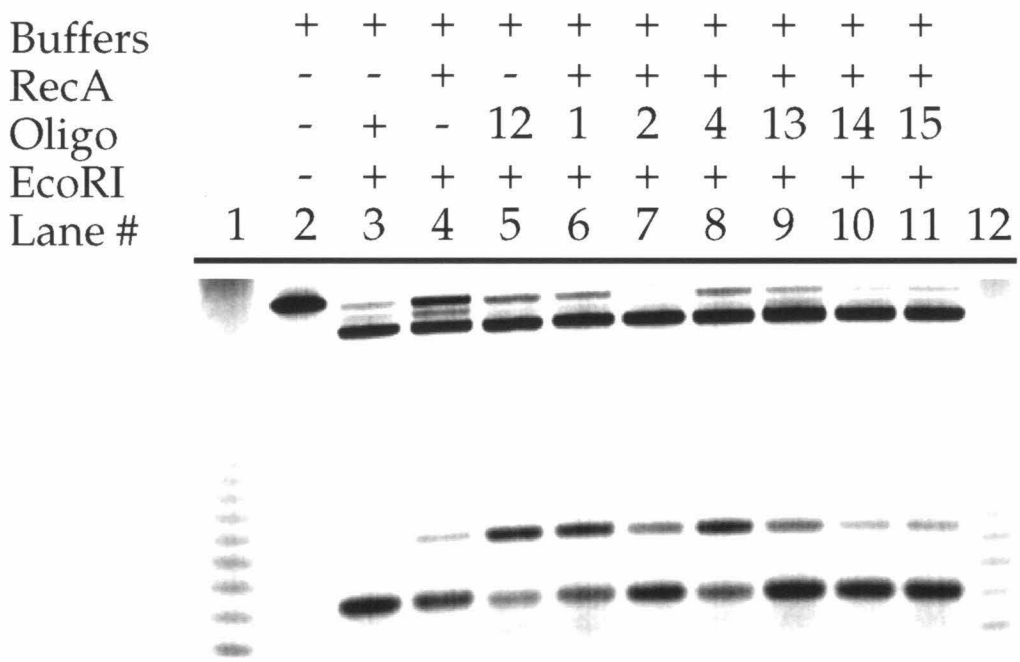

4 3'-T T G C T G C C G G T C A C T T*A A G T C A A G A G G A G C T -5'

12 3'-T T G C T G C C G G T C A C T T A A G T C A A G A G G A G C T -5'

13 3'-T*T G C T G C C G G T C A C T T A A G T C A A G A G G A G C T*-5'

14 3'-T*T G C T G C C G G T C A C T T*A A G T C A A G A G G A G C T*-5'

15 3'-T*T G C T G C C G G T*C A C T T A A G T*C A A G A G G A G C T*-5'

Double strand cleavage using nucleoprotein filaments

Since one of the goals for directing chemical cleavage to arbitrary sites on duplex DNA is to obtain efficient double-strand cleavage in order to physically isolate segments of DNA of interest, each of the oligonucleotides used in the earlier studies was incubated under the standard conditions for affinity cleavage with EcoO109I linearized pRBNN. The products from affinity cleavage reactions were resolved on a 5% non-denaturing polyacrylamide gel. The expected 225 bp cleavage product was not present at a detectable level for any of the oligonucleotides used. It is clear from the data obtained for site occupancy that the oligonucleotides are binding their target sites. Therefore the non-detectable level of double-strand cleavage are likely due to inefficiency of the cleavage reaction under the conditions of our experiments. The use of more efficient chemistry compatible with the binding of RecA will be needed to achieve higher cleavage efficiencies.

Effect of RecA on the autocleavage of T oligonucleotides*

To observe the effect of binding of RecA on the autocleavage of an oligonucleotide carrying T* at an internal position, a 60 base long oligonucleotide with T* incorporated at a central position (**16**) was ^{32}P labeled at its 5'-end. Cleavage reactions carried out for the indicated times both in the presence and absence of RecA showed comparable amounts of cleavage, indicating that the binding of RecA does not inhibit the auto-cleavage reaction (Figure 2.12). The maximum amount of auto-cleavage observed is only ~20% indicating an upper bound to the amount of cleavage that can be

Figure 2.12: Storage phosphor autoradiogram of 15% denaturing polyacrylamide gel containing the products from autocleavage reactions carried out using RecA in presence of 5'-end labeled 60 mer oligonucleotide **16** 3'-ACTCTGACAGATTTTGCTGCCGGTCACT**T***AAGTCAAGAGGAG CTTCATGATCCGGACCGC-5'. Autocleavage reactions were carried out under standard conditions for the indicated times. Non-specific protein (BSA) and recA storage buffer were added to reactions without RecA to maintain all other components of the reactions at the same concentration. Lanes marked A* and A are products of adenine specific reaction (16) carried out on **16** or an oligonucleotide of the same sequence but lacking the T*, respectively.

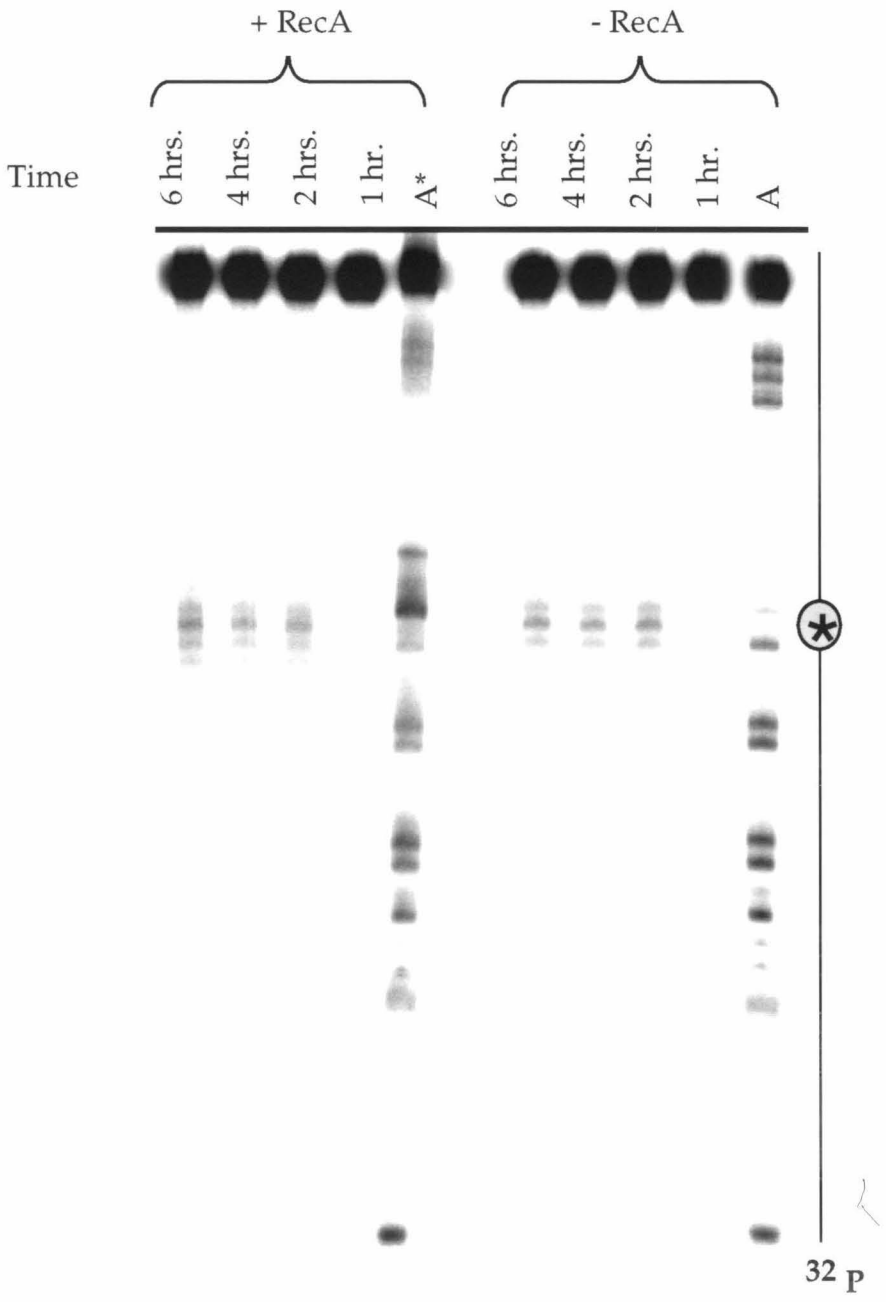
+ RecA
- RecA
Time
6 hrs.
4 hrs.
2 hrs.
1 hr.
A*
6 hrs.
4 hrs.
2 hrs.
1 hr.
A
32 P

Figure 2.13: Storage phosphor autoradiogram of 15% denaturing polyacrylamide gel containing the products from cleavage reactions carried out using RecA in presence of 5'-end labeled 75 mer oligonucleotide **17** 3'-ACTCTGACAGATTTTGCTGCCGGTCACTTAAGTCAAGA GGAGCTTCATGATCCGGACCGC$(T)_{15}$-5' hybridized to a complementary 40 mer **18** 5'-TATGAGACTGTCTAAAACGACGGCCAGTGAA**T***TCAGTTCT-3'. Cleavage reactions were carried out under standard conditions for the indicated times. Non-specific protein (BSA) and RecA storage buffer were added to reactions without RecA to maintain all other components of the reactions at the same concentration. Lanes marked A are products of adenine specific reaction (16) carried out on **17** .

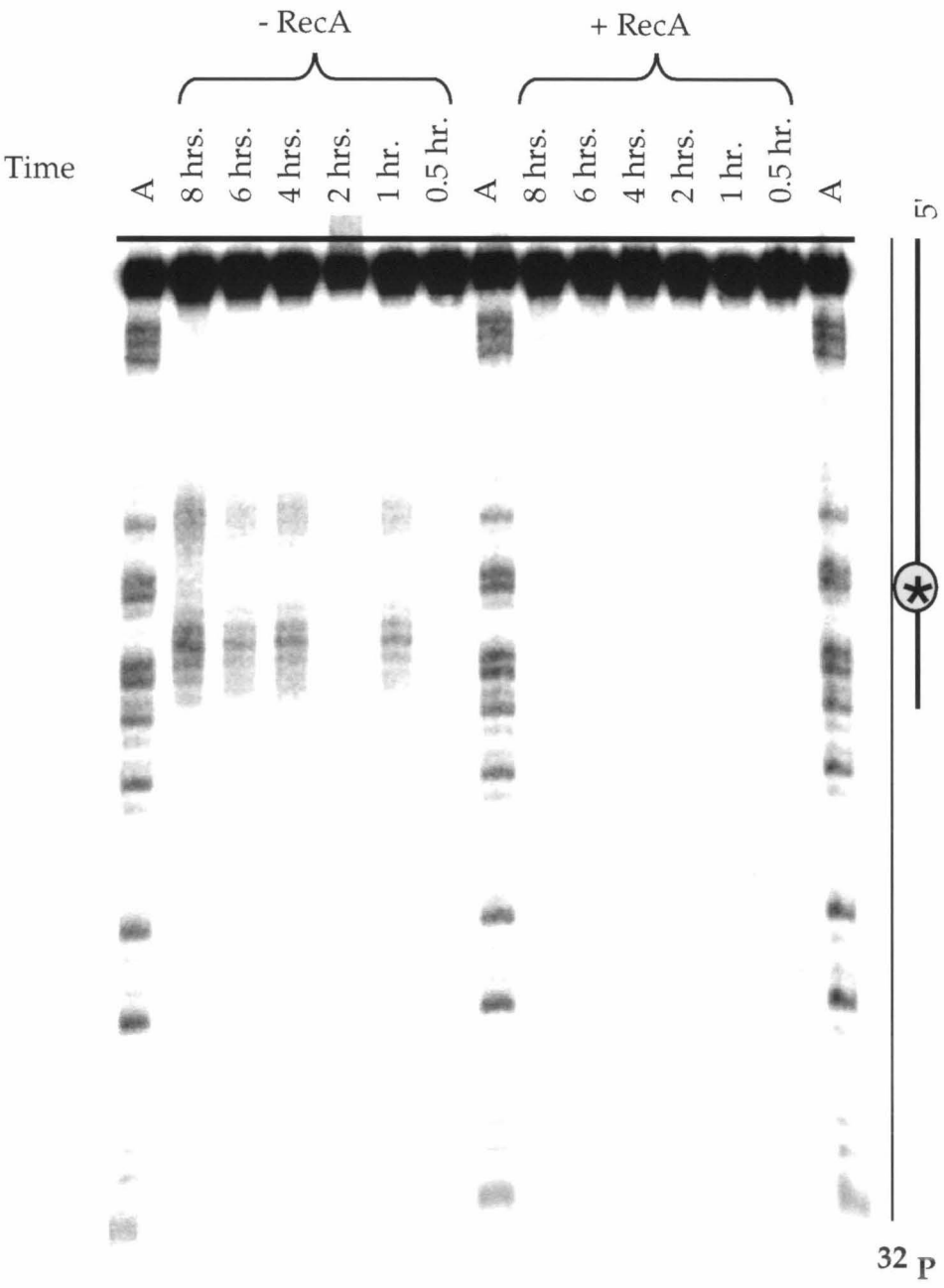
- RecA
+ RecA
Time
A
8 hrs.
6 hrs.
4 hrs.
2 hrs.
1 hr.
0.5 hr.
A
8 hrs.
6 hrs.
4 hrs.
2 hrs.
1 hr.
0.5 hr.
A
5'
32 P

achieved by T* oligonucleotides under the buffer conditions used in the experiment.

Effect of RecA on the cleavage of complementary strands by T oligonucleotides*

The binding of RecA to duplexes suffers from a kinetic barrier that can be overcome by appending a single stranded tail to the duplex (22). To observe the effect of binding of RecA on the cleavage of a duplex with an iron atom located in the major groove, a 75 base long oligonucleotide (**17**) was labeled at its 5'-end, hybridized with a 40 base long complementary oligonucleotide carrying a T* at an internal position (**18**). Cleavage reactions carried out for the indicated times, both in the presence and absence of RecA show that binding of RecA completely inhibits the cleavage of the complementary strand (Figure 2.13). It has been proposed that the reactivity of duplex DNA to hydroxyl radicals is greater in the minor groove compared to the major groove (23). RecA protein is known to bind in the minor groove of duplex DNA (24). This result is therefore indicative of quantitative inhibition of hydroxyl radical mediated cleavage in the minor groove due to binding of RecA.

Conclusions

A number of parameters have been optimized to increase the cleavage yields obtainable from RecA. The minimum length of an oligonucleotide for efficient cleavage is less than 24 nucleotides. The lower limit of oligonucleotide length for observable cleavage appears to be sequence

dependent. Under the conditions of the experiment, in the three-strand reaction, between 20-40% of available sites are occupied. A small amount of non-specific binding of RecA to the target duplex is also observed. The binding of RecA to single-stranded oligonucleotides carrying an appended T* does not affect the autocleavage reaction. However, the binding of RecA to tailed duplexes carrying the chelated metal atom in the major groove quantitatively inhibits cleavage, presumably due to inaccessibility of the more reactive minor groove to hydroxyl radicals. In summary, the experiments described in this chapter have helped us to better understand the use of RecA• oligonucleotide-EDTA filaments to direct affinity cleavage at arbitrary sites on duplex DNA.

EXPERIMENTAL

General. Sonicated, deproteinized calf thymus DNA (Pharmacia) was dissolved in H_2O to a final concentration of 2.0 mM in base pairs and was stored at 4 °C. Glycogen was obtained from Boehringer-Mannheim as a 20 mg/ml aqueous solution. γ-S-ATP purchased from Sigma, was found to contain <10% ADP by HPLC analysis and stored in 100 mM aliquots -20 °C. Nucleoside triphosphates labeled with ^{32}P were obtained from Amersham or ICN and were used as supplied. Cerenkov radioactivity was measured with a Beckman LS 2801 scintillation counter. Restriction endonucleases were purchased from Boehringer Mannheim or New England Biolabs and were used according to the supplier's recommended protocol in the activity buffer provided. Klenow fragment and T4 polynucleotide kinase were obtained from Boehringer Mannheim. Phosphoramidites were purchased from Glen Research.

Construction of pUCRBNN. This plasmid was prepared by standard methods (15) by annealing two synthetic oligonucleotides, 5'- TATGAGAC TGTCTAAAACGACGGCCAGTGAATTCAGTTCTCCTCGAAGTACTAGGCC TGG-3' and 3'- ACTCTGACAGATTTTGCTGCCGGTCACTTAAGTCAA GAGGAGCTTCATGATCCGGACCGC-5' followed by ligation of the resulting duplex with pUC18 DNA previously digested with NdeI and NarI; this ligation mixture was used to transform *E. Coli* XL1-Blue competent cells (Stratagene). Plasmid DNA from transformants was isolated, and the

presence of the desired insert was confirmed by restriction analysis and Sanger sequencing. Preparative isolation of plasmid DNA was performed using a Qiagen plasmid kit.

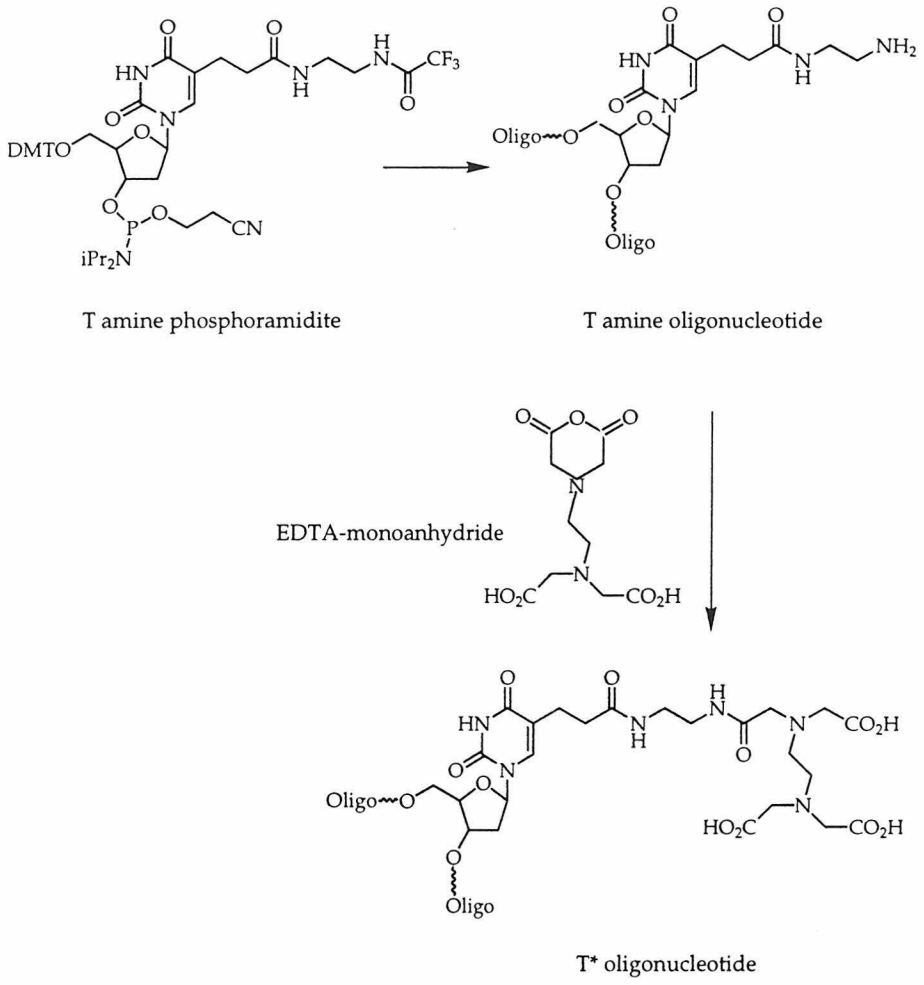

Figure 2.14: Incorporation of T* precursor amine into oligonucleotides and postsynthetic modification with EDTA monoanhydride to generate T* containing oligonucleotides.

Synthesis and Purification of Oligodeoxyribonucleotides.

Incorporation of T into oligonucleotides*

Incorporation of thymidine EDTA into oligonucleotides using the β-cyanoethyl phosphoramidite of the triethyl ester of Thymidine EDTA has previously been described (5). For incorporation of T* at the 5' terminus or at

internal sites in this study, a modified procedure wherein T* is incorporated using β-cyanoethyl phosphoramidite of the trifluoroacetyl protected amine precursor(Figure 2., followed by post-synthetic modification with EDTA-mono-anhydride (15). For incorporation of T* at the 3' end T*-CPG was used as described in the literature (16).

Oligodeoxyribonucleotides were synthesized using standard automated solid-support chemistry on an Applied Biosystems Model 380B DNA synthesizer and *O*-cyanoethyl-*N*,*N*-diisopropyl phosphoramidites. Crude oligonucleotide products containing the 5'-terminal dimethoxytrityl protecting group were purified by reverse phase FPLC using a ProRPC 16/10 (C_2-C_8) column (Pharmacia LKB) and a gradient of 0-40% CH_3CN in 0.1 M triethylammonium acetate, pH 7.0, detritylated in 80% aqueous acetic acid, and chromatographed a second time.

Modified thymidine was incorporated at the 5' termini of oligonucleotides (Figure 2.3) using the β-cyanoethyl-*N*,*N*-diisopropylchloro - phosphoramidite of a thymidine derivative containing an appropriately protected linker-amine (Amino modifier C2-dT, Glen Research). Deprotection was carried out in concentrated NH_4OH at 55 °C for 24 h. Following trityl-on FPLC purification, dry oligonucleotide containing a free amine attached to C5 of the 5'-thymidine was detritylated in 80% acetic acid for 20 minutes at room temperature. Following thorough lyophilization, the oligo-amine was post-synthetically modified with EDTA monoanhydride as described (17) to give the T* oligonucleotide **1**. The modified oligonucleotide was

chromatographed a second time by FPLC using a gradient of 0-40 % CH_3CN in 0.1 M NH_4OAc.

Purified oligonucleotides were desalted on Pharmacia NAP-5 Sephadex columns. The concentrations of single-stranded oligonucleotides were determined by UV absorbance at 260 nm using extinction coefficients calculated by addition of the monomer nucleoside values (values for T were used in place of T* in the calculation). Oligonucleotide solutions were lyophilized to dryness for storage at -20 °C. Presence of T* and/or T-amine was confirmed by degradation of 10 n mole aliquots with snake venom phosphodiesterase and calf intestinal phosphatase followed by HPLC analysis on a Microsorb MV reverse phase column.

DNA Manipulations. The 300 bp HindIII/NdeI restriction fragment of the plasmid pUCJWII47 (12) was isolated and labeled at the 5′- or 3′-end on the HindIII side by standard procedures (15). Adenine-specific sequencing reactions were carried out as previously described (16).

Affinity Cleavage Reactions. A dried aliquot of oligonucleotide-EDTA was dissolved in enough MilliQ water to give a concentration of 40 μM. This concentration was verified by checking the UV absorbance before addition of iron. An equal volume of a 40μM solution of aqueous $Fe(NH_4)_2(SO_4)_2 \bullet 6H_2O$ was added to produce a solution that was 20 μM in oligonucleotide and Fe(II). This solution was allowed to equilibrate for at least 15 min. at room temperature. A stock solution was prepared containing 75 μl 10x buffer (250

mM Tris-acetate, 40 mM Mg-acetate, 1 mM EGTA, 5 mM spermidine, 8 mM β-mercaptoethanol, pH 7.5), 37.5 μl of 2 mM bp calf thymus DNA (added to supress background oxidative cleavage of target DNA), and 25 μl acetylated BSA (3 mg/ml). To a given reaction was added 5.5 μl stock solution, 3 μl of either the oligonucleotide-EDTA•Fe(II) at 20 μM or H_2O (for control reactions, 3 μl of RecA solution (7.4 mg RecA/ml in RecA storage buffer) plus RecA storage buffer (20 mM Tris-HCl, 0.1 mM EDTA, 1 mM DTT, 50% glycerol, pH 7.5) to give the designated nucleotide to monomer ratio (excess RecA storage buffer was added to ensure that each reaction was run under the same conditions), and enough H_2O to give a final reaction volume of 30 ml after ascorbate addition. Following a 1 min incubation at 37 °C, nucleoprotein filament formation was initiated by addition of 1 μl 30 mM γ-S-ATP. After 10 min, approximately 20,000 cpm (~ 1 nM) of 3'- or 5'-labeled duplex was added and joint molecule formation was allowed to proceed for 30 min at 37 °C. The cleavage reactions were initiated by the addition of 1 μl 30 mM sodium ascorbate. The final reaction conditions were 25 mM Tris-acetate, 6 mM Tris-HCl, 4 mM $Mg(OAc)_2$, 1 mM EGTA, 32 μM EDTA, 0.5 mM spermidine, 0.8 mM β-mercaptoethanol, 5% glycerol, 100 mM bp calf thymus DNA approximately 1 mM sodium ascorbate, pH 7.5. After 8 h, the cleavage reactions were stopped by phenol/chloroform extraction and precipitation of the DNA by the addition of glycogen, NaOAc (pH 5.2), and $MgCl_2$ to final

concentrations of 140 μg/ml, 0.3 M, and 10 mM, respectively, and 100 μl ethanol. The DNA was isolated by centrifugation and removal of the supernatant. The precipitate was dissolved in 20 μl H_2O, frozen, and lyophilized to dryness. The DNA solutions were assayed for Cerenkov radioactivity by scintillation counting and was resuspended in enough formamide-TBE loading buffer containing 0.1% SDS. to give 5000 cpm/μl. The DNA was denatured at 90 °C for 5 min, and loaded onto an 8% denaturing polyacrylamide gel. Residual radioactivity was counted to determine the amount loaded in each lane. The DNA cleavage products were electrophoresed in 1x TBE buffer at 50 V/cm. The gel was dried on a slab dryer and then exposed to a storage phosphor screen. The gel was visualized with a Molecular Dynamics 400S PhosphorImager. Cleavage intensities at each nucleotide position were measured using the ImageQuant™ software and the pixel values obtained were plotted in the form of histograms using Kaleidagraph™ software.

Restriction enzyme inhibition studies

Reaction conditions were identical to those described above except pRBNN linearized with EcoO109I and 3'-end labeled with α-^{32}P dCTP was used as the substrate. Folowing the formation of synaptic complexes, 20 units of EcoRI were added and digestion was carried out for 1hr. or the indicated time. Reactions were terminated by phenol/chloroform extraction and ethanol precipitation. Products were resolved by electrophoresis on a 1%

agarose gel in TAE buffer at 120V for 1 hr. The gel was blotted on to a nylon membrane (Nytrans, Schleicher and Schuell) and visualized with a Molecular Dynamics 400S PhosphorImager.

References

1. Collectively reviewed in Methods in Enzymology (1993) **208**, Robert T. Sauer Ed.

2. Pogozelski, W.K., McNeese, T. J., Tullius, T.D. (1995) *J. Am. Chem. Soc.*, **117**, 6428-6433.

3. Hertzberg, R. P., Dervan P. B. (1982) *J.Am.Chem.Soc.* **104**, 313-315.

4. Schultz, P. G., Taylor,J. S., Dervan, P. B. (1982) *J.Am.Chem.Soc.* **104**, 6861-6863.

5. Dreyer, G. B., Dervan, P. B. (1985) *Proc. Natl. Acad. Sci. USA* **82**, 968-972.

6. Moser, H. E., Dervan, P. B. (1987) *Science* **238**, 645-650; Beal, P. A., Dervan, P. B. (1991) *Science* **251**, 1360-1363.

7. Strobel, S. A., Moser, H. E., Dervan, P. B. (1988) *J. Am. Chem. Soc.* **110** 7927-7929; Strobel, S. A., Dervan, P. B. (1990) *Science* **249**, 73-75; Strobel, S.A., Doucette-Stamm, L. A., Riba, L., Housman, D. E., Dervan,P.B. (1991) *Science* **254**, 1639-1642.

8. For recent reviews see: Kowalczykowski, S. C., Eggleston, A. K. (1994) *Annu. Rev. Biochem.* **63**, 991-1043; West, S. C. (1992) *Ann. Rev.Biochem.* **61**, 603-640.

9. Flory, J., Radding, C. M. (1982) *Cell* **28**, 747-756; Egelman, E. H. , Yu, X. (1989) *Science* **245,** 404-407.

10. Honigberg, S. M., Gonda, D. K., Flory, J., Radding, C. M. (1985) *J. Biol. Chem.* **260**, 11845-11851; Radding, C. M. (1991) *J. Biol. Chem.* **266**, 5355-5358.

11. Reddy, G., Jwang, B., Rao, B.J., Radding, C.M. (1994) Biochemistry **33**, 11486-11492.

12. Hsieh, P., Camerini-Otero, C. S., Camerini-Otero, R. D. (1992) *Proc. Natl. Acad. Sci. USA* **89**, 6492-6496.

13. Howard-Flanders, P., West, S. C. & A. Stasiak (1984) *Nature* **309**, 215-220; Umlauf, S. W., Cox, M. M., Inman, R. B. (1990) *J. Biol. Chem.* **265**, 16898-6912; Rao, B. J., Dutreix, M., Radding, C. M. (1991) *Proc. Natl. Acad. Sci. USA* **88**, 2984-2988; Takahashi, M., Kubista, M., Norden, B. (1991), *Biochimie* **73**, 219-226; Adzuma, K. (1992) *Genes Devel.* **6**, 1679-1694; Kim, M. G., Zhurkin, V. B., Jernigan, R. L., Camerini-Otero, R. D. (1995) *J.Mol.Biol.* **247**, 874-889.

14. Singleton, J.W. (1994) Master's Dissertation, California Institute of Technology.

15. Sambrook, J., Fritsch, E. F. & Maniatis, T. (1989) *Molecular Cloning, 2nd ed.* Cold Spring Harbor Laboratory Press, New York.

16. Iverson, B. L., Dervan, P. B. (1987) *Nucleic Acids Res.* **15**, 7823-7830.

17. Han, H., Dervan, P. B. (1994) *Nucleic Acids Res.***22,** 2837-2844.

18. Dixon, W., et al. (1991) *Meth. Enzymol.* **208**, 380-413.

19. Singleton, S.F., Dervan, P.B. (1992) *J. Am. Chem. Soc.*. **114**, 6957-6965; Singleton, S.F. (1995) Doctoral Dissertation, California Institute of Technology.

20. Hertzberg, R.P., Dervan, P.B. (1984) *J. Am. Chem. Soc.*. **23**, 3934-3945.

21. Strobel, S.A., Moser, H.E. , Dervan, P.B. (1988) *J. Am. Chem. Soc.*. **110**, 7927-7929.

22. Cassuto, E., Howard-Flanders, P. (1986) *Nuc. Acids Res.* **14**, 1149-1157.

23. Oakley, M.G., Dervan, P.B. (1990) *Science* **248**, 847-850.

24. Capua, E. D. & Muller, B. (1987) *EMBO J.* **6**, 2492-2498.

CHAPTER THREE

Cooperative Binding Of RecA•Oligonucleotide Filaments On Double-stranded DNA Detected By Affinity Cleavage

(The text for this chapter is taken in part from a manuscript in preparation for Nucleic Acids Research, co-authored with Prof. Peter B. Dervan)

Introduction

Cooperative binding in Nature

The binding affinities of transcription regulators (activators/repressors) typically fall in the range of low micromolar to sub-nanomolar. The binding affinity at the target site is a result of specific contacts with bases at the target site, local flexibility and also a number of *non-specific contacts* with the DNA backbone. This results in a low (often not measurable) affinity for non-specific sequences. For larger genomes, where larger amounts of non-specific competing sequences are present, this would mean that correspondingly higher specificities would be needed to find target sites of the same size. As pointed out by Kodadek(1), in the hypothetical case of a human cell containing one molecule of an activator that must bind a single site in the 10^9 bp human genome, this would mean that the ratio of K_d(non-specific)/ K_d(specific) would have to be 10^9 for the target site to be occupied 50% of the time. This figure rises to 10^{10} for 90% occupancy. At 30ºC this corresponds to an extremely large free energy difference–approximately 13.9 kcal mol^{-1}. High occupancy of a specific target site against such an overwhelming amount of non-specific genomic DNA can be accomplished in one of three ways–expressing a very large amount of the activator, evolving the activator to achieve extremely high binding affinities, or more simply through *cooperativity*. Cooperative binding of a transcription factor as a multimer or through contacts with heterologous DNA binding proteins can be used to dramatically enhance the binding affinity and specificity of transcriptional regulators. A simple demonstration of this concept is an example

taken from Ptashne (2). Consider the case where a repressor interacts with its operator site with a binding energy of 10 kcal mol^{-1} and with another molecule of the repressor with an interaction energy of 2 kcal Mol^{-1}. If theoretical curves are drawn to represent the fractional occupancy of an operator site, it is easily seen that approximately 30 or 100 fold more repressor molecules are needed to achieve 99% or 99.9% occupancy respectively, in the single-site case versus where

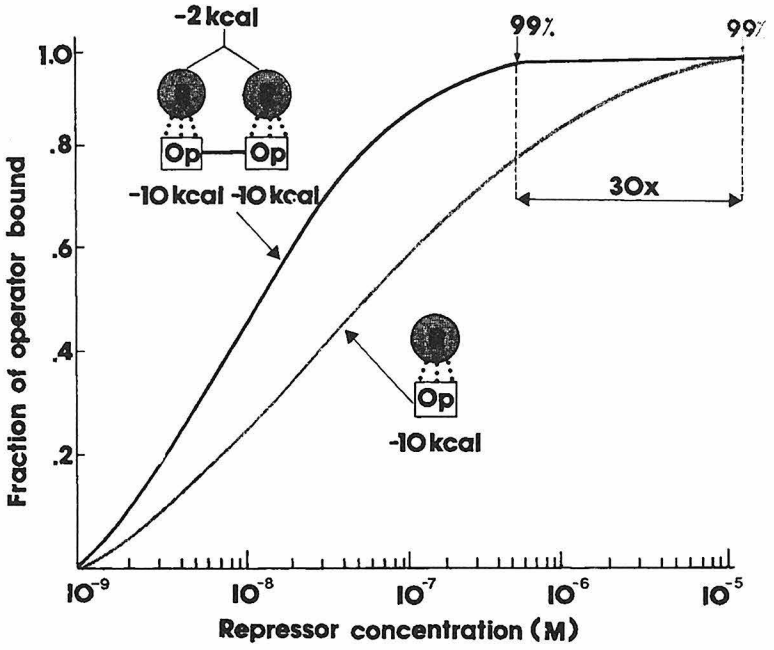

An example of how cooperative interactions can increase the binding affinity of a ligand (1).

two molecules of the repressor bind adjacent sites.

Transmission of cooperative effects can take place via a number of mechanisms such as protein-protein contacts in distinct "dimerization domains" (3), distortion of adjacent sites on DNA to enable accomodation of the second ligand (4), or sliding and intermolecular transfer (5).

Cooperative oligonucleotide directed triplex formation

Using the well established affinity cleavage technique (6), Strobel and Deravan have demonstrated how two triple helix forming oligonucleotides, each 9 bases long, can bind cooperatively to adjacent homopurine sites in genomic DNA from bacteriophage λ (7). Using a short Watson-Crick duplex as a dimerization domain in a binding motif analogous the binding of leucine -zipper proteins, Distefano, Shin and Dervan demonstrated that stronger cooperativity can be obtained beween two pyrimidine oligonucleotides binding to homopurine targets separated by two base pairs (8). Stabilization of the dimerization domain by binding of a small molecule such as echinomycin was shown to further enhance coperative binding energy (9). The cooperative binding energy of short oligonucleotides binding to directly abutting sites in a homopurine tract in the absence of a dimerization domain can be quantitated using affinity cleavage titrations (10). Under the conditions of the experiment the free energy of interaction between oligonucleotides bound to adjacent sies was reported to be 1.8-2.1 kcal•mol^{-1}. The stacking of bases at the junction has been shown to be the basis for this cooperative interaction using studies where the magnitude of observed cooperativity was dependent on the specific bases at the junction and single mismatches at the junction could disrupt cooperativity (11). An impressive demonstration of the gain in binding energy due to cooperativity was a recent study by Colocci and Dervan where three pyrimidine oligonucleotides only 6 bases in length, carrying favorable modifications such as

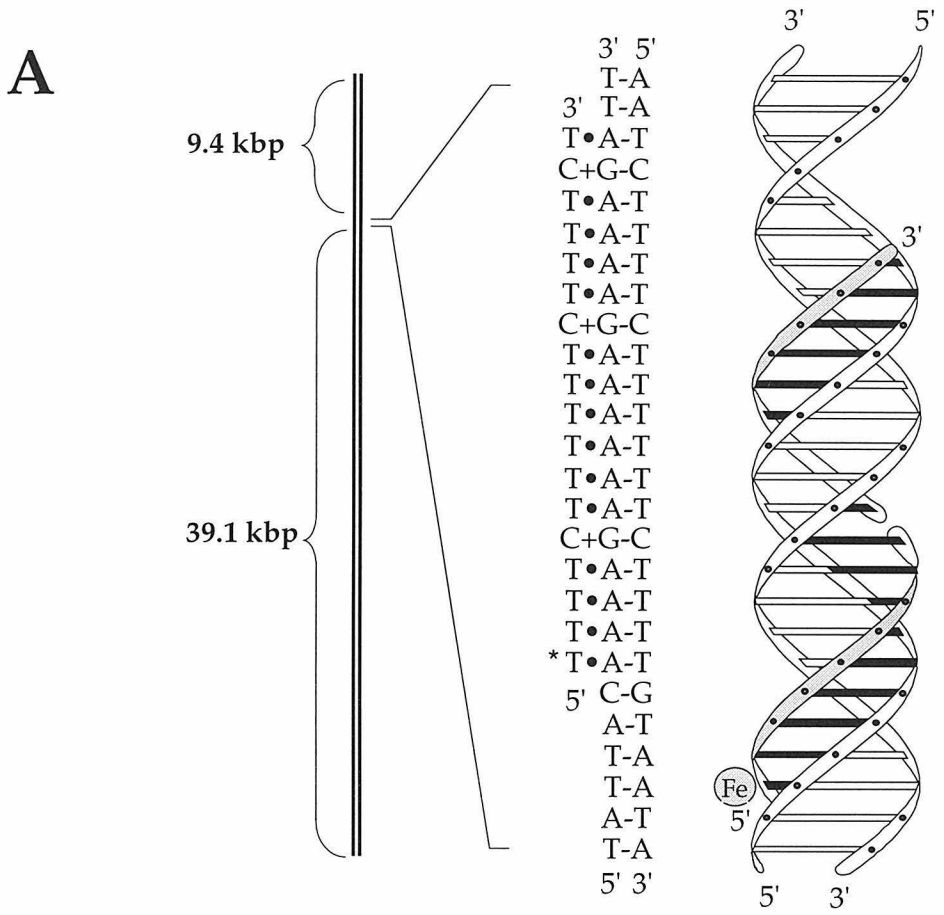

Figure 3.1: A historical perspective of cooperative systems using oligonucleotide mediated triple helix formation.

A. Cooperative binding of two 9 base pyrimidine oligonucleotides to adjacent homopurine sites in the bcteriophage λ genome. Adapted from reference 7.

B. Schematic diagram of a Y-shaped triple-helical complex composed of two oligonucleotides, **1** and **2**, binding cooperatively to double-helical DNA through the formation of a Watson-Crick minihelix. Adapted from reference 8.

C. Schematic representation of a complex composed of three triple helix forming oligonucleotides binding to adjacent sites on double-helical DNA. ^{P}U and ^{m}C designate 5-(1-propynyl)-2'-deoxyuridine and 5-methyl-2'-deoxycytidine, respectively.Adapted from reference 12.

B

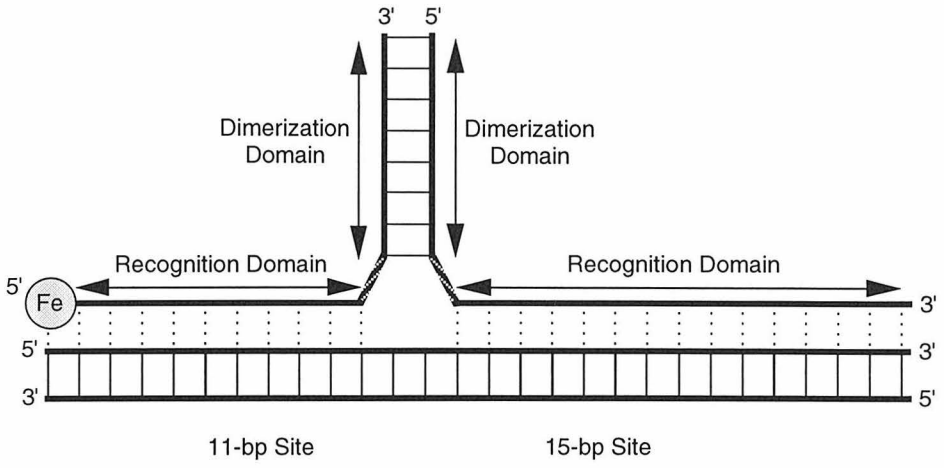

5'-AAAAAAGGAAA A AAAAAAGAGAGAGAGA-3'
3'-TTTTTTTCCTTT T TTTTTTCTCTCTCTCT-5'

1 5'-*TTTTTTTTCCTTTC GTCAATCG **(11-bp Site)**

2 5'-CGATTGACCTTTTTCTCTCTCTCT **(15-bp Site)**

C

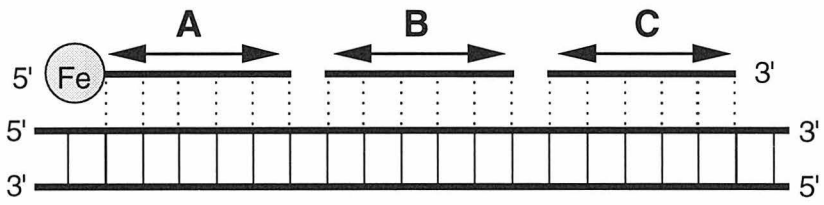

5'-A A A AAAGGA AAGAAA AGAGAG AGA-3'
3'-T T T TTTCCT TTCTTT TCTCTC TCT-5'

A 5'-*TUUCCU

B 5'-UUCUUU

C UCUCUC -3'

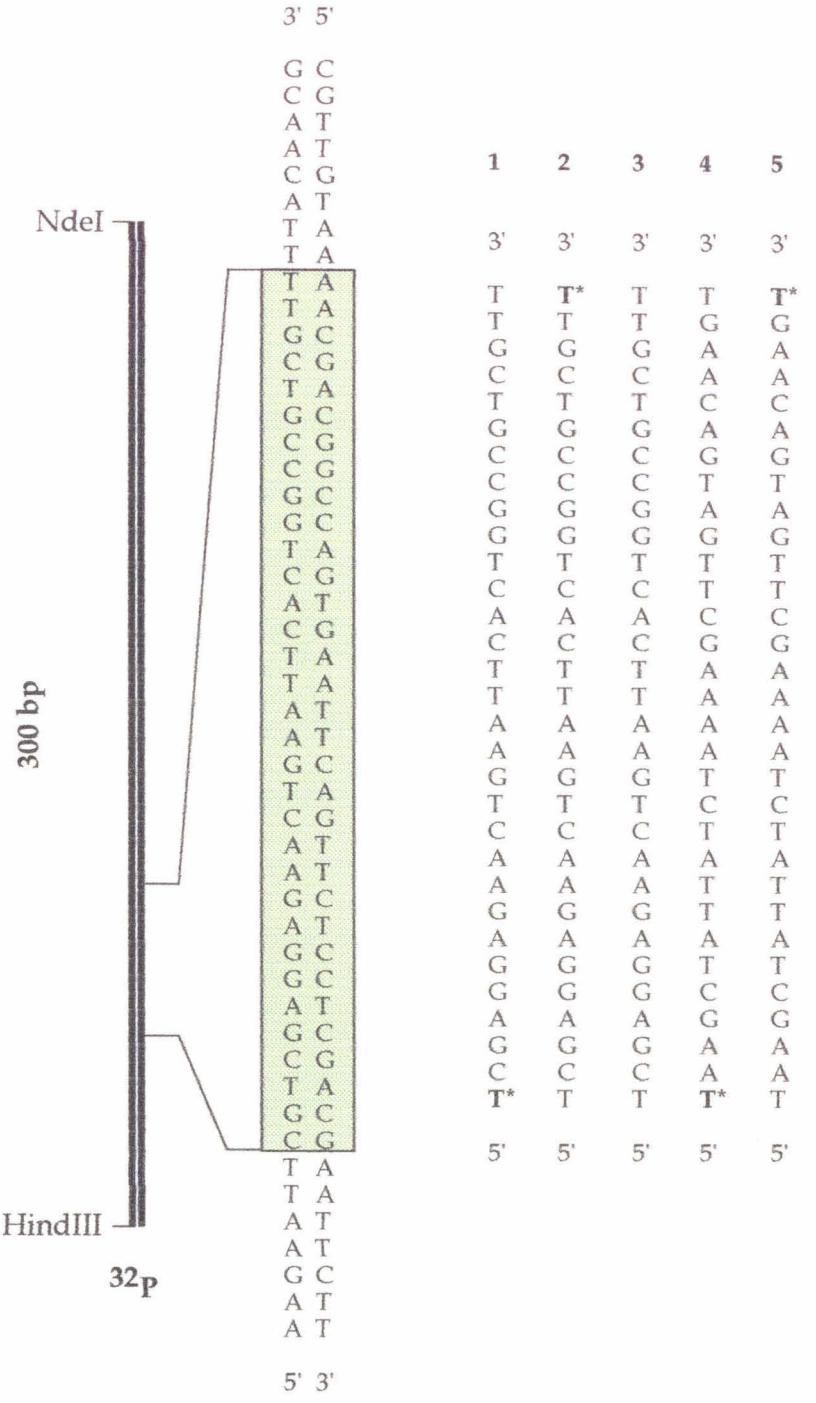

Figure 3.2: Schematic diagram of the restriction fragment, target site and oligonucleotides used to investigate the origin of the secondary clevage pattern for terminal T* oligonucleotide.

methyl cytidine and 5-propynyl uridine, have been used to bind cooperatively to three adjacent homopurine targets (12).

The RecA protein from *E.Coli* , in the presence of the slowly hydrolyzed cofactor ATP-γ-S, can bind single-stranded DNA to form stable nucleoprotein filaments which can then bind to homologous sites on double-stranded DNA (13) forming a three stranded complex that exists in a dynamic state (14). Binding of these filaments to DNA can be observed by incorporating into the oligonucleotide part of the filament, the modified thymidine derivative, T*, wherein the DNA cleaving moiety EDTA•Fe is covalently attached at C5 of a thymine heterocycle (15). Here we report the detection of cooperative binding of short nucleoprotein filaments to homologous sites on duplex DNA using affinity cleavage.

RESULTS AND DISCUSSION

Affinity cleavage directed by a RecA•oligonucleotide filaments with a modified thymidine residue T* incorporated at a single terminal position on the oligonucleotide, has recently been used for studying the three-strand reaction catalyzed by RecA (15). When the T* residue is incorporated at either the 5′- or the 3′- terminus (**1** or **2** , Figure 3.2) a major cleavage pattern is observed at the site expected by antiparallel binding of the third strand to it's homologous sequence, together with a minor cleavage pattern at the *opposite* end (Lanes 6 and 7, Figure 3.3). This minor cleavage pattern could in principle arise by two distinct mechanisms. Since the 31 base oligonucleotide used to form the filament contains a central region that is palindromic, the minor cleavage could result

Figure 3.3. Storage phophor autoradiogram of an 8 % denaturing polyacrylamide gel used to separate affinity cleavage products. The cleavage reactions were carried out as described in the experimental section. Lane 2: Untreated 3′-labeled duplex. Lane 3: Intact 3′-labeled duplex obtained from control reaction in the absence of RecA and oligonucleotide-EDTA•Fe. Lane 4: RecA (20 μM) with no oligonucleotide-EDTA•Fe. Lane 5: Oligonucleotide **1** with no RecA. Affinity cleavage products produced by RecA-**1** (Lanes 6) or RecA-**2** (Lanes 7) filaments. Lanes 5-15: Affinity cleavage products of reactions in which **3** was co-incubatedwith **4** or **5** at concentrations indicated above the figure. The nucleotide-to-monomer ratio in lanes 5-15 was 3:1. Lanes 1 and 17 contain the products of adenine-specific sequencing reaction of 3′-labeled duplex (22).

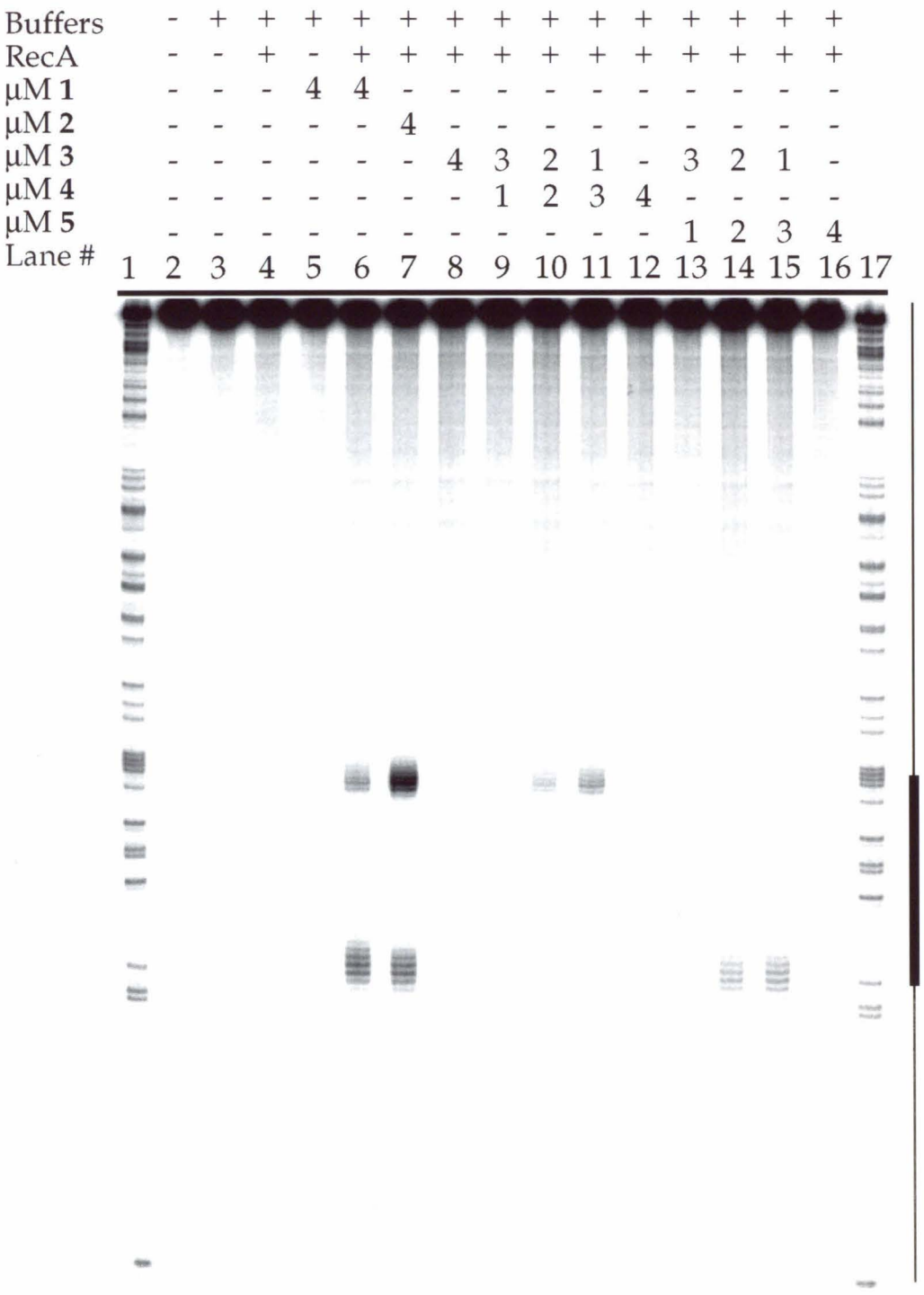
Buffers - + + + + + + + + + + + + + +
RecA - - + - + + + + + + + + + + +
μM 1 - - - 4 4 - - - - - - - - - -
μM 2 - - - - - 4 - - - - - - - - -
μM 3 - - - - - - 4 3 2 1 - 3 2 1 -
μM 4 - - - - - - - 1 2 3 4 - - - -
μM 5 - - - - - - - - - - - 1 2 3 4
Lane # 1 2 3 4 5 6 7 8 9 10 11 12 13 14 15 16 17

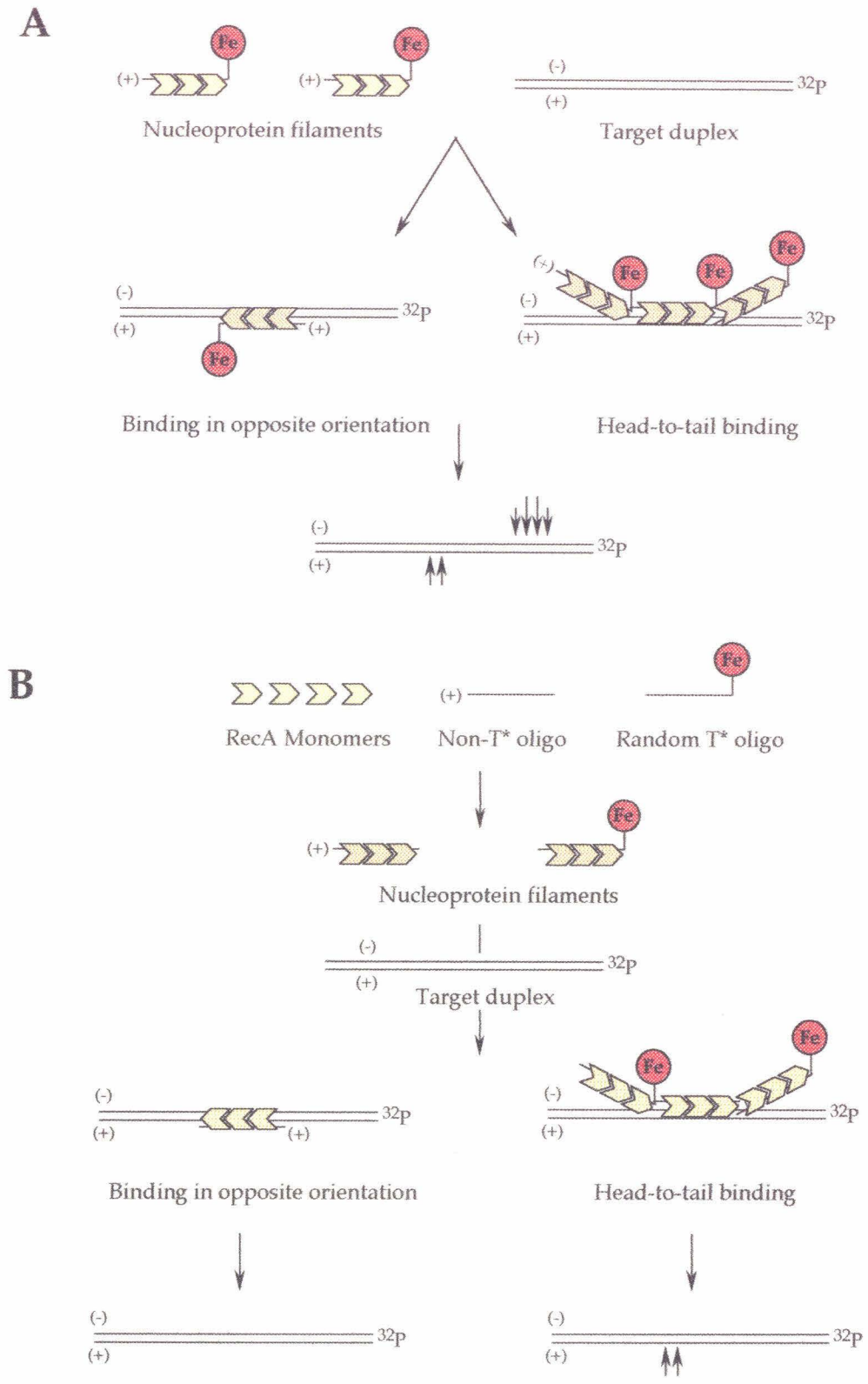

Figure 3.4: A. Alternate models for the observation of affinity cleavage at the minor cleavage site.
B. Experimental design for determining the cause for affinity cleavage at the minor cleavage site.

from binding of a small number of filaments in the opposite orientation. On the other hand, because RecA filaments have been shown to polymerize in a head-to-tail fashion (16), the 3'-end of the filament positioned at the target site would be associated with the 5'-end of a second filament such that the 5'-T* of **1** in the second filament would be pulled in close enough to the duplex to affect cleavage at the minor cleavage site observed with the RecA-**1** filaments (Figure 3.4 A). Similarly, the 3'-T* of a filament containing **2**, if associated with the 5'-end of the filament located at the target site, would be positioned correctly to produce the weaker cleavage observed with the RecA-**2** filaments. Because the associated nucleoprotein filaments adjacent to the filament bound at the target site do not make sequence-specific contacts with the duplex DNA, the sequence of the oligonucleotide in the associated filament is not required to be identical to that of the bound filament.

In order to test each model, an experiment (Figure 3.4 B) was designed where the target site would be occupied by a homologous filament made using an oligonucleotide with the same sequence as **1**, but not carrying a T* at either of its termini (Fig. 3.2, oligo **3**). Secondary site cleavage should now be affected by filaments made from oligonucleotides of random sequence that had T* appended to either the 5'- or 3'- end (Fig. 3.2, oligos **4** and **5** respectively). The results of this experiment are shown in Figure 3.3. No cleavage is observed in the absence of both RecA and oligonucleotide-EDTA•Fe (lane 3), oligonucleotide-EDTA•Fe (lane 4), RecA (lane 5). Lanes 6 and 7 show cleavage patterns obtained with 4μM **1** and **2** respectively. In lanes 8-16, the concentration of either oligonucleotide **4**

(lanes 7-11) or **5** (lanes 12-15) is varied from 4 μM to 0 μM as the concentration of oligonucleotide **3** is adjusted to maintain 4 μM total oligonucleotide concentration. The nucleotide to monomer ratio is held at the optimum value of 3:1. Both the filaments of random sequence RecA-**4** and RecA-**5** give cleavage patterns that are consistent with the head-to-tail binding model. This study clearly indicated the possibility of using contacts between RecA monomers at the termini of nucleoprotein filaments as a means for achieving cooperative binding of shorter filaments (Figure 3.5). Since the shortest reported length for binding of a RecA• oligonucleotide filament to double stranded DNA is 15 bases (17), we decided to use this as a starting point for investigating the cooperative binding of short nucleoprotein filaments to homologous targets.

Figure 3.5. Proposed scheme for sequence-specific cleavage of duplex DNA directed by cooperative binding of two RecA nucleoprotein filaments, one of which is formed with an oligonucleotide containing thymidine-EDTA•Fe (T*) at its 3' terminus. In the first step, RecA monomers polymerize on the T* oligonucleotide to form a nucleoprotein filament. Synapsis follows in which the two nucleoprotein filaments bind cooperatively to their respective homologous sequences on a ^{32}P-labeled duplex substrate forming a joint molecule. The cleavage reaction is then initiated by the addition of of a reducing agent (sodium ascorbate).

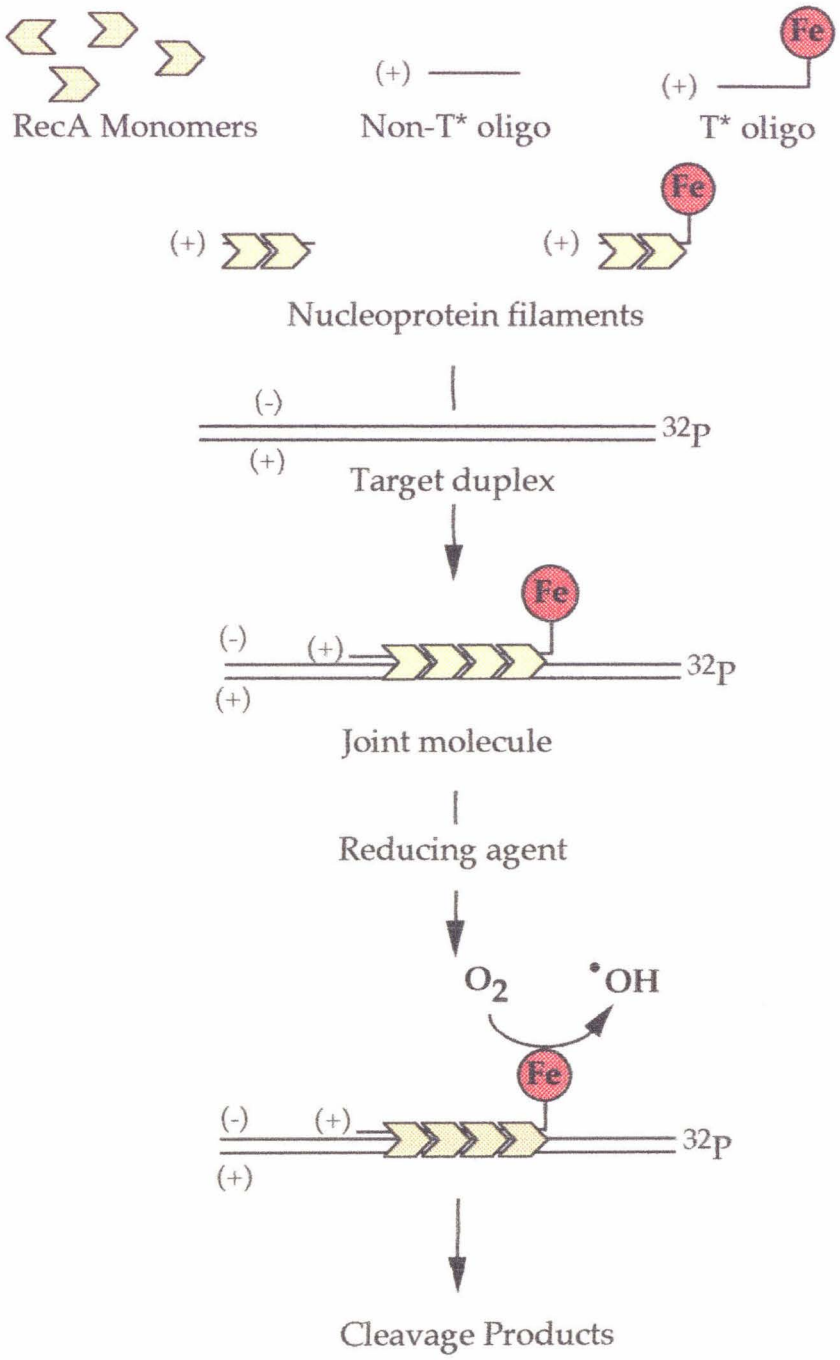
RecA Monomers
(+)
Non-T* oligo
Fe
(+)
T* oligo
(+)
Fe
(+)
Nucleoprotein filaments
(-)
32P
(+)
Target duplex
Fe
(-)
(+)
32P
(+)
Joint molecule
Reducing agent
O2
•OH
Fe
(-)
(+)
32P
(+)
Cleavage Products

A

```
                        Filament I          Filament II
5'- CGT TGT AAA ACG ACG GCC AGT GAA TTC AGT TCT CCT CGA CGA ATT CTT - 3'
3'- GCA ACA TTT TGC TGC CGG TCA CTT AAG TCA AGA GGA GCT GCT TAA GAA - 5'
```

B

```
6        3' -   T*GC TGC CGG TCA CTT - 5'

7                              3' -  AAG TCA AGA GGA GCT*      - 5'
8                              3' -  AAG TCA AGA GGA GCT       - 5'
9                              3' -  AAG TCA AGA GGA GC        - 5'
10                             3' -  AAG TCA AGA GGA G         - 5'
11                             3' -  AAG TCA AGA GGA           - 5'
12                             3' -  AAG TCA AGA GG            - 5'

13                             3' -   AG TCA AGA GGA GCT G     - 5'
14                             3' -    G TCA AGA GGA GCT GC    - 5'
15                             3' -      TCA AGA GGA GCT GCT   - 5'
16                             3' -       CA AGA GGA GCT GCT T - 5'

17       3' -   T*GC TGC CGG TCA CTA - 5'
18       3' -   T*GC TGC CGG TCA CTC - 5'
19       3' -   T*GC TGC CGG TCA CTG - 5'
20       3' -   T*GC TGC CGG TCA CTΦ - 5'

21                             3' -  TAG TCA AGA GGA GCT*      - 5'
22                             3' -  CAG TCA AGA GGA GCT*      - 5'
23                             3' -  GAG TCA AGA GGA GCT*      - 5'

24                              5' - T*TC AGT TCT CCT CGA       - 3'
25                             5' -  TTC AGT TCT CCT CGA       - 3'
```

Figure 3.6: A. Schematic representation of the 30 base pair target site and the two adjacent subsites used for observing cooperative binding.

B. Sequences of olgonucleotides used for studying the limitations of cooperative binding.

Length and polarity requirements

The oligonucleotides **6** - **12** (Figure 3.6) were designed to determine the shortest filament that can bind cooperatively with a filament made using the 15-mer oligonucleotide carrying a T* residue at its 3'- end (oligonucleotide **6**), with each oligonucleotide at a final concentration of 3 μM. The results from these experiments are shown in figure 3.7. As seen in lanes 3 and 4, oligonucleotide **7** binds its site weakly whereas no binding is observable for oligonucleotide **6**. However when the two filaments are present in the reaction simultaneously, strongly cooperative binding is observed (lane 4). Oligonucleotides **8**, **9**, **10** and **11** clearly show cooperative binding while only weak cooperative binding is observed for the 11 base oligonucleotide **12** at the concentrations used in the experiment. Since the length of the shortest oligonucleotide that can form stable filaments with RecA has been reported to be 9 bases (18), it is likely that shorter oligonucleotides at higher concentrations could be made to bind cooperatively.

Binding to non-adjacent sites

The oligonucleotides **24** and **25** were designed to bind to a site abutting oligonucleotide **6** but on the opposite strand. Filaments made with olgonucleotide **24** do not show any observable binding (Lane 11). No cooperative binding was observed when olgonucleotides **6** and **24** were used in tandem (Lane 13). This is evidence that protein-protein contacts between RecA monomers, which are highly directional in nature, are the basis for cooperative binding of filaments.

Figure 3.7. Storage phophor autoradiogram of an 8 % denaturing polyacrylamide gel used to separate affinity cleavage products. The cleavage reactions were carried out as described in the experimental section. Lane 2: Untreated 3′-labeled duplex. Lane 3 -12: Reactions with RecA (20 μM) with oligonucleotides as indicated above the figure. The nucleotide-to-monomer ratio in each lane was 3:1. Lane 13 contains the standard full length 31 mer **2**. Lanes 1 and 14 contain the products of adenine-specific sequencing reaction of 3′-labeled duplex (22).

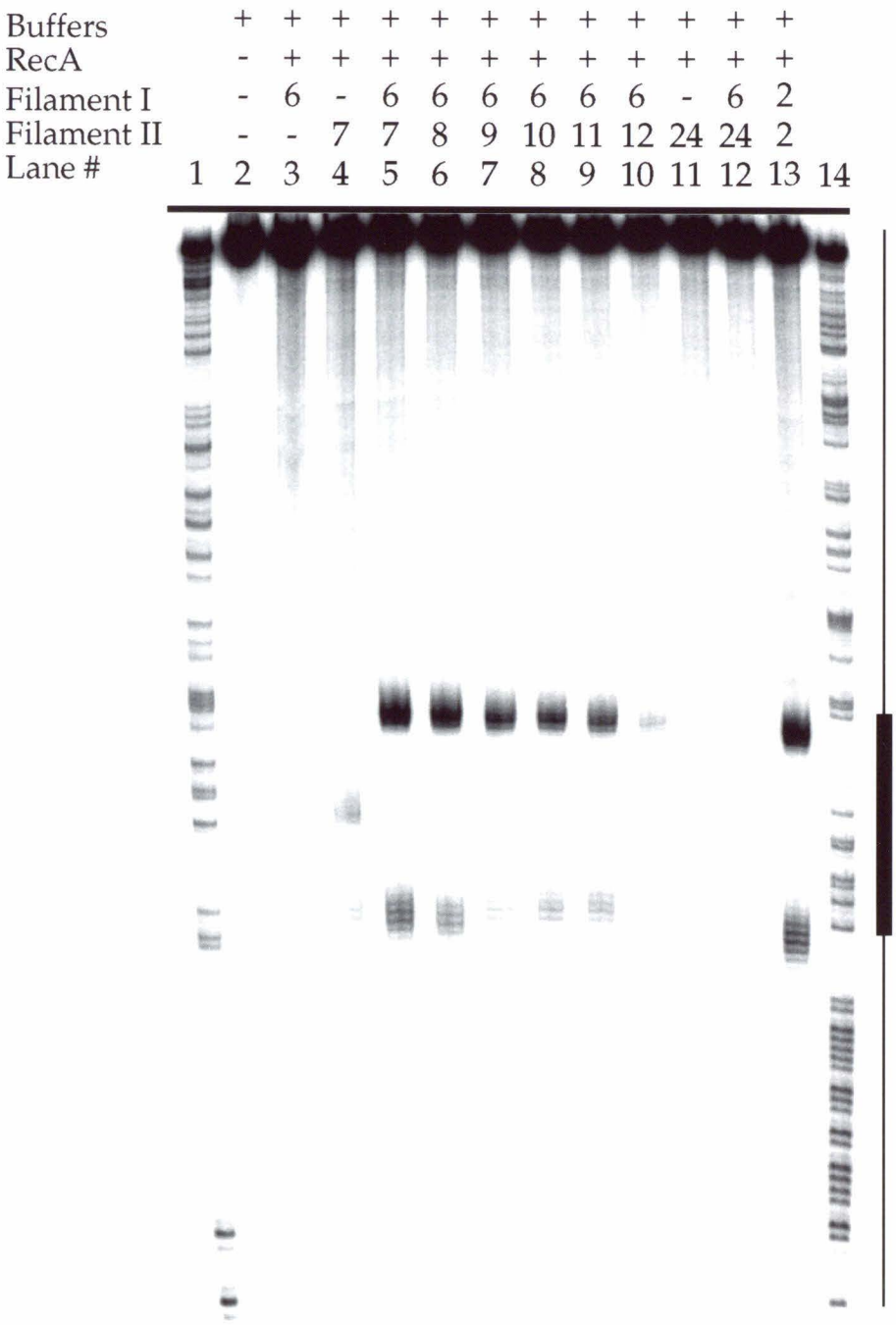
Buffers + + + + + + + + + + + +
RecA - + + + + + + + + + + +
Filament I - 6 - 6 6 6 6 6 6 - 6 2
Filament II - - 7 7 8 9 10 11 12 24 24 2
Lane # 1 2 3 4 5 6 7 8 9 10 11 12 13 14

Effect of gaps between binding sites

The cooperative binding of short nucleoprotein filaments observed in the experiment above could arguably have been caused by a structural distortion of the adjacent sequence by binding of the first filament which predisposes it to binding by a second filament. Oligonucleotides **13, 14, 15** and**16** designed to bind adjacent sites separated by one, two, three or four base-pairs were synthesized to test this possibility. As seen in lanes 7-10 (Figure 3.8) cooperative binding is completely abolished by a gap of as little as a single base pair, and is not recovered when the gap is made large enough to accomodate a single RecA monomer.

Figure 3.8. Storage phophor autoradiogram of an 8 % denaturing polyacrylamide gel used to separate affinity cleavage products. The cleavage reactions were carried out as described in the experimental section. Lane 11: Untreated 3′-labeled duplex. Lane 2-10: Reactions with RecA (20 μM) with oligonucleotides as indicated above the figure. The nucleotide-to-monomer ratio in each lane was 3:1. Lanes 1 contains the products of adenine-specific sequencing reaction of 3′-labeled duplex (22).

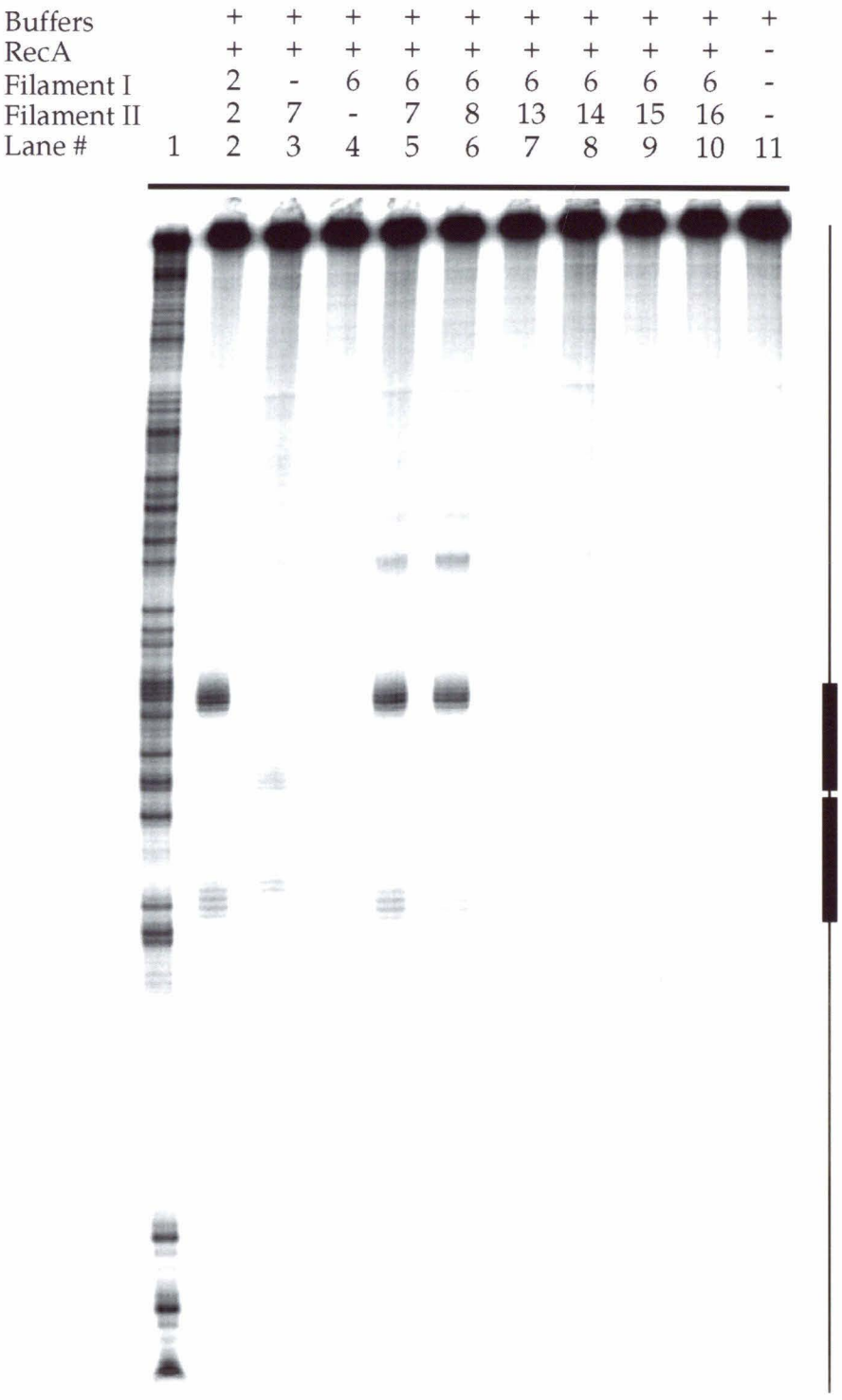
Buffers + + + + + + + + + +
RecA + + + + + + + + + -
Filament I 2 - 6 6 6 6 6 6 6 -
Filament II 2 7 - 7 8 13 14 15 16 -
Lane # 1 2 3 4 5 6 7 8 9 10 11

Effect of single base mismatches at the junction

In order to determine if the cooperative binding seen was indeed due to protein mediated contacts and not due to base stacking, oligonucleotides **17**, **18** and **19** were synthesized where the base at the 5'- end of the junction was changed to each of the other three bases. No significant differences in cooperative binding were observed in any case (Lanes 4-7, Fig.7). Similarly, replacing the base at the 3'- end of the junction (oligonucleotides **21-23**) had no effect on cooperative binding (Lanes 9-11, Fig.7). In fact, cooperative binding was seen even when filaments were made with oligonucleotide **20**, where the nucleotide at the 5'- side of the junction was changed to an abasic sugar (lane 8, Fig. 7). Together, these studies clearly demonstrate that the basis for cooperative interaction of the two filaments is not base stacking, but protein mediated interactions between the filaments.

Figure 3.9. Storage phophor autoradiogram of an 8 % denaturing polyacrylamide gel used to separate affinity cleavage products. The cleavage reactions were carried out as described in the experimental section. Lane 2-13: Reactions with RecA (20 μM) with oligonucleotides as indicated above the figure. The nucleotide-to-monomer ratio in each lane was 3:1. Lanes 1 contains the products of adenine-specific sequencing reaction of 3'-labeled duplex (22).

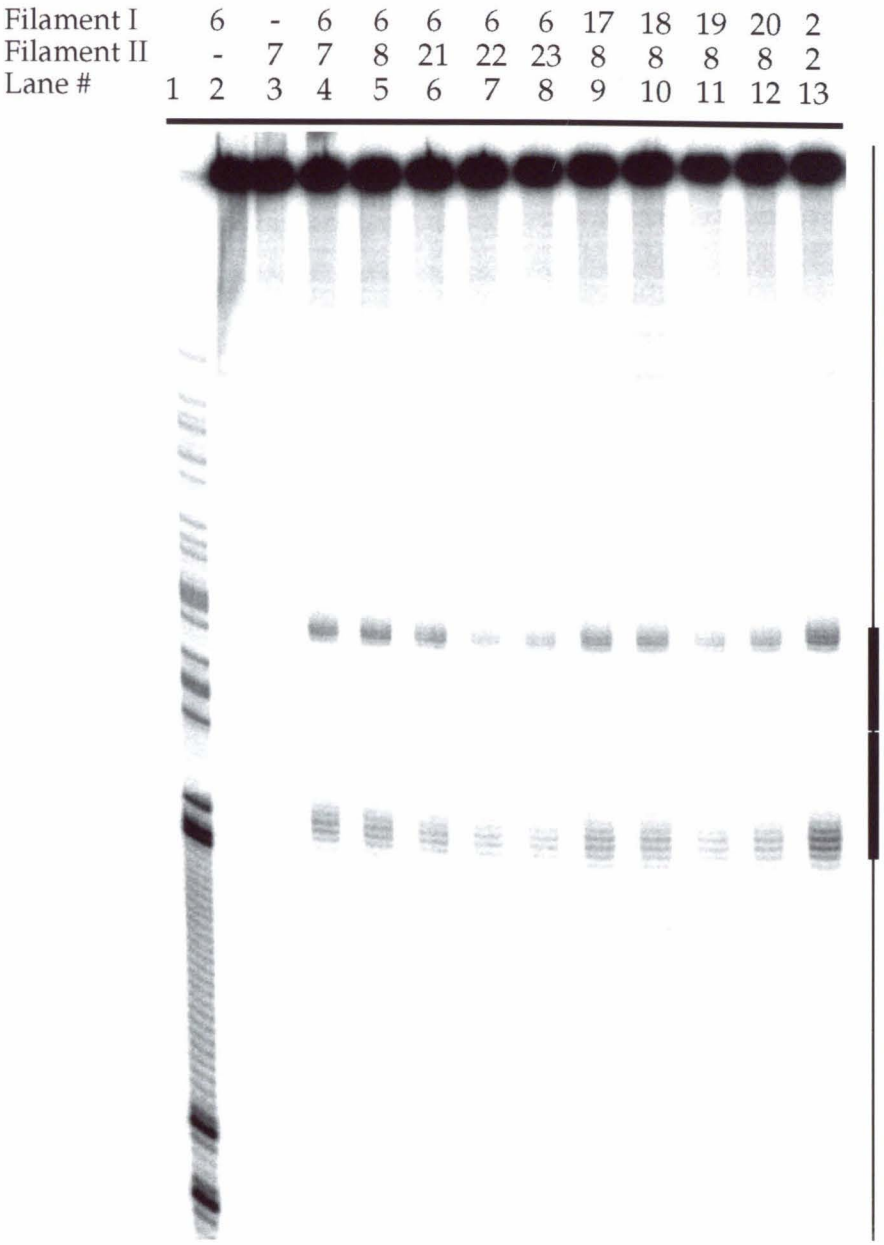
Filament I 6 - 6 6 6 6 17 18 19 20 2
Filament II - 7 7 8 21 22 23 8 8 8 8 2
Lane # 1 2 3 4 5 6 7 8 9 10 11 12 13

MATERIALS AND METHODS

General

RecA protein was isolated from the strain JC12772 using a modified version of published procedures. Sonicated, deproteinized calf thymus DNA (Pharmacia) was dissolved in H_2O to a final concentration of 2.0 mM in base pairs and was stored at 4 °C. Glycogen was obtained from Boehringer-Mannheim as a 20 mg/ml aqueous solution. γ-S-ATP was purchased from Sigma and was stored at -20 °C. Nucleoside triphosphates labeled with ^{32}P were obtained from Amersham or ICN and were used as supplied. Cerenkov radioactivity was measured with a Beckman LS 2801 scintillation counter. Restriction endonucleases were purchased from Boehringer Mannheim or New England Biolabs and were used according to the supplier's recommended protocol in the activity buffer provided. Klenow fragment, calf intestinal alkaline phosphatase and snake venom phosphodiesterase were obtained from Boehringer Mannheim. Phosphoramidites were purchased from Glenn Research.

Synthesis and Purification of Oligodeoxyribonucleotides

All ogonucleotides were synthesized and purified as described in Chapter Two. Each oligonucleotide was further characterized by digestion with calf intestinal alkaline phosphatase and snake venom phosphodiesterase followed by analysis of the digested oligos using reversed phase HPLC to confirm complete post-synthetic modification of the primary amine appended to C-5 of the terminal thymidine residues.

DNA Manipulations

The 300 bp HindIII/NdeI restriction fragment of the plasmid pUCJWII47 was isolated and labeled at the 3'-end at the HindIII site by standard procedures (23). Adenine-specific sequencing reactions were carried out as previously described (22) .

Affinity Cleavage Reactions

A dried pellet of oligonucleotide-EDTA was dissolved in a solution of aqueous $Fe(NH_4)_2(SO_4)_2 \bullet 6H_2O$ to produce a solution that was 20 μM in oligonucleotide and Fe(II). This solution was allowed to equilibrate for at least 15 minutes at room temperature. A stock solution was prepared containing 75 μl 10x buffer (250 mM Tris-acetate, 40 mM Mg-acetate, 1 mM EGTA, 5 mM spermidine, 8 mM -mercaptoethanol, pH 7.5), 20 μl calf thymus DNA (2 mM in bp), and 35 μl acetylated BSA (3 mg/ml). To a given reaction was added 5.5 μl stock solution, 3 μl of each oligonucleotide-EDTA•Fe(II) at the 20 μM or H_2O (for control reactions), 3 μl of RecA solution (7.5 mg RecA/ml RecA storage buffer) plus RecA storage buffer (20 mM Tris-HCl, 0.1 mM EDTA, 1 mM DTT, 50% glycerol, pH 7.5) to give the designated nucleotide to monomer ratio (appropriate amounts of RecA storage buffer were added to ensure that each reaction was run under the same conditions), and enough H_2O to give a final reaction volume of 30 μl after DTT addition. Where two oligonucleotide filaments were made for observing cooperative binding, 1.5 μl of each partner

was added at a concentration of 40 μM. Following a 1 min incubation at 37 °C, nucleoprotein filament formation was initiated by addition of 1 μl 30 mM γ-S-ATP. After 10 min, approximately 20,000 cpm (~1 nM) 3'- labeled duplex was added and joint molecule formation was allowed to proceed for 30 min at 37 °C. The cleavage reactions were initiated by the addition of 1 μl 30 mM sodium ascorbate. The final reaction conditions were 25 mM Tris-acetate, 6 mM Tris-HCl, 4 mM $Mg(OAc)_2$, 1 mM EGTA, 32 mM EDTA, 0.5 mM spermidine, 0.8 mM β-mercaptoethanol, 5% glycerol, 1 mM sodium ascorbate, pH 7.5. After 8 h, the cleavage reactions were phenol/chloroform extracted and the DNA was precipitated by the addition of glycogen, NaOAc (pH 5.2), and $MgCl_2$ to final concentrations of 140 μg/ml, 0.3 M, and 10 mM, respectively, and 100 μl ethanol. After centrifugation and removal of the supernatant, the dried pellet was dissolved in 20μl H_2O, frozen, and lyophilized to dryness. The DNA in each tube was resuspended in 5 μl of formamide-TBE loading buffer containing 0.1% SDS . The DNA solutions were assayed for Cerenkov radioactivity by scintillation counting and diluted to 5000 cpm/μl with more formamide-TBE loading buffer containing 0.1% SDS. The DNA was denatured at 90 °C for 5 min, and loaded onto an 8% denaturing polyacrylamide gel. The DNA cleavage products were electrophoresed in 1x TBE buffer at 50 V/cm. The gel was dried on a slab dryer and then exposed to a storage phosphor screen. The gel was visualized with a Molecular Dynamics 400S PhosphorImager.

REFERENCES

1. Kodadek, T. (1995) *Chem. and Biol.* **2**, 267-279.
2. Ptashne, M. (1986)*A Genetic Switch* Blackwell Scientific Publications and Cell Press: Palo Alto, CA.
3. Giniger, G., Ptashne, M. (1988) *Proc. Natl. Acad. U.S.A.*, **85**, 382-386.
4. Wilson, W. D. (1987) *Prog. Drug Res.* **31**, 193-221.
5. Ruusala, T., Crothers, D. M. (1992) *Proc. Natl. Acad. U.S.A.* **89**, 4903-4907.
6. For a review on affinity cleaving see Dervan, P. B. (1991), *Meth. Enzym*. **208**, 497-515.
7. Strobel, S. A., Dervan, P. B. (1989) *J.Am. Chem. Soc.*, **111**, 7286-7287.
8. Distefano, M. D., Shin, J. A., Dervan, P. B. (1991) *J. Am. Chem. Soc.* **113**, 5901-5902.
9. Distefano, M. D., Dervan, P. B. (1992) *J.Am. Chem. Soc.*, **114**, 11006-
10. Distefano, M. D., Dervan, P. B. (1993) *Proc. Natl. Acad. Sci. USA* **90**, 1179-1183; Colocci, N., Distefano, M. D., Dervan, P.B. (1993) *J. Am. Chem. Soc.* **115**, 4468-4473.
11. Colocci, N., Dervan, P.B. (1994) *J. Am. Chem. Soc.* **116**, 785-786.
12. Colocci, N. (1996) Doctoral Dissertation, California Institute of Technology.
13. Flory, J., Tsang, S.S., Muniyappa, K. (1984) *Proc. Natl. Acad. Sci. USA* **81**, 7026-7030.

14. Reddy, G., Jwang, B., Rao, B. J., Radding, C.M. (1994) *Biochemistry* **33**, 11486-11492.

15. Baliga, R., Singleton, J. W., Dervan, P. B. (1995) *Proc. Natl. Acad. Sci. USA* **92**, 10393-10397.

16. Register, J. C., Griffith, J. (1986) *Proc. Natl. Acad. of Sci., USA* **83**, 624- 628.

17. Hsieh, P., Camerinio tero, C. S., Camerinio tero, R. D. (1992) *Proc. Natl. Acad. Sci. USA* **89**, 6492-6496.

18. Leahy, M. C., Radding, C. M. (1986) *J. Biol. Chem.* **261**, 6954-6960.

19. Golub, E. I., Ward, D. C., Radding, C. M. (1992) *Nucleic Acids Res.* **20**, 3121-3125.

20. Golub, E. I., Radding, C. M., Ward, D. C. (1993) *Proc. Natl. Acad. Sci.USA* **90**, 7186-7190.

21. Han, H., Dervan, P. B. (1994) *Nucleic Acids Res*.**22**, 2837-2844.

22. Iverson, B. L., Dervan, P. B. (1987) *Nucleic Acids Res.* **15**, 7823-7830.

23. Sambrook, J., Fritsch, E. F., Maniatis, T., *Molecular Cloning, 2nd ed.* (Cold Spring Harbor Laboratory Press, New York, (1989).

CHAPTER FOUR

Groove Location of RecA•Oligonucleotide Filaments in Complexes with Homologous Double-stranded DNA Characterized by Affinity Cleavage

(The text for this chapter is taken in part from a published manuscript co-authored with Jennifer W. Singleton and Professor Peter B. Dervan.)

Introduction

The RecA protein of *E. coli* (38 kD) plays a central role in DNA recombination and repair. *In vitro*, RecA protein directs strand exchange between two DNA molecules of homologous sequence when one of the segments of DNA is completely or partially single-stranded (1-4). In the presence of adenosine triphosphate (ATP), or its slowly-hydrolyzed analog γ-S-ATP, RecA polymerizes on single-stranded DNA forming a right handed helical nucleoprotein filament with a binding stoichiometry of approximately one RecA monomer for every three bases (5-8). The filament then binds to a site on duplex DNA which is homologous to the sequence of the single strand bound within the filament (9-12). In this synapsis step, a joint molecule is formed which contains the three strands of DNA and numerous RecA monomers. The final step is the release of the products of strand exchange–a displaced single strand and a heteroduplex. In the presence of topological constraints, such as when the 5'-end of the strand to be displaced is at an internal site within duplex DNA, the reaction does not proceed past synapsis and the three strands of DNA remain bound in the joint molecule (13-14).

Although it is generally accepted that all three strands of DNA are held stably in the form of a joint molecule during synapsis (15-19), two different mechanisms of strand exchange can be envisaged which require different joint molecule structures (20,21). The first mechanism involves local opening of a region of duplex followed by Watson-Crick base-pairing of the single strand with its complementary strand. The outgoing strand is either completely

displaced (22) or held associated with the newly formed heteroduplex by non-Watson-Crick interactions in the form of a three stranded structure (23). For the second mechanism, a fully base-paired duplex makes additional base-specific interactions with the homologous single strand within the RecA-associated complex giving rise to a three stranded structure in which all three strands are held together in a triple helical complex which is then processed to give the products of strand exchange (24-25). The biochemical evidence for each of these models is briefly discussed below.

Studies with protein associated joint molecules

Joint molecules formed using a linear single strand targeted to an internal site of target duplex molecules, in the presence γS-ATP have been studied by Adzuma using restriction enzyme protection and chemical modification studies (22). Chemical modification experiments carried in presence of bound RecA revealed that the N7 of guanine residues of all three DNA strands and N3 of cytosine residues of the outgoing strand of the complex reacted with DMS. All three strands reacted with potassium permanganate ($KMnO_4$) but the incoming and complementary strands showed less uniform reactivity than did the outgoing strand. This was interpreted as an indication that the outgoing strand of the RecA-coated joint molecule is single-stranded in character while the other two strands behave more like a canonical duplex. This supports a mechanism of homologous alignment where strand separation occurs *before* pairing.

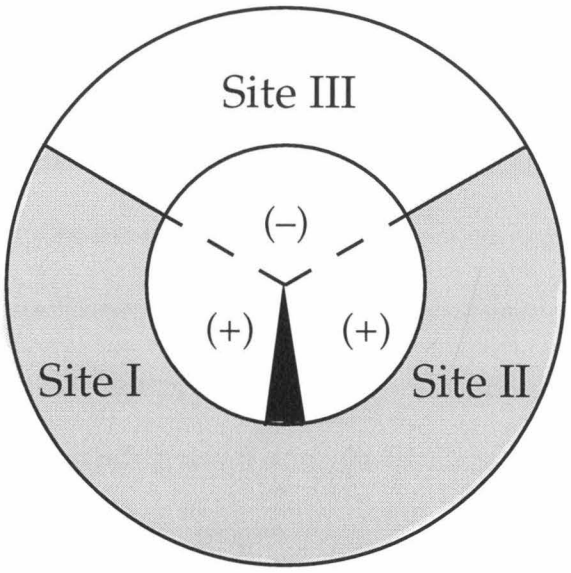

Figure 4.1 : A model of a cross-section of a RecA filament illustrating its three DNA binding sites. The sites are numbered I, II, and III in the order that they are bound by ssDNA. Based on nuclease accessibility studies Site III is placed at the groove of the filament (unshaded sector). The dark wedge symbolizes the inability of strands bound in site I and site II to base-pair. Strands in site I and II are bound parallel (+), and the strand in site III is bound with opposite polarity (–). Adapted from Norden et al. (18).

Norden and coworkers have proposed the three-site model for recognition of homology based on findings from linear dichroism spectroscopy and small angle neutron scattering studies of RecA-DNA complexes formed in the presence of γS-ATP (18). The RecA protein polymer is proposed to have three DNA binding sites each of which can bind a single strand of DNA (Figure 4.1). The sites are designated I, II, and III based on the order in which they are occupied by successively added single-stranded DNA (ssDNA) molecules. A DNA strand bound in site III is susceptible to nuclease cleavage whereas strands bound in

sites I or II are resistant to cleavage. Site III is thus proposed to be a more open binding site with weaker DNA binding affinity than sites I or II. The sites also differ in their DNA binding affinities and in the relative polarity of the bound strands. The polarity of the strand bound in site III is opposite to the other two strands allowing site III-site I base-pairing and site III-site II base-pairing. Homologous alignment is proposed to take place when a single strand bound in site I scans a duplex bound in site II and site III till homology is located, followed by spontaneous flipping of the strand in site III from its Watson-Crick partner in site II to form a new base pair with a base from the strand in site I. Interestingly, the complexes formed were shown to depend on the order of addition of the components– RecA-ssDNA-dsDNA complexes had different LD signatures form RecA-dsDNA-ssDNA complexes (18). It must be noted that linear dichroism is a macroscopic assay and interpretations of LD signatures can only be used to *infer indirectly* the polarities of the strands involved and their possible groove location.

Studies with deproteinized joints

Reports from a few laboratories, including Radding and coworkers, as well as Camerini-Otero and coworkers have described the RecA-mediated formation of triple-stranded joint molecules which, after deproteinization, are thermostable and show chemical reactivity consistent with a novel triplex structure (26-31).

In deproteinized joint molecules formed using RecA, ATP, ssDNA, and hairpin duplexes containing regions complementary to the ssDNA, Radding and coworkers have shown that the two strands of the deproteinized joint which

would be destined to form heteroduplex DNA in strand exchange show chemical modification and enzymatic digestion patterns indistinguishable from those of control duplex DNA (27). The outgoing strand shows nuclease resistance and chemical reactivity different from both ssDNA and dsDNA, with most of the purine residues, especially adenines showing hyperreactivity toward DEPC. Methylation of functional groups in the major goove–N7 of guanosine bases, N4 of adenosine bases and N4 of cytosine bases– showed no effect on the rate and extent of three stranded joint formation but decreased the thermal stability of resultant complexes. The authors proposed a structure where the incoming strand and its complement are base paired in the Watson-Crick sense and the outgoing strand is associated through contacts in the major groove of the newly formed heteroduplex–a structure that would require local melting of the duplex and insertion of the third strand in the *minor groove* . The planar base-triplets proposed by Radding and coworkers are shown in Figure 4.3A.

Figure 4.2: Planar base triplets for the three-stranded joint molecule formed by RecA protein proposed by (A) Radding and coworkers and (B) Camerini-Otero and coworkers. The strands from the target duplex are shown in blue and the incoming strand is shown in red. Note that the G•GC base triplet proposed by Radding does not have a specific interaction between the N7 of G in the incoming strand and the 2-amino proton of the outgoing strand.

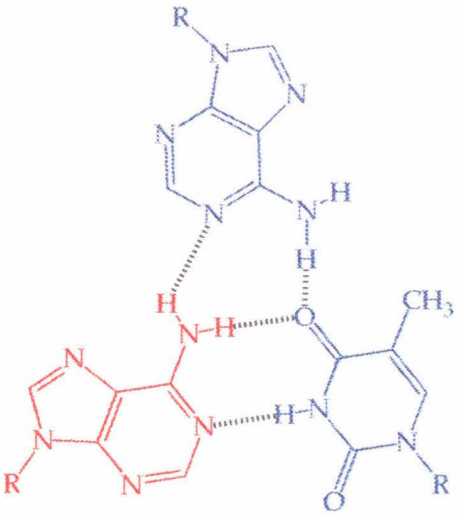

A•AT

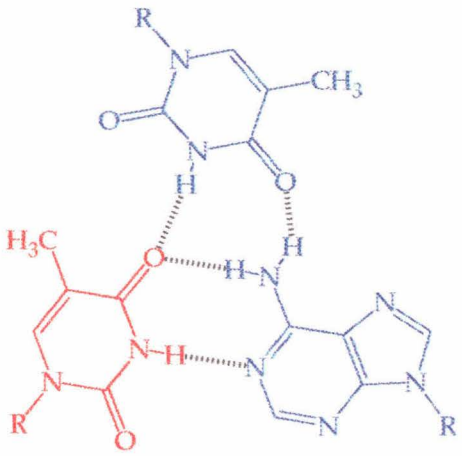

T•TA

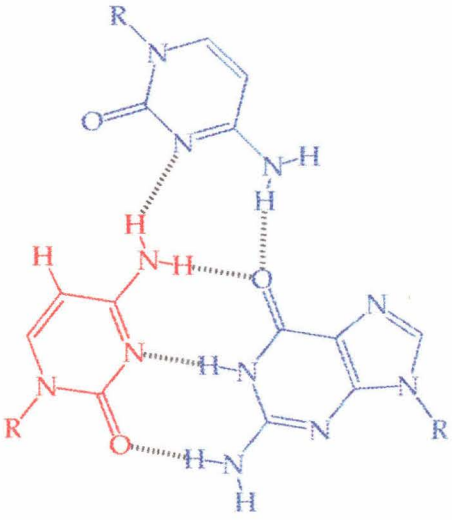

C•CG

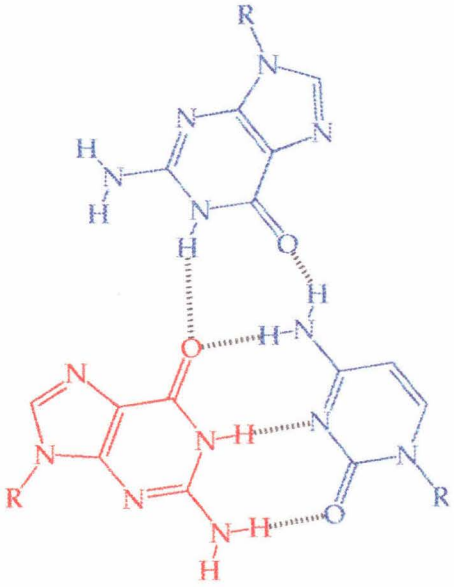

G•GC

Figure 4.2 A

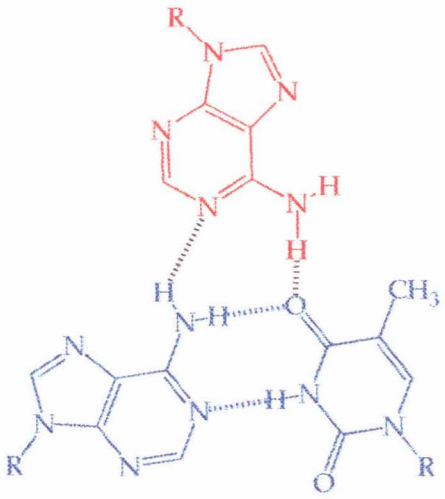

A•AT

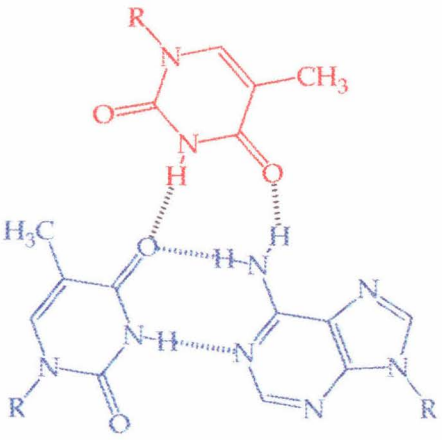

T•TA

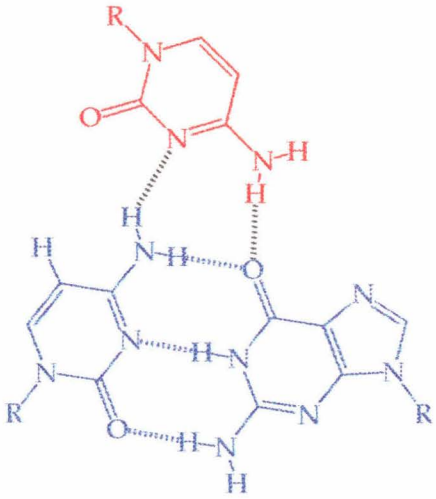

C•CG

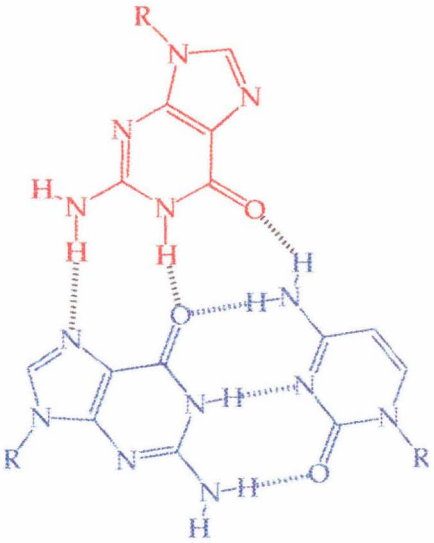

G•GC

Figure 4.2 B

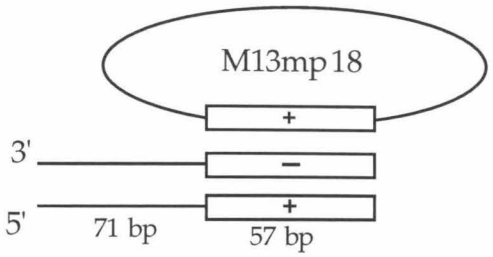

Figure 4.3. Schematic representation of the distal joints studied by Camerini-Otero and coworkers. Boxes indicate regions of homology between duplex and single-stranded DNA, thin lines indicate heterologous regions. "+" and "–" indicate complementary sequences. Adapted from Kim et.al.(25).

Camerini-Otero and coworkers have studied deproteinized distal joints formed using RecA, ATP, M13mp18 (circular ssDNA), and a 128 bp duplex DNA which contains 57 base pairs at its terminus which are homologous to a region of M13mp18 (Figure 4.3). Using 7deazaA and 7deazaG bases in either or both strands in the target duplex they measured the thermal stabilities of deproteinized joint molecules of substituted duplexes and M13 DNA. Modest decreases (~5-10°C) in stability were observed for duplexes where 7deazaG or 7deazaA were incorporated in the homologous strand. A slightly lower decrease (2-5°C) was observed for incorporation of these analogs in the complementary strand. The authors also report a partial DMS footprint of the incoming strand on the homologous strand. Based on this data Camerini-Otero and coworkers favor an intermediate where the incoming strand is located in the *major groove* of the duplex at the homologous site – a configuration consistent with *pairing before*

strand separation.. The planar base-triplets proposed by Camerini-Otero and coworkers are shown in Figure 4.2 B. A comparison of the proposed triplets shows that they are similar in the placement of the three bases but differ in the strands to which the bases are assigned.

Determination of groove location by affinity cleavage

Affinity cleavage is a technique wherein a redox-active metal ion tethered to a DNA-binding molecule, upon exposure to a reductant produces a small diffusible oxidant- presumably hydroxyl radicals- to cause localized cleavage of the DNA backbone (31). Affinity cleavage can be used as a reliable assay for determining the groove location and orientation of a DNA binding ligand (Figure 4.4).

Figure 4.4: Affinity cleavage patterns observed from placing a chelated iron atom in the major or minor groove of B-form DNA. Δ indicates the distance in base pairs between the location of the iron atom and the site of maximal cleavage.

Figure 4.5 A: Expected cleavage patterns for the two possible binding modes of RecA• oligonucleotide (EDTA)•Fe(II) filaments.

Figure 4.5 B: The location of the coordinated iron atom in each of the two possible intermediates for the three-strand exchange reaction mediated by RecA protein. W, C and R represent the Watson (homologous), Crick (complementary) and recombinant (incoming) strands respectively.

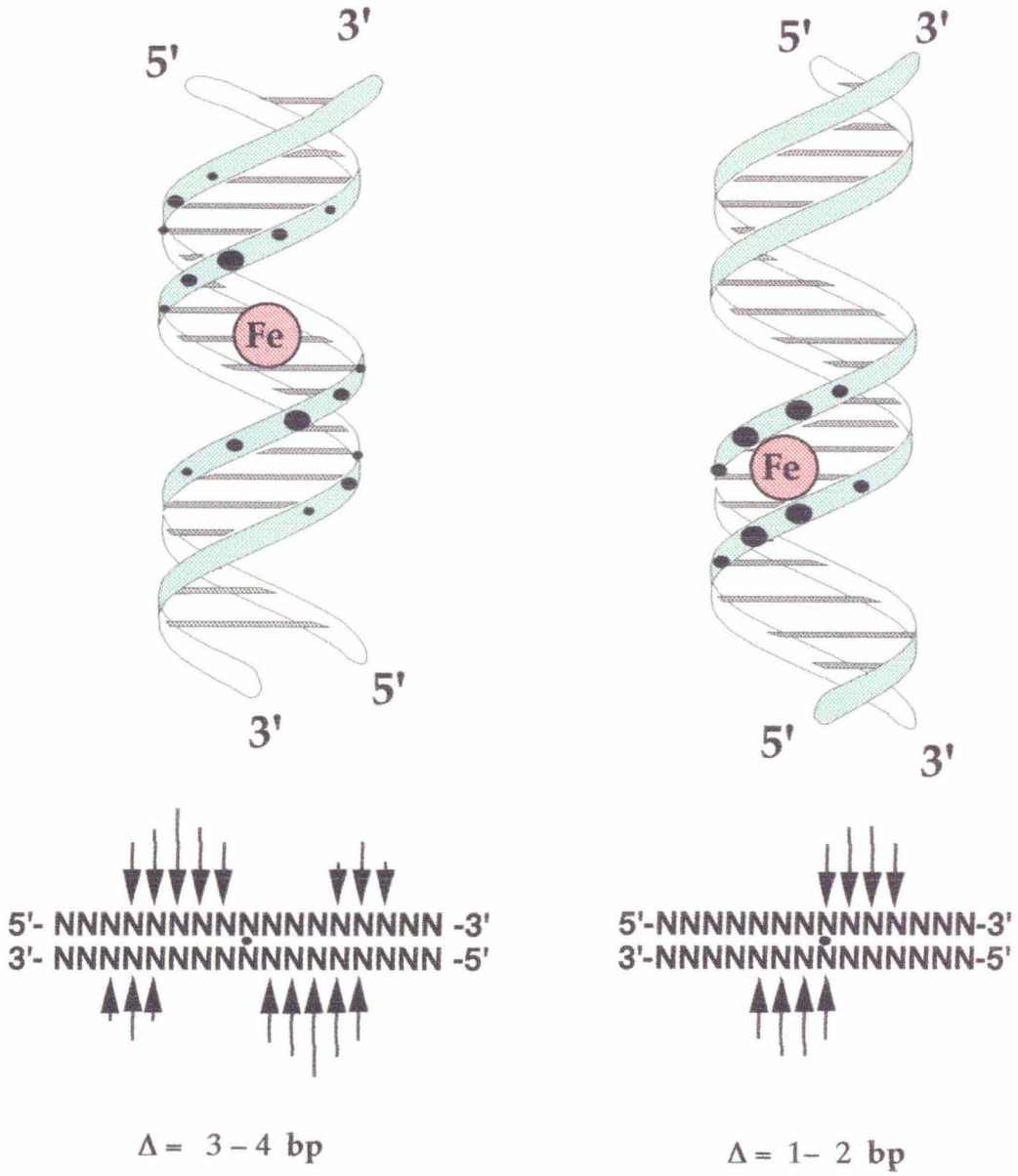

Δ = Distance in base pairs between location of chelated iron atom and site of maximal cleavage

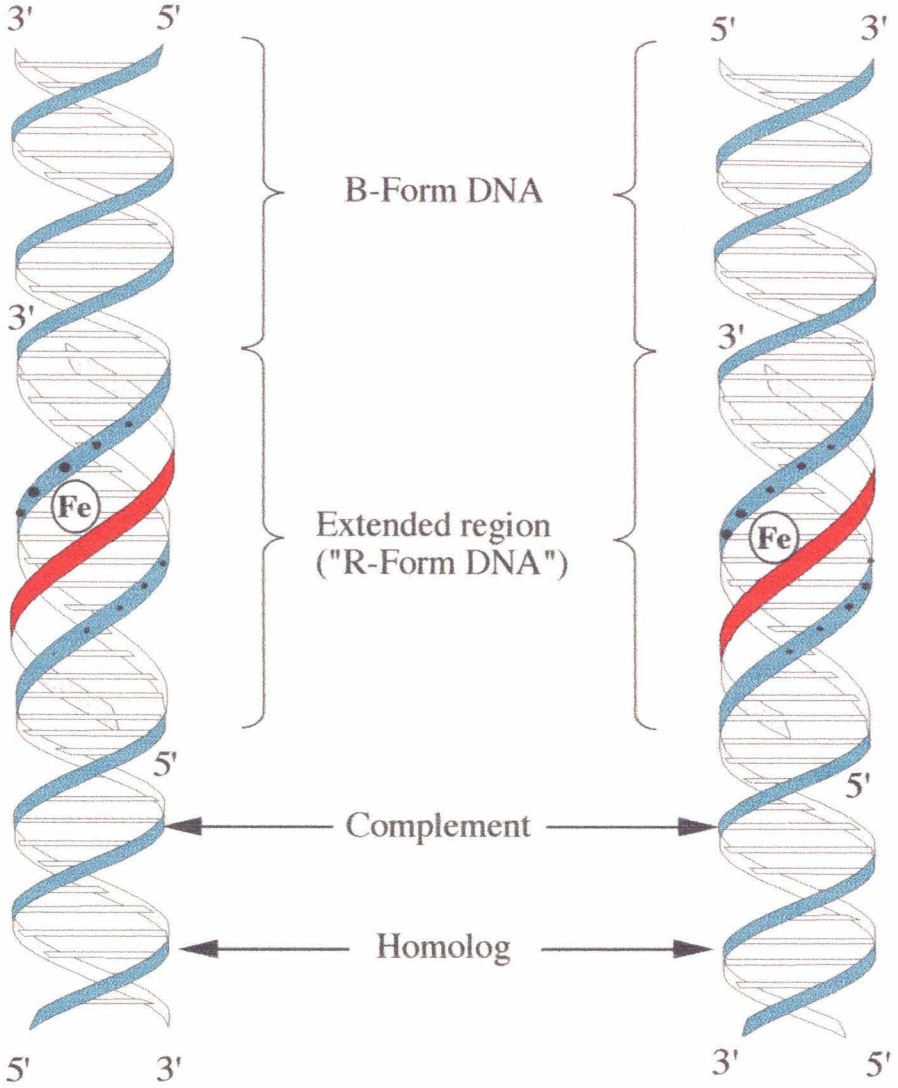

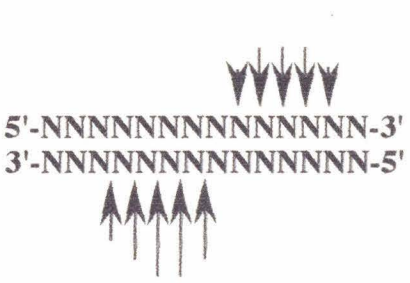

Minor groove binding

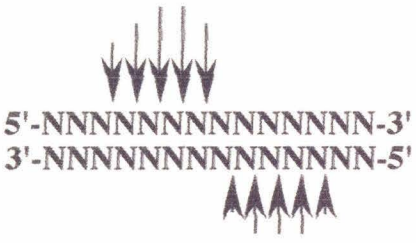

Major groove binding

Major groove binding

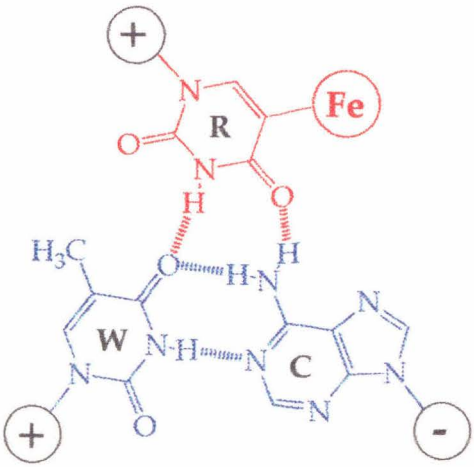

Minor groove binding

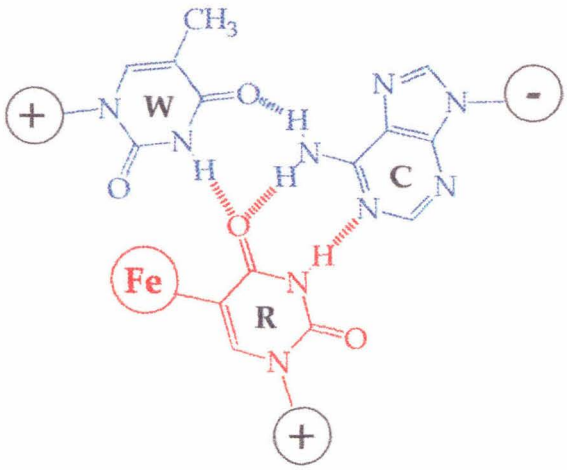

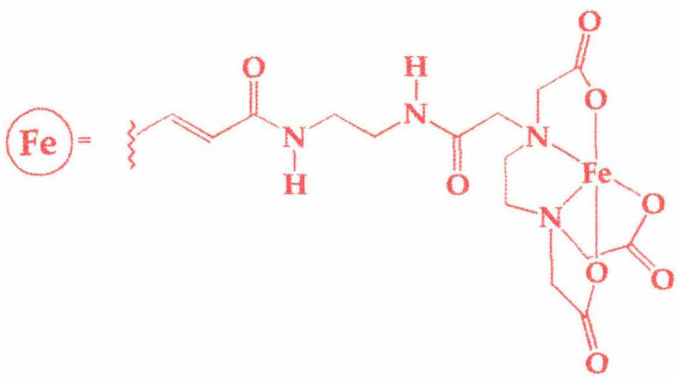

In our laboratories affinity cleavage with a variety of DNA binding molecules–intercalators, peptides, proteins and oligonucleotides, has provided detailed information about the binding site, groove location and orientation of these ligands (31,34-39). Because B-form DNA is right-handed, a binding mode that places the coordinated metal ion in the major groove of duplex DNA produces a cleavage pattern that is shifted toward the 5'- end on opposite strands whereas, if the metal ion is located in the minor groove, the cleavage pattern is shifted in the 3'- direction (Figure 4.4). To study the binding of oligonucleotide third strands in non-enzymatic triple helices, a modified thymidine derivative, T*, wherein the DNA cleaving moiety EDTA•Fe is covalently attached at C5 of the thymine heterocycle, can be incorporated into the oligonucleotides (36,37,39). It should be noted that in this case the intensity of the cleavage pattern generated on the two strands is dissymmetric because of the shielding of one of the strands by the oligonucleotide carrying the T*. The interpretation of groove location based on the 5'- or 3'- shifts of the cleavage pattern is therefore made using a set of oligonucleotides that carry T* at either terminal or internal sites.

Results and Discussion

The expected groove locations of the coordinated metal atom based on two proposed T•(TA) triplets, and the cleavage patterns that are expected for the two binding modes of the third strand in the three-stranded joint formed in the presence of RecA are illustrated in figure 4.5A and 4.5B respectively.

First, the set of oligonucleotides described in Chapter Two were used under reaction conditions that were strong enough to achieve cleavage on both

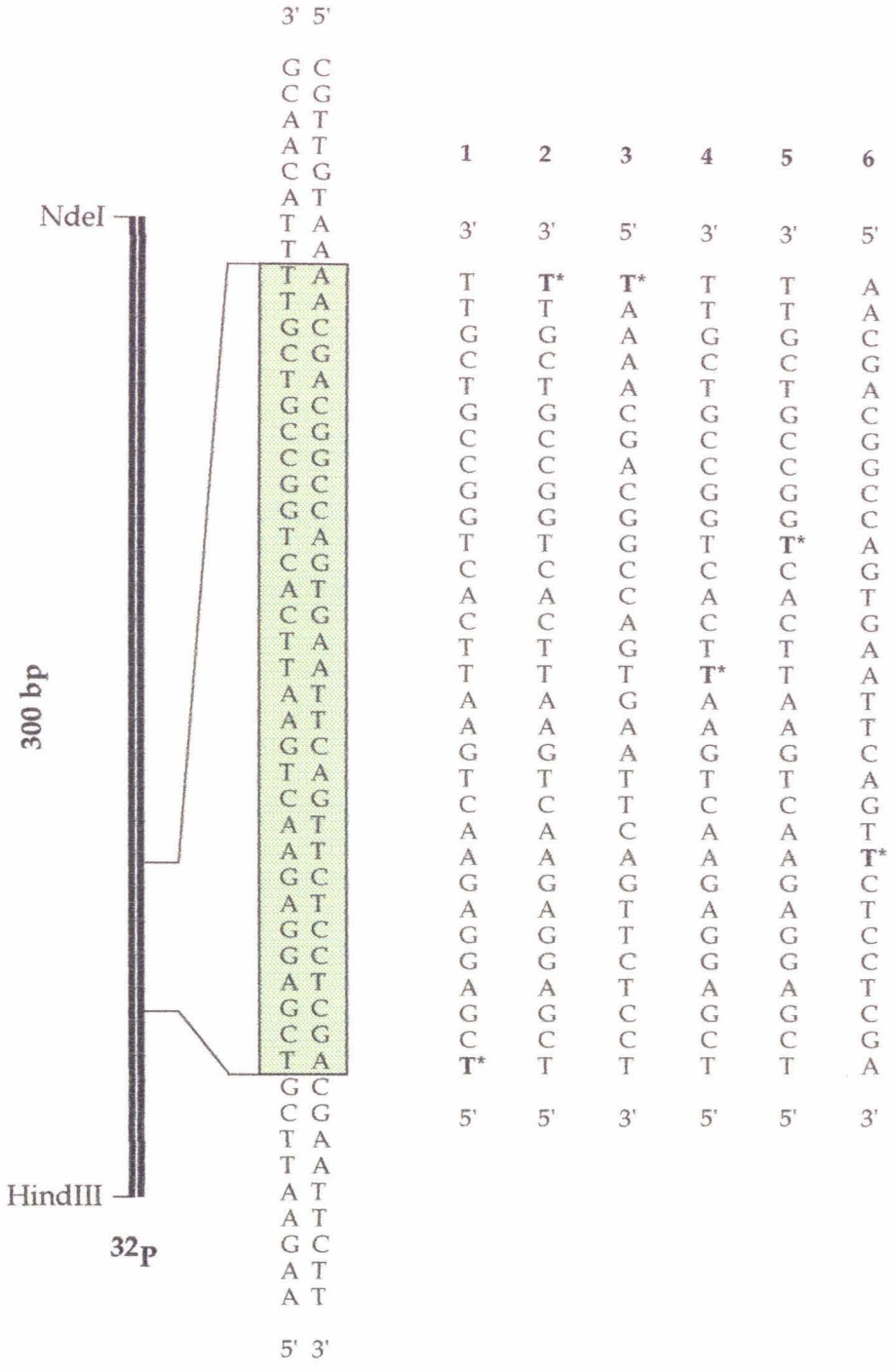

Figure 4.6: Schematic diagram of the restriction fragment, target site and oligonucleotides used to investigate groove location of the incoming strand.

Figure 4.7. **(A)** Storage phosphor autoradiogram of an 8% denaturing polyacrylamide gel containing the products of affinity cleavage reactions from terminal T* oligonucleotides. Lanes 2, 5, 8 and 11 contain cleavage products from DNA labeled on the 5′-end at the Hind III site and lanes 3, 6, 9 and 12 contain products from DNA labeled on the 3′-end at the Hind III site. Lanes 1, 7 and 13 contain the products of adenine-specific reaction (44) on 5'-end labeled duplex and lanes 4 and 10 contain the products from 3'-end-labeled duplex. Reaction components for all other lanes were as indicated in the figure under conditions described in Experimental.

(B) Histogram representations of the observed cleavage pattern. The lengths of the arrows represent the relative cleavage intensity at each nucleotide position.

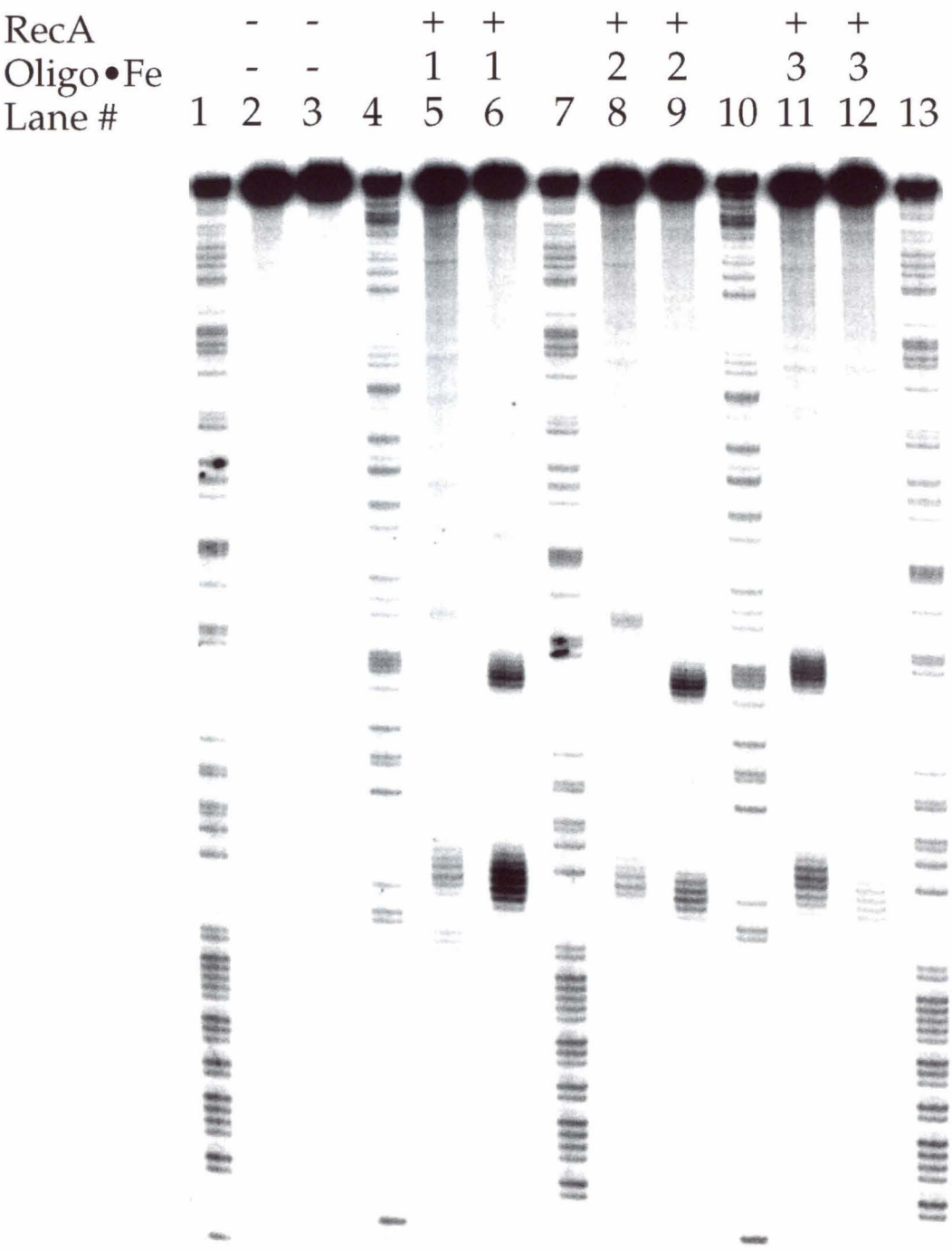
RecA - - + + + + +
Oligo•Fe - - 1 1 2 2 3 3
Lane # 1 2 3 4 5 6 7 8 9 10 11 12 13

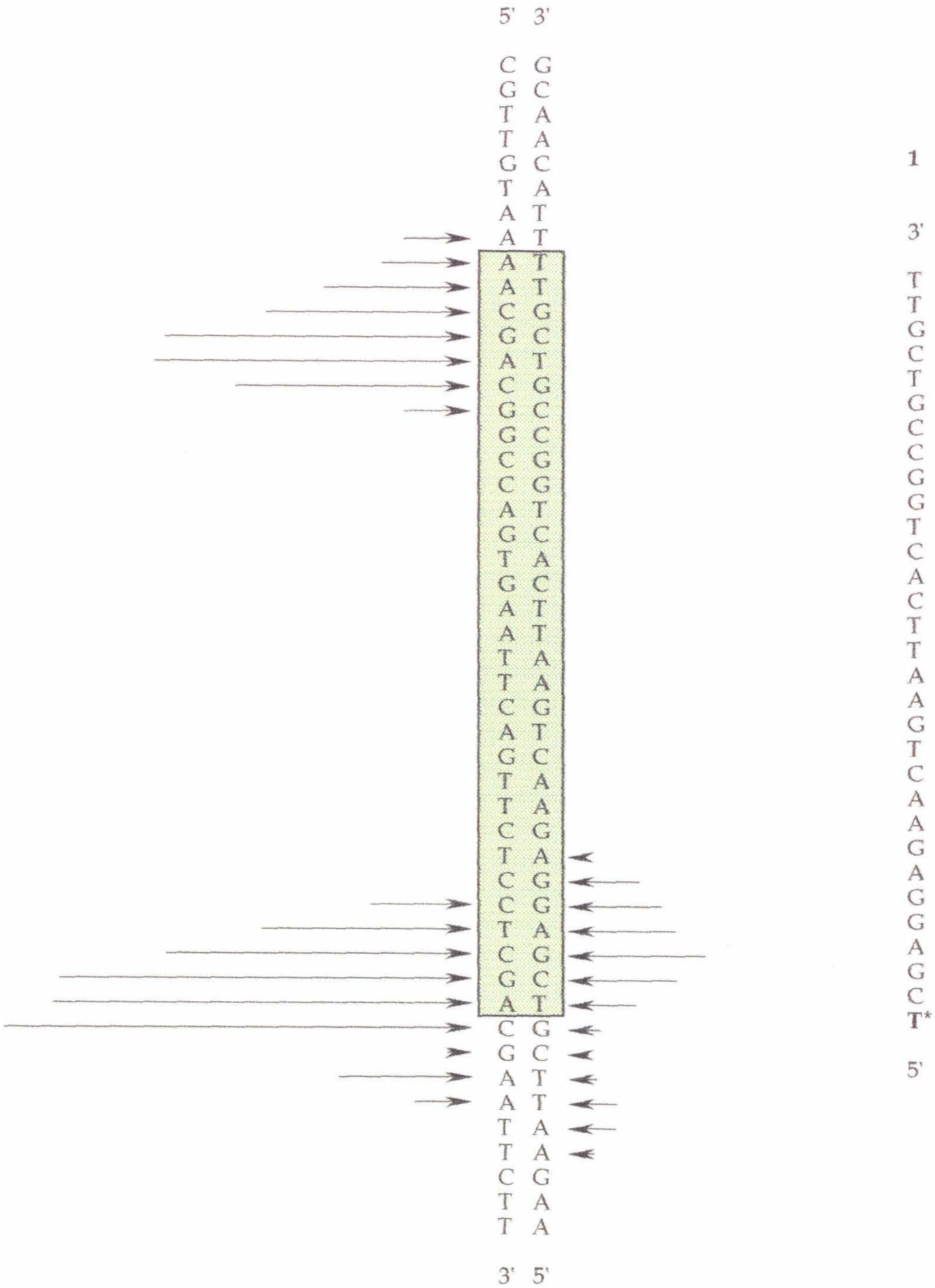
5' 3'
C G
G C
T A
T A
G C
T A
A T
A T
A T
A T
C G
G C
A T
C G
G C
G C
C G
C G
A T
G C
T A
G C
A T
A T
T A
T A
C G
A T
G C
T A
T A
C G
T A
C G
C G
T A
C G
G C
A T
C G
G C
A T
A T
T A
T A
C G
T A
T A
3' 5'
1
3'
T
T
G
C
T
G
C
C
G
G
T
C
A
C
T
T
A
A
G
T
C
A
A
G
A
G
G
A
G
C
T*
5'

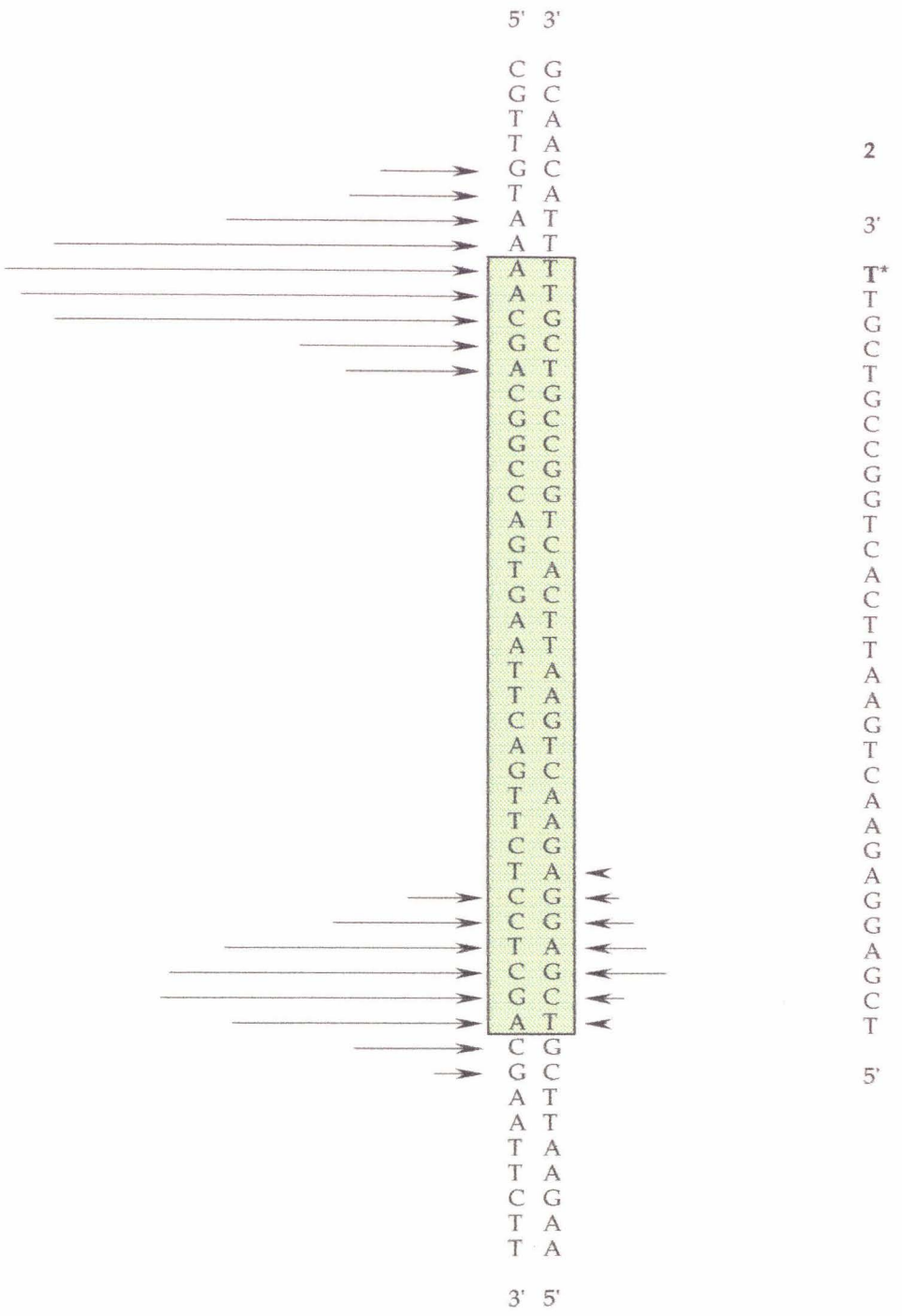
5' 3'
3' 5'
2
3'
T*
5'

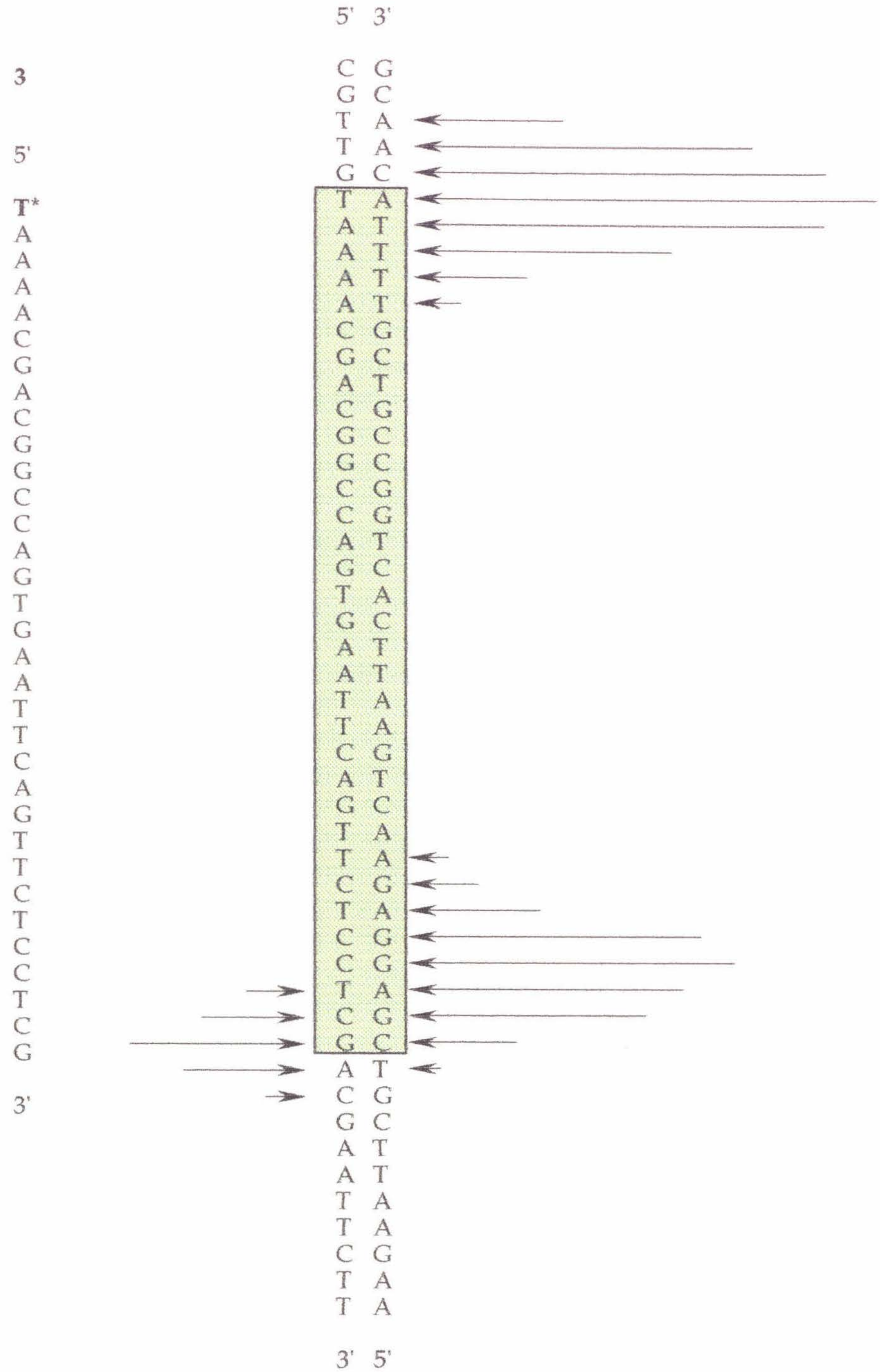
3
5'
T*AAAACGACGGCCAGTGAATTCAGTTCTCCTCG
3'
5' CGTTGTAAAACGACGGCCAGTGAATTCAGTTCTCCTCGACGAATTCTT 3'
3' GCAACATTTTGCTGCCGGTCACTTAAGTCAAGAGGAGCTGCTTAAGAA 5'

strands of the target duplex. As shown in figure 4.7, where cleavage is observable on both strands, a 3' shifted pattern is clearly visible. This is consistent with a chelated iron atom lying in the minor groove of the target duplex.

Since the cleavage patterns obtained by using the terminal T* oligonucleotides probably reflect the structure of the duplex-triplex junction, T* was next incorporated at a central position in an oligonucleotide which was homologous to a 31-bp target site in the plasmid pUCJWII47 (Figure 2, **1**). The results from this experiment are shown in Figure 4.8 A. Cleavage is observed on both strands only when both RecA and **4**•Fe are present in the reaction. The efficiency of cleavage produced at each nucleotide was measured (lanes 14,15)

Figure 4.8. **(A)** Storage phosphor autoradiogram of an 8% denaturing polyacrylamide gel containing the products of affinity cleavage reactions from oligonucleotide central T*. Lanes 2, 5, 8, 11 and 14 contain cleavage products from DNA labeled on the 5'-end at the Hind III site and lanes 3, 6, 9, 12 and 15 contain products from DNA labeled on the 3'-end at the Hind III site. Lanes 1, 7 and 13 contain the products of adenine-specific reaction (44) on 5'-end labeled duplex and lanes 4, 10 and 16 contain the products from 3'-end-labeled duplex. Reaction components for all other lanes were as indicated in the figure under conditions described in "Materials and Methods". **(B)** Histogram representation of the observed cleavage pattern. The lengths of the arrows represent the relative cleavage intensity at each nucleotide position.

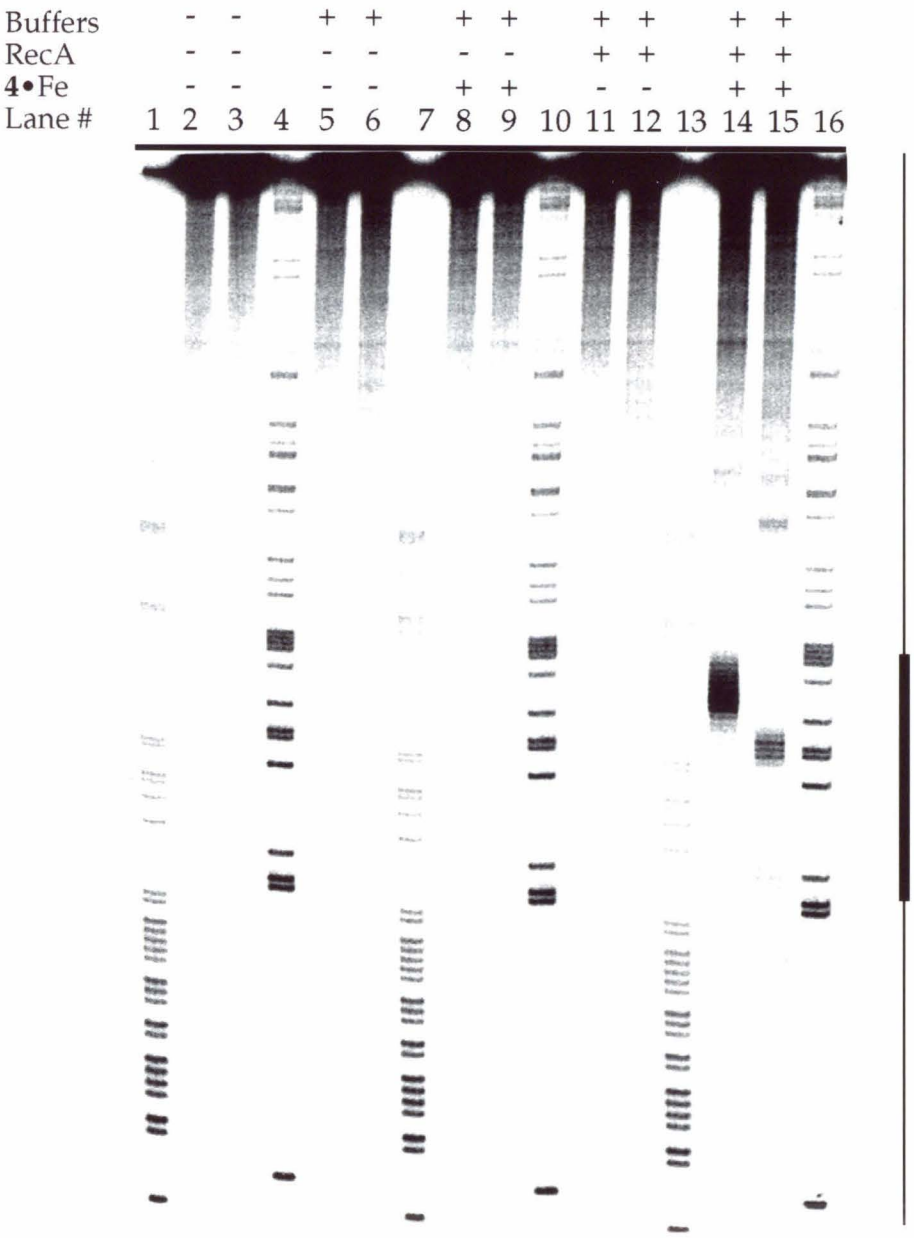
Buffers - - + + + + + + + +
RecA - - - - - - + + + +
4•Fe - - - - + + - - + +
Lane # 1 2 3 4 5 6 7 8 9 10 11 12 13 14 15 16

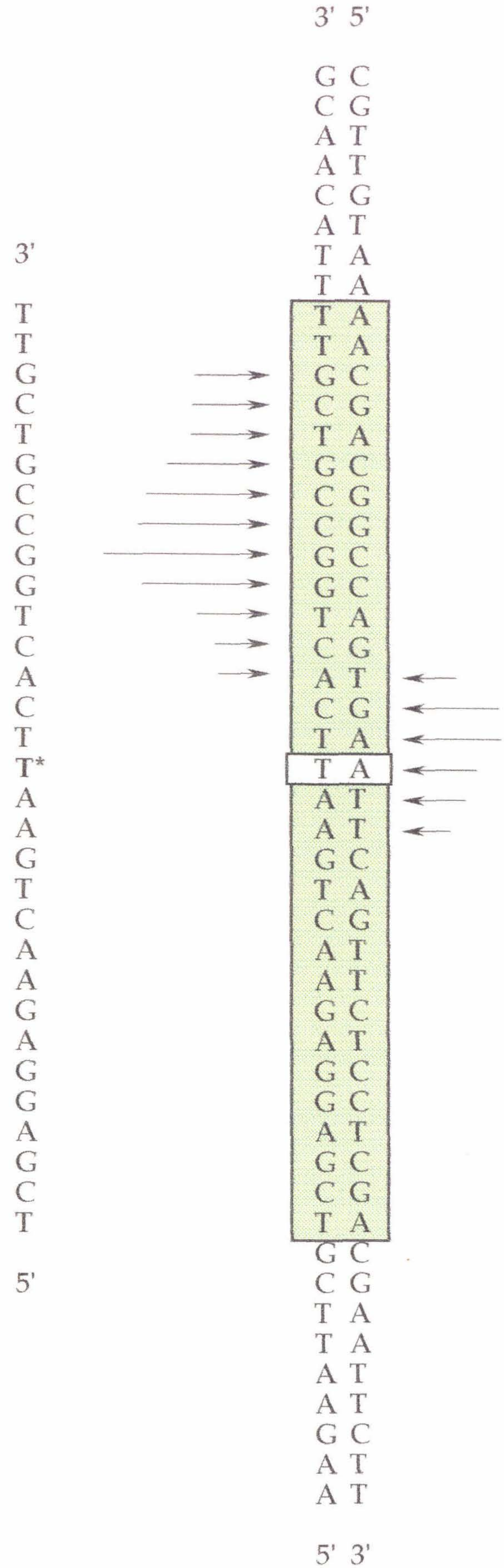
3' 5'
3'
TTGCTGCCGGTCACTT*AAGTCAAGAGGAGCT
5'
GCAACATTTTGCTGCCGGTCACTTAAGTCAAGAGGAGCTGCTTAAGAA
CGTTGTAAAACGACGGCCAGTGAATTCAGTTCTCCTCGACGAATTCTT
5' 3'

from the storage phosphor autoradiogram in Fig. 4.8A and the results of this analysis presented in histogram form are shown in Figure 4.8B. A 3'-shifted cleavage pattern is clearly visible. Again, the cleavage pattern is consistent with an intermediate in which the incoming strand has invaded the target duplex from the minor groove, leaving the outgoing strand located in the major groove of the nascent heteroduplex (23).

Formation of the products of strand exchange–an interwound heteroduplex and a completely displaced strand would be expected to give a cleavage pattern on only the complementary strand (36), and the fact that such a pattern is not observed suggests that the structure being studied is not simply a D-loop but one in which the displaced homologous strand is held in close association with the nascent heteroduplex. Shown in figure 4.10 is the case where **4** is simply hybridized to its complement and the affinity cleavage reactions are carried out for the indicated time.

Figure 4.9. Storage phosphor autoradiogram of an 8% denaturing polyacrylamide gel containing the products of affinity cleavage reactions from **4** hybridized to its complementary strand from the 300 bp restriction fragment from pUCJW. Lanes 3 -8 contain products from reactions carried out from 75 min. to 0 min. in 15 min. steps. Lanes 1 and 9 contain the products of adenine-specific reaction (44) on 3'-end labeled duplex and lanes 2 contains the products from 5'-end-labeled duplex. Histogram representation of the observed cleavage pattern is shown alongside.

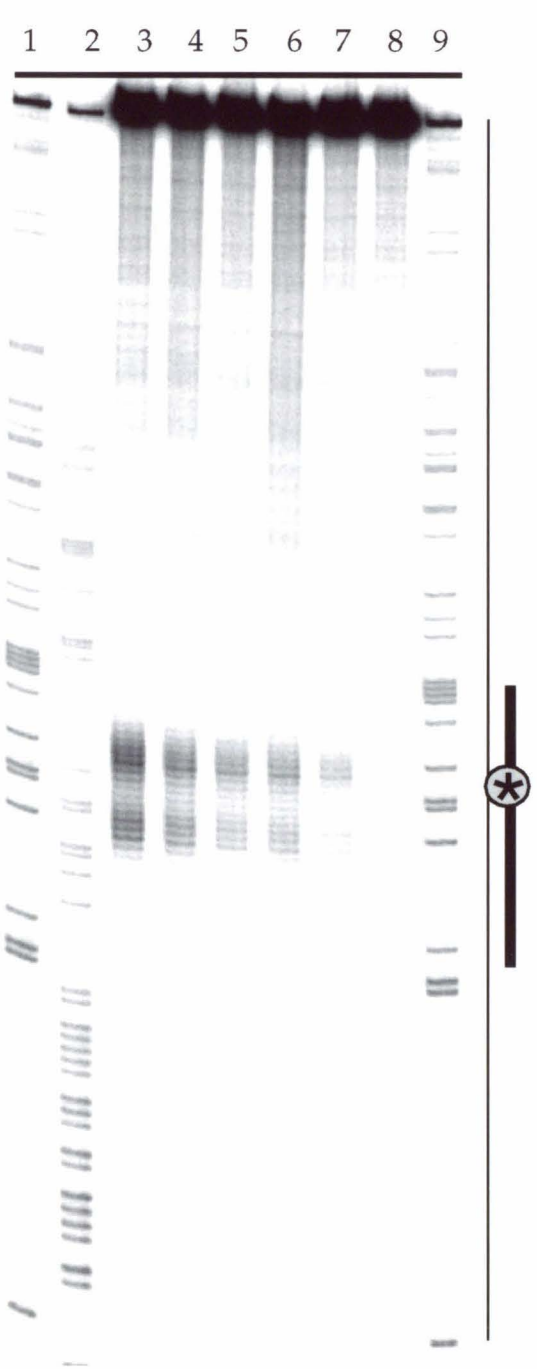
1 2 3 4 5 6 7 8 9

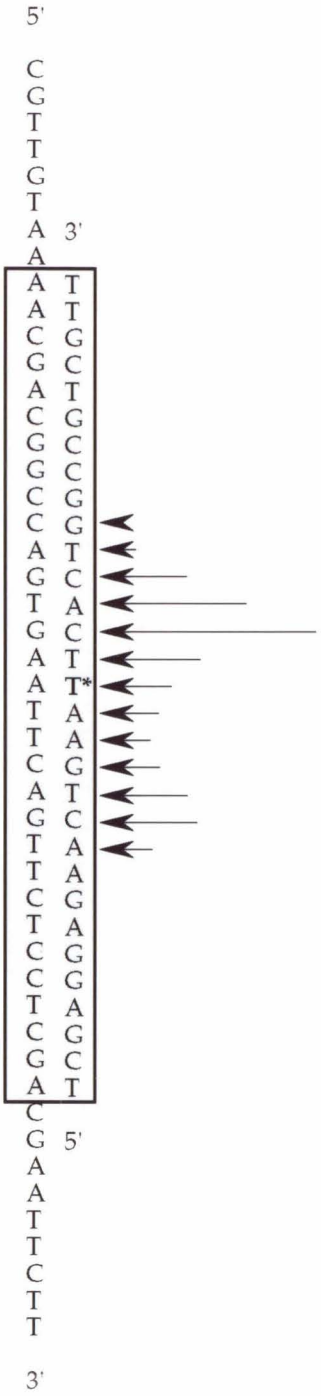
5'
CGTTGTAA
AACGACGGCCAGTGAATTCAGTTCTCCTCGA
3'
TTGCTGCCGGTCACTTT*AAGTCAAGAGGAGCT
5'
CGAATTCTT
3'

In order to more rigorously test the possibility that the outgoing strand is not simply a D-loop, we designed an experiment where the 31 mer with internal T* was hybridized to a synthetic D-loop as shown in figure 4.10A. The cleavage patterns obtained from this complex(Figure 4.10 B) show little if any reproducible cleavage is seen on the D-looped strand. The cleavage pattern obtained from the bulged hybrid is therefore clearly different from that obtained in the three stranded complex. This is further evidence that the outgoing strand is not simply a D-loop but a strand held in close proximity to the major groove of the nascent heteroduplex.

For oligonucleotide **4** it is intriguing that although the 3'-shift remains intact upon transferring the T* from the termini to a central site, the magnitudes of cleavage observed are reversed and the displacement of the center of the observed cleavage pattern from the location of the T* residue is also changed from 1 bp in the 3'- direction to between 3 and 4 bp in the 3' direction. To observe the effect of transferring the T* to a position internal to the oligonucleotide but not central, we designed oligonucleotide **5** (Figure 4.6). The cleavage pattern observed using this oligonucleotide is shown in figure 4.11. A 3'-shifted cleavage pattern is clearly observable. However the center of the cleavage pattern is displaced by ~4 nucleotide positions from the location of the T* residue.

As pointed out earlier, in cases where affinity cleavage patterns from oligonucleotides carrying a T* residue at an internal position, are used to make interpretations about the groove location of the chelated metal atom, the protection of one of the strands of the target duplex by the third strand

Figure 4.10: A. Synthetic D-loop complex formed using 60 base long oligonucleotides **7** and **8** hybridized to oligonucleotide **4**.

B. Storage phosphor autoradiogram of an 15% denaturing polyacrylamide gel containing the products of affinity cleavage reactions. Lanes 1 and 5 contain the products of adenine-specific reaction (44) on **8** and lanes 4 and 8 contain the products from A-reaction on **7**. Affinity cleavage reactions were carried out as previously described both in the presence and absence of RecA.

A

```
7 5'-TATGAGACTGTCTAA----AACGACGGCCAGTGAA TTCAGTTCTCCTC---GAAGTACTAGGCCTGG---3'
8 3'---ACTCTGACAGATT 3'-TTGCTGCCGGTCACT T*AAGTCAAGAGGAG-5'CTTCATGATCCGGACCGC-5'
                      \                                  /
                       CCAAGATTACAGTTACCTGTACGTTATACTA
```

B

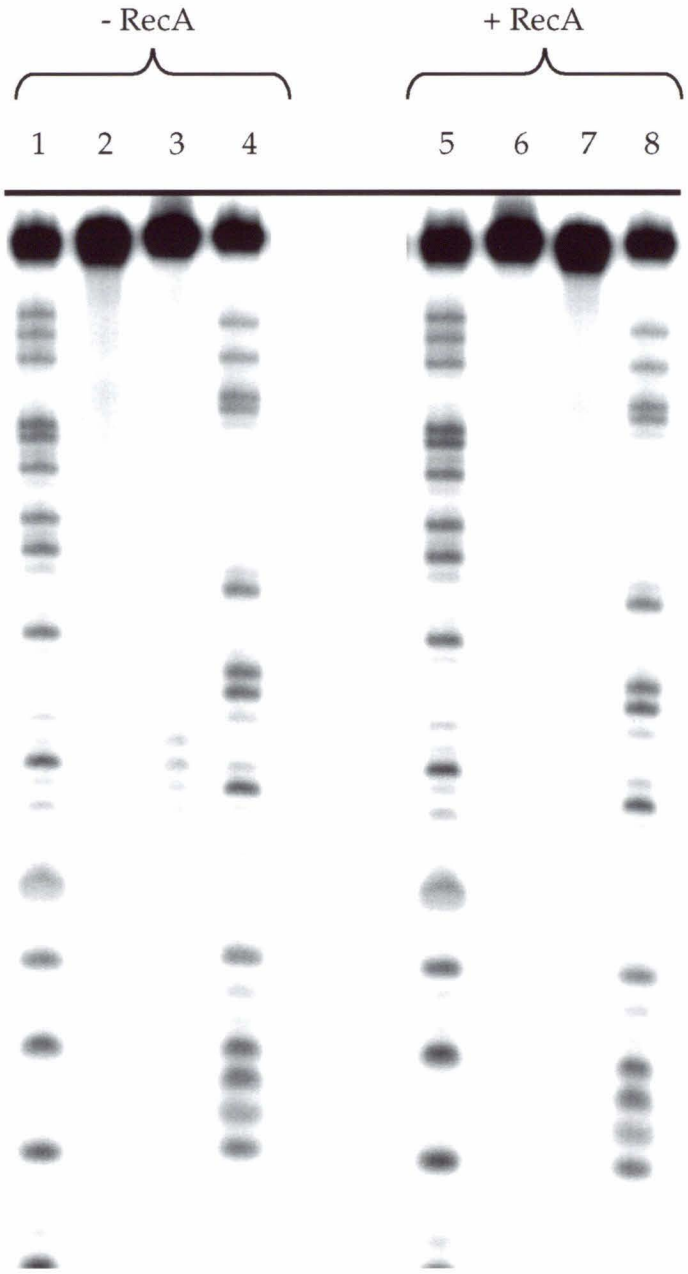

Figure 4.11. Storage phosphor autoradiogram of an 8% denaturing polyacrylamide gel containing the products of affinity cleavage reactions from oligonucleotide **5**. Lanes 3 contains the cleavage products from DNA labeled on the 3′-end at the Hind III site and lane 4 contains products from DNA labeled on the 5′-end at the Hind III site. Lane 1 contains the products of adenine-specific reaction (44) on 5'-end labeled duplex and lane 2 contains the products from 3'-end-labeled duplex. Histogram representation of the observed cleavage pattern is shown alongside.

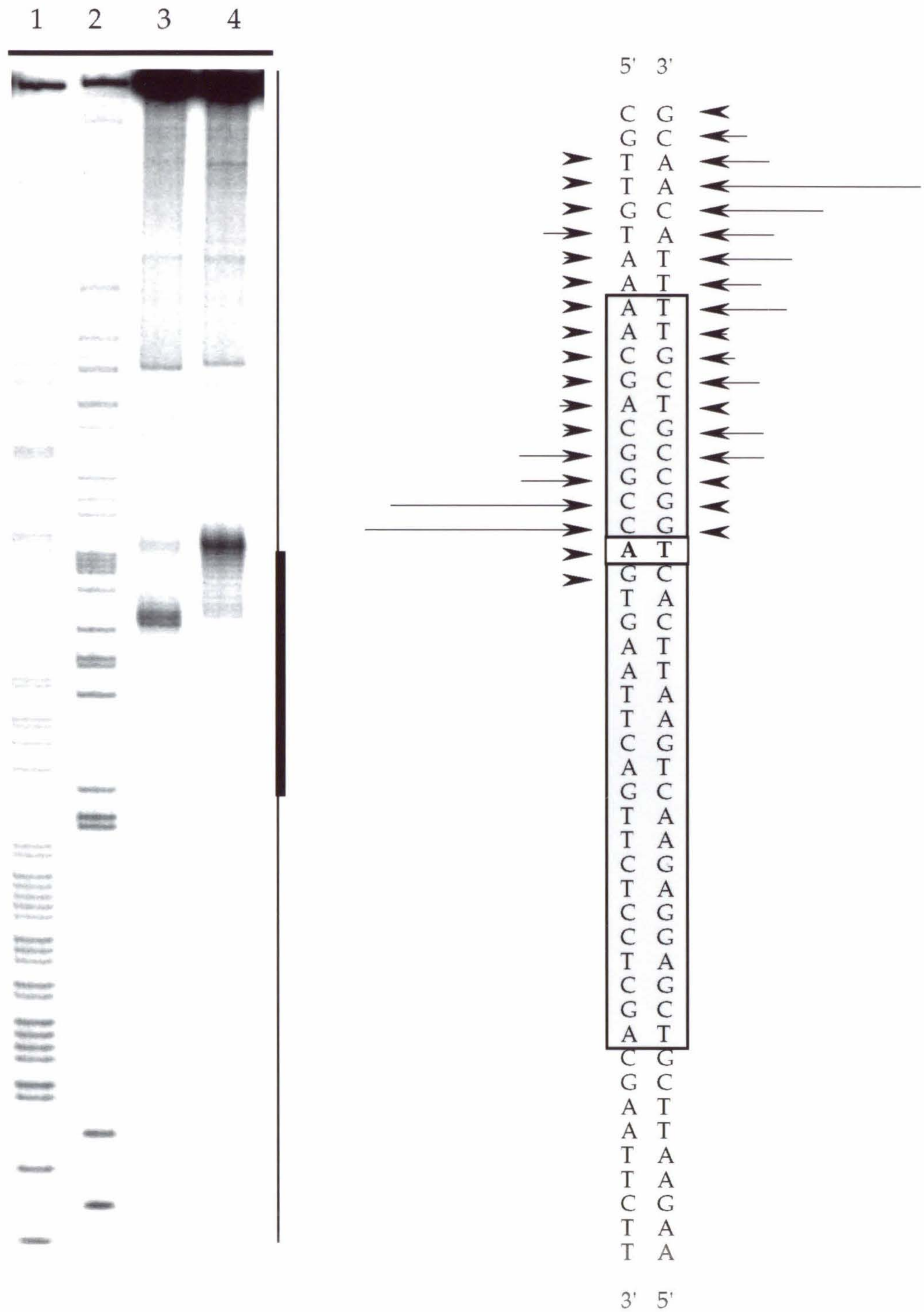
1 2 3 4
5' 3'
C G
G C
T A
T A
G C
T A
A T
A T
A T
A T
C G
G C
A T
C G
G C
G C
C G
C G
A T
G C
T A
G C
A T
A T
T A
T A
C G
A T
G C
T A
T A
C G
T A
C G
C G
T A
C G
G C
A T
C G
G C
A T
A T
T A
T A
C G
T A
T A
3' 5'

sometimes causes cleavage patterns that are *apparently 3'- shifted*. However in these cases the site *proximal* to the location of the T* residue is cleaved more efficiently than sites distal from T*. The histogram in figure 4.12 clearly shows that this is not the case. However, to verify that the differences in the magnitude of cleavage observed were not a result of different labeling efficiencies, an oligonucleotide complementary to **4** and carrying a T* at an internal site was designed (Oligonucleotide **6**, Figure 4.6). The results from this study are shown in figure 4.12. As expected, the 3'-shift remains intact but the magnitude of cleavage observed on either strand is reversed.

The finding that the nucleoprotein filament in the recombination intermediate is lodged in the minor groove of the target duplex is consistent with a number of observations from different laboratories. First, as mentioned in the introduction, Radding and coworkers found that methylation of functional groups in the major groove – the N4 position of cytosine, N6 of adenine and N7 of guanine, did not effect the rate or extent of joint molecule formation, but reduced the thermal stability of the deproteinized complex (27). Second, Jain and Cox have shown that the N7 position of guanine bases in the target duplexes are not involved in the formation of the three stranded complexes(40). And finally, Kumar and Muniyappa recognized the possibility of minor groove contacts when they observed the inhibition of joint molecule formation by a minor groove binding ligand- distamycin, but not by a major groove binder–methyl green (41).

Before concluding, it is of interest to examine more critically the evidence presented by Camerini-Otero and coworkers for major groove binding of the

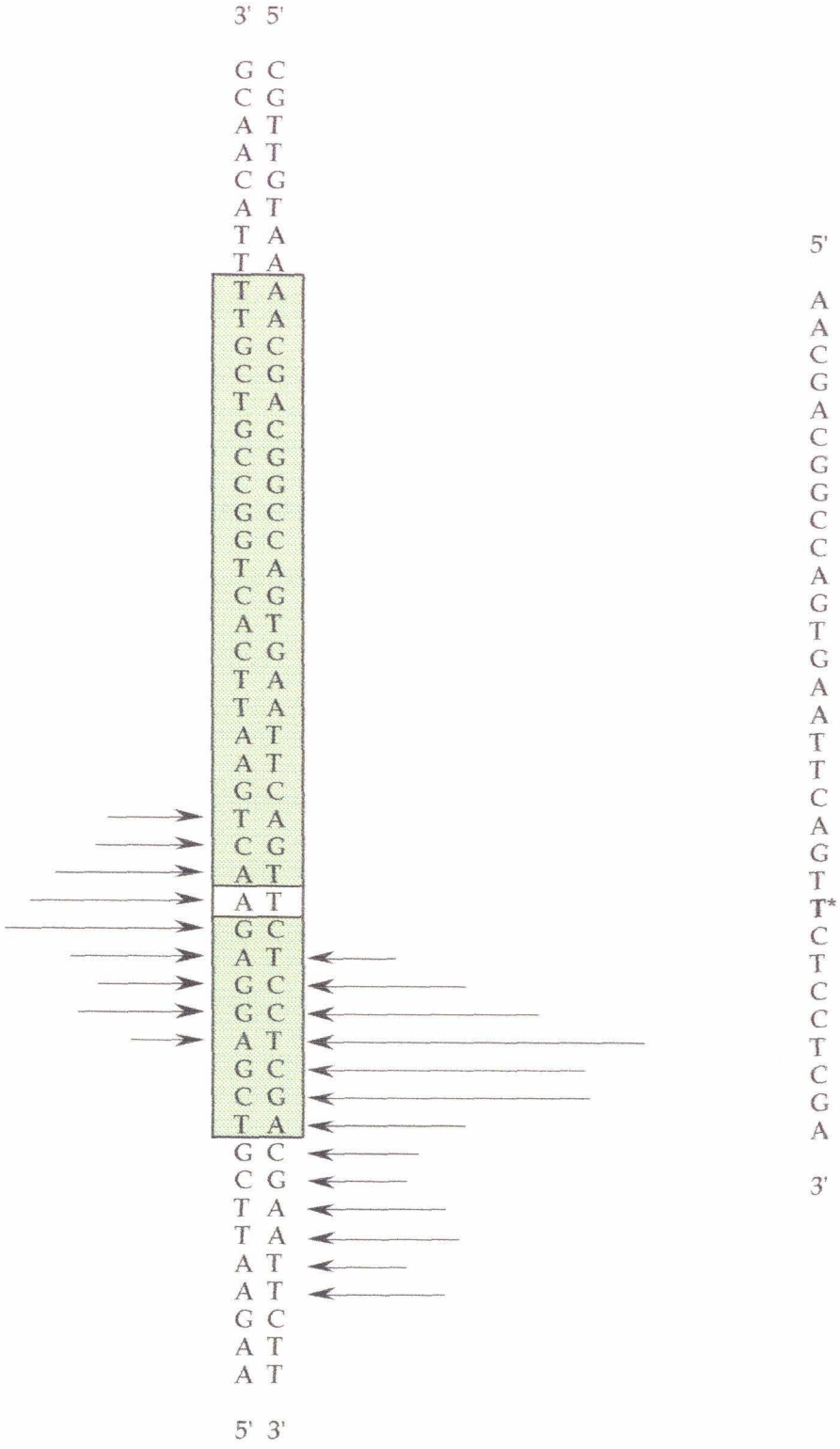

Figure 4.12. Histogram representation of the observed cleavage pattern from affinity cleavage reactions with oligonucleotide **6**.

third strand. First we note that the inclusion of 7-deaza-purines is known to destabilize duplexes, presumably due to the change in electronic character of the purine ring (45). Therefore, it is not unlikely that these substitutions would cause destabilization of a three-stranded complex formed by insertion of the incoming strand in the minor groove. Such an effect should be observable for incorporation of the 7-deaza analogs in either strand of the target duplex since the triplex intermediate involves hydrogen bonding between all three strands. In fact, Kim et.al. report lower melting temperatures for the three stranded complex when 7-deaza purines are incorporated into either strand of the duplex (25). Surprisingly, using a *single* determination for each of the Tm's of duplexes containing 7-deaza adenosine and 7-deaza guanosine bases, the authors concluded that the modified duplexes were of stability comparable to the parent duplex. Kim et al. also report absence of DMS hyperreactivity in the minor groove of the target duplex in triplexes generated using RecA compared to non-enzymatic triplexes, which they interpret as "a distinctive structural signature of parallel triplexes". We believe that this is more evidence for the minor grove location of the third strand.

CONCLUSIONS

We have used affinity cleaving techniques to probe the structure of the protein associated joint molecule formed between a RecA-oligonucleotide filament and Watson-Crick double helical DNA using an oligonucleotides with EDTA•Fe attached at a terminal or internal positions. We observed cleavage of both the homologous and complementary strands at the site predicted by antiparallel binding of the filament to its complementary sequence. The cleavage

pattern was shifted toward the 3'-end on opposite strands, clearly indicating the minor groove location of the incoming oligonucleotide. Comparison with a bulged hybrid showed that the outgoing strand is not simply a D-loop. Complementary oligonucleotides with internal T* residue gave cleavage patterns that were also 3'-shifted and showed the expected reversal of intensities on the two labeled strands on the target duplex. Taken together, our data argues strongly for minor groove approach of the incoming strand in a three strand reaction initiated by formation of ssDNA•RecA filaments.

There is a growing consensus regarding the existence of a three-stranded intermediate and the positioning of the three bases according to the energy minima described by Zhurkin *et.al.* (42). In fact, in a recent report Van Meervelt *et.al.* show crystallographic evidence for the feasibility of the proposed G•(GC) base triplet (43). While we acknowledge the possibility of existence of the proposed base triplets in the strand exchange intermediate, our affinity cleavage analysis does not directly address this issue and only indicates the close association of the third strand with the nascent heteroduplex. The initial recognition step may therefore involve either recognition of specific functional groups in the minor groove or local melting of the duplex following the insertion of the third strand in the minor groove.

EXPERIMENTAL

General. RecA protein was isolated from the strain JC12772 using standard protocols as modified by Kowalczykowski. Sonicated, deproteinized calf thymus DNA (Pharmacia) was dissolved in H_2O to a final concentration of 2.0 mM in base pairs and was stored at 4 °C. Glycogen was obtained from Boehringer-Mannheim as a 20 mg/ml aqueous solution. γ-S-ATP purchased from Sigma, was found to contain <10% ADP by HPLC analysis and stored in 100 mM aliquots -20 °C. Nucleoside triphosphates labeled with ^{32}P were obtained from Amersham or ICN and were used as supplied. Cerenkov radioactivity was measured with a Beckman LS 2801 scintillation counter. Restriction endonucleases were purchased from Boehringer Mannheim or New England Biolabs and were used according to the supplier's recommended protocol in the activity buffer provided. Klenow fragment and T4 polynucleotide kinase were obtained from Boehringer Mannheim. Phosphoramidites were purchased from Glen Research.

Construction of pUCJWII47. This plasmid was prepared by standard methods (32) by annealing two synthetic oligonucleotides, 5'-AATTCAGTTCTCCTCGACGAATTCTTTTTCTTTCTTCTTTTCTTCGAGTCGAGTCGAG-3' and 5'-GATCCTCGACTCGACTCGAAGAAAAGAAGAAAGAAAAAGAATTCGTCGAGGAGAACTG-3', followed by ligation of the resulting duplex with pUC19 DNA previously digested with EcoRI and BamHI; this ligation mixture was used to transform *E. Coli* XL1-Blue competent cells (Stratagene). Plasmid DNA from transformants was isolated, and the presence

of the desired insert was confirmed by restriction analysis and Sanger sequencing. Preparative isolation of plasmid DNA was performed using a Qiagen plasmid kit.

Synthesis and Purification of Oligodeoxyribonucleotides.

Oligodeoxyribonucleotides were synthesized using standard automated solid-support chemistry on an Applied Biosystems Model 380B DNA synthesizer and *O*-cyanoethyl-*N,N*-diisopropyl phosphoramidites. Crude oligonucleotide products containing the 5′-terminal dimethoxytrityl protecting group were purified by reverse phase FPLC using a ProRPC 16/10 (C_2-C_8) column (Pharmacia LKB) and a gradient of 0-40% CH_3CN in 0.1 M triethylammonium acetate, pH 7.0, detritylated in 80% aqueous acetic acid, and chromatographed a second time.

Modified thymidine was incorporated at a central position in oligonucleotide **1** (Figure 2) using the β-cyanoethyl-*N,N*-diisopropylchlorophosphoramidite of a thymidine derivative containing an appropriately protected linker-amine (Amino modifier C2-dT, Glen Research). Deprotection was carried out in concentrated NH_4OH at 55 °C for 24 h. Following trityl-on and trityl-off FPLC purification, the oligonucleotide containing a free amine attached to C5 of the 5′-thymidine was post-synthetically modified with EDTA monoanhydride as described (33) to give the T* oligonucleotide **1**. The modified oligonucleotide was chromatographed a third time by FPLC using a gradient of 0-40 % CH_3CN in 0.1 M NH_4OAc.

Purified oligonucleotides were desalted on Pharmacia NAP-5 Sephadex columns. The concentrations of single-stranded oligonucleotides were determined by UV absorbance at 260 nm using extinction coefficients calculated by addition of the monomer nucleoside values (values for T were used in place of T* in the calculation). Complete postsynthetic modification was verified by degradation to nucleosides using snake venom phosphodiesterase and calf alkaline phosphatase folowed by HPLC analysis on a MicrosorbMV (Rainin) reverse phase column. Repeated attempts at MALDI-TOF spectroscopy were unsuccessful. Oligonucleotide solutions were lyophilized to dryness for storage at -20 °C.

DNA Manipulations. The 300 bp HindIII/NdeI restriction fragment of the plasmid pUCJWII47 (Figure 2) was isolated and labeled at the 5′- or 3′-end on the HindIII side by standard procedures (32). The hybrid with the synthetic D-loop was isolated by first hybridizing the three oligonucleotides **4, 7** and **8,** followed by purification of the hybrid on a 25% non-denaturing gel. The bulged hybrid does not run as a punctate band and some smearing is seen. Adenine-specific sequencing reactions were carried out as previously described (44) .

Affinity Cleavage Reactions. A dried pellet of oligo-nucleotide-EDTA was dissolved in a solution of aqueous $Fe(NH_4)_2(SO_4)_2 \bullet 6H_2O$ to produce a solution that was 20 μM in oligonucleotide and Fe(II). This solution was allowed to equilibrate for at least 15 min at room temperature. A stock solution was prepared containing 60 μl 10x buffer (250 mM Tris-acetate, 40 mM Mg-acetate, 1 mM EGTA, 5 mM spermidine, 8 mM β-mercaptoethanol, pH 7.5), 30 ml of 2 mM

bp calf thymus DNA (added to supress background oxidative cleavage of target DNA), and 20 ml acetylated BSA (3 mg/ml). To a given reaction was added 5.5 µl stock solution, 3 µl of either the oligonucleotide-EDTA•Fe(II) at 20 mM or H_2O (for control reactions, 3 µl of RecA solution (7.4 mg RecA/ml RecA storage buffer) plus RecA storage buffer (20 mM Tris-HCl, 0.1 mM EDTA, 1 mM DTT, 50% glycerol, pH 7.5) to give the designated nucleotide to monomer ratio (excess RecA storage buffer was added to ensure that each reaction was run under the same conditions), and enough H_2O to give a final reaction volume of 30 µl after ascorbate addition. Following a 1 min incubation at 37 °C, nucleoprotein filament formation was initiated by addition of 1 ml 30 mM γ-S-ATP. After 10 min, approximately 20,000 cpm (~ 1 nM) of 3'- or 5'-labeled duplex was added and joint molecule formation was allowed to proceed for 30 min at 37 °C. The cleavage reactions were initiated by the addition of 1 ml 30 mM sodium ascorbate. The final reaction conditions were 25 mM Tris-acetate, 6 mM Tris-HCl, 4 mM $Mg(OAc)_2$, 1 mM EGTA, 32 mM EDTA, 0.5 mM spermidine, 0.8 mM β-mercaptoethanol, 5% glycerol, 100 mM bp calf thymus DNA approximately 1 mM sodium ascorbate, pH 7.5. After 8 -14 h, the cleavage reactions were stopped by phenol/chloroform extraction and precipitation of the DNA by the addition of glycogen, NaOAc (pH 5.2), and $MgCl_2$ to final concentrations of 140 mg/ml, 0.3 M, and 10 mM, respectively, and 100 ml ethanol. The DNA was isolated by centrifugation and removal of the supernatant. The precipitate was dissolved in 20 µl H_2O, frozen, and lyophilized to dryness. DNA in each tube was

resuspended in 5 µl of formamide-TBE loading buffer containing 0.1% SDS and transferred to a new tube. The DNA solutions were assayed for Cerenkov radioactivity by scintillation counting and diluted to 5000 cpm/ml with more formamide-TBE loading buffer containing 0.1% SDS. The DNA was denatured at 90 °C for 5 min, and loaded onto an 8% denaturing polyacrylamide gel. The DNA cleavage products were electrophoresed in 1x TBE buffer at 50 V/cm. The gel was dried on a slab dryer and then exposed to a storage phosphor screen. The gel was visualized with a Molecular Dynamics 400S PhosphorImager. Cleavage intensities at each nucleotide position were measured using the ImageQuant™ software and the pixel values obtained were plotted in the form of histograms using Kaleidagraph™ software.

References

1. Stasiak, A. and Egelman, E.H. (1994), *Experientia* **50**, 192-203.
2. Kowalczykowski, S. C. & Eggleston, A. K. (1994), *Annu. Rev. Biochem.* **63**, 991-1043
3. West, S. C. (1992), *Annu. Rev.Biochem.* **61**, 603-640.
4. Radding, C. M. (1991), *J. Biol. Chem.* **266**, 5355-5358.
5. Egelman, E. H. &Yu, X. (1989), *Science* **245,** 404-407.
6. Flory, J. & Radding, C. M. (1982), *Cell* **28**, 747-756.
7. Dunn, K., Chrysogelos, S. & Griffith, J. (1982), *Cell* **28**, 757-765.
8. Flory, J., Tsang, S. S. & Muniyappa, K. (1984), *Proc. Natl. Acad. Sci. USA* **81**, 7026-7030.
9. Stasiak, A. , Egelman, E. H. & P. Howard-Flanders (1988), *J.Mol.Biol.* **202**, 659-662.
10. Gonda, D. K. & Radding, C. M. (1983), *Cell* **34**, 647-654.
11. Julin, D. A., Riddles, P. W. & Lehman, I. R. (1986), *J. Biol. Chem.* **261**, 1025-1030.
12. Tsang, S. S., Chow, S. A. & Radding, C. M. (1985), *Biochemistry* **24**, 3226-3232.
13. Honigberg, S. M., Gonda, D. K., Flory, J. & Radding, C. M. (1985), *J. Biol. Chem.* **260**, 11845-11851.
14. Menetski, J. P., Bear, D. G. & Kowalczykowski, S. C. (1990), *Proc. Natl. Acad. Sci. USA* **87**, 21-25.

15. Register, J. C., Christiansen, G. & Griffith, J. (1987), *J. Biol. Chem.* **262**, 12812-12820.

16. Umlauf, S. W., Cox, M. M. & Inman, R. B. (1990), *J. Biol. Chem.* **265**, 16898-16912.

17. Jain, S., Cox, M. M. & Inman, R. B. (1995), *J. Biol. Chem* **270**, 4943-4949.

18. Takahashi, M., Kubista, M. & Norden, B. (1991), *Biochimie* **73**, 219-226.

19. Rao, B.J., Jwang, B. & Dutreix, M. (1990), *Biochemie* **73**, 363-370.

20. Stasiak, A. (1992), *Molecular Microbiology* **6**, 3267-3276.

21. Howard-Flanders, P., West, S. C. & A. Stasiak (1984), *Nature* **309**, 215-220.

22. Adzuma, K. (1992), *Genes Devel.* **6**, 1679-1694.

23. Rao, B. J., Chiu, S. K. & Radding, C. M. (1993), *J. Mol. Biol.* **229,** 328-343.

24. Camerini-Otero, R.D. & Hsieh, P., *Cell* (1993). **73**, 217-223.

25. Kim, M. G., Zhurkin, V. B., Jernigan, R. L. & R. D. Camerini-Otero (1995), *J.Mol.Biol.* **247**, 874-889.

26. Rao, B. J., Dutreix, M. & Radding, C. M. (1991), *Proc. Natl. Acad. Sci. USA* **88**, 2984-2988.

27. Chiu, S. K., Rao, B. J., Story, R. M. & Radding, C. M. (1993), *Biochemistry* **32**, 13146-13155.

28. Hsieh, P., Camerini-Otero, C. S. & Camerini-Otero, R. D. (1990), *Genes Devel.* **4**, 1951-1963.

29. Hsieh, P., Camerini-Otero, C. S. & Camerini-Otero, R. D. (1992), *Proc. Natl. Acad. Sci. USA* **89**, 6492-6496.

30. Muller, B., Burdett, I. & West, S. C. (1992), *The EMBO Journal* **11**, 2685-2693.

31. For a review on affinity cleaving see Dervan, P. B. (1991), *Meth. Enzym*. **208**, 497-515.

32. Sambrook, J., Fritsch, E. F. & Maniatis, T., *Molecular Cloning, 2nd ed.* (Cold Spring Harbor Laboratory Press, New York, (1989).

33. Han, H. & Dervan, P. B. (1994), *Nucleic Acids Res*.**22,** 2837-2844.

34. Hertzberg, R. P. & Dervan P. B. (1982), *J.Am.Chem.Soc.* **104**, 313-315.

35. Schultz P. G. , Taylor,J.S. & Dervan, P. B. (1982), *J.Am.Chem.Soc.* **104**, 6861-6863.

36. Dreyer, G. B. & Dervan, P. B. (1985), *Proc. Natl. Acad. Sci. USA* **82**, 968-972.

37. Moser, H. E. & Dervan, P. B. (1987), *Science* **238**, 645-650.

38. Oakley M. G. & Dervan P. B. (1990), *Science* **248**, 847-850.

39. Beal, P. A. & Dervan, P. B. (1991), *Science* **251**, 1360-1363.

40. Jain, S. K., Inman, R. B. & Cox, M. M. (1992), *J. Biol. Chem.* **267**, 4215-4222.

41. Kumar, K.A & Muniyappa, K. (1992), *J.Biol.Chem.* **267**, 24824-24832.

42. Zhurkin ,V. B., Raghunathan, G., Ulyanov, N. B., Camerini-Otero, R. D. & Jernigan, R. L. (1994), *J.Mol.Biol.* **239**, 181-200.

43. Van Meervelt, L., Vlieghe, D., Dautant, A., Gallois, B., Precigoux, G. & Kennard, O. (1995), *Nature* **374**, 742-744.

44. Iverson, B. L. & Dervan, P. B. (1987), *Nucleic Acids Res.* **15**, 7823-7830.

45. Grein, T., et al. (1994) *Bioorganic & Medicinal Chemistry Letters*,. **4**,971-976.

CHAPTER FIVE

Progress toward defining functional group determinants of alignment of homologous DNA sequences by RecA nucleoprotein filaments

Introduction

The RecA protein from *E.Coli* , in the presence of the slowly hydrolyzed cofactor ATP-γ-S, can bind single-stranded DNA to form stable nucleoprotein filaments which can then bind to homologous sites on double-stranded DNA(1), forming a three-stranded complex that exist in a dynamic state (2). Binding of these filaments to DNA can be observed by incorporating the modified thymidine derivative, T*, into the oligonucleotide part of the filament (3). While we have established the minor groove location of the incoming strand in the three-stranded complex, the sequence of events leading to the formation of the complex remain unclear. Two basic mechanisms can be envisioned–formation of a pre-exchange complex by recognition of the Watson-Crick base paired double helical target by formation of specific contacts between bases on the incoming strand and functional groups in the minor groove or alternatively, local melting of the duplex followed by sliding of a locally melted region along duplex DNA until a region of homology is located by stable base pairing (Figure 5.1).

The technique of "functional group mutations" has been used by several laboratories to study how specific functional groups on nucleic acids can contribute to their structure, function or recognition by macromolecular ligands (4-6). Here we describe attempts to use of this technique in combination with affinity cleavage to investigate the functional group determinants of alignment of homologous sequences by RecA nucleoprotein filaments.

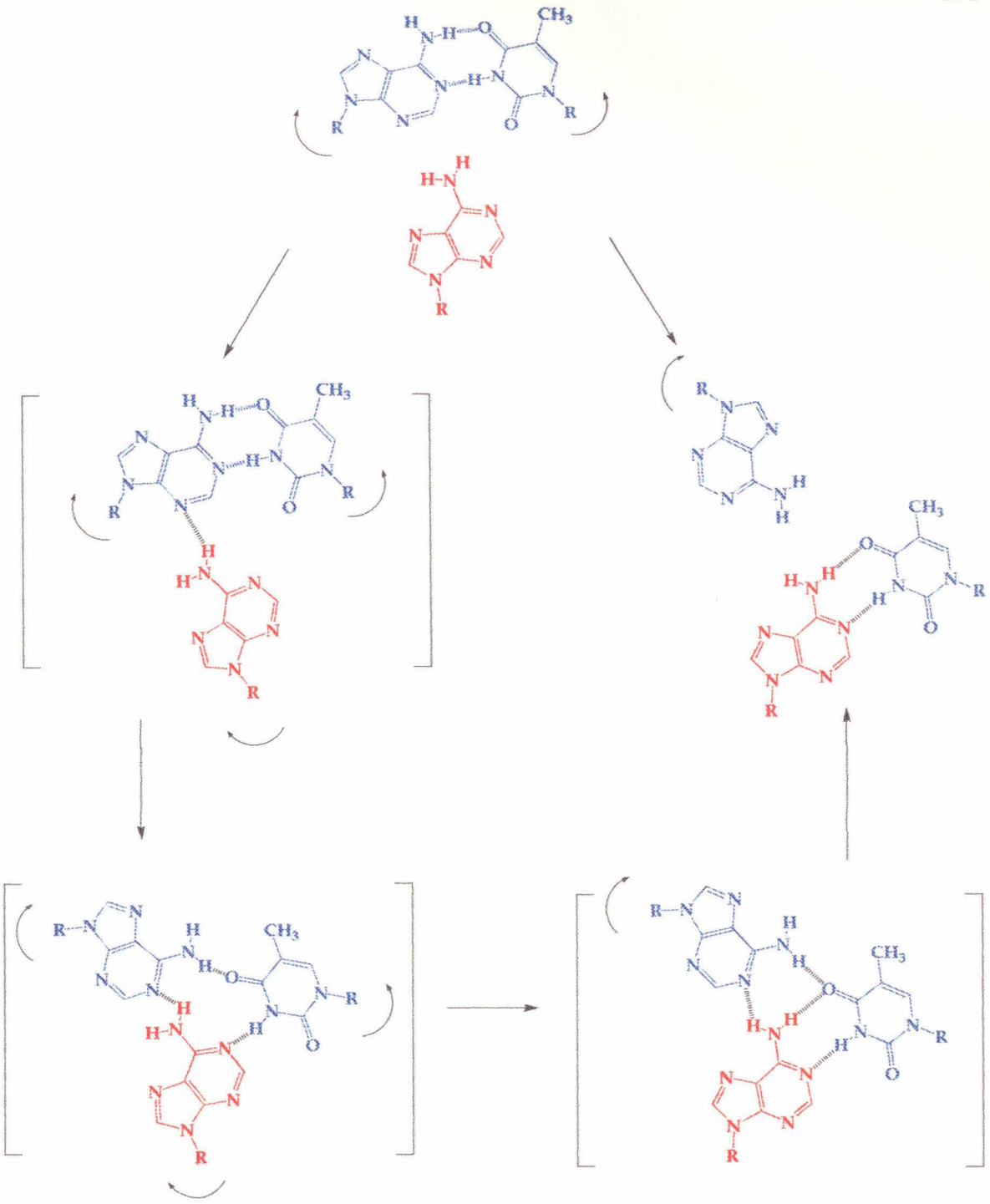

Figure 5.1 : Alternate modes for homologous alignment by RecA.
(a) Recognition in minor groove followed by formation of a post-exchange triplex that is processed to give products.
(b) Simple melting of duplex followed by strand switching by complementary strand.

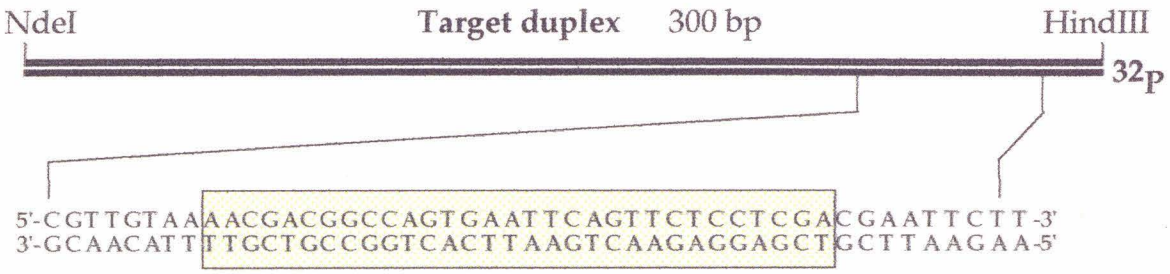

$\Phi =$ 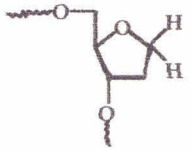

Oligo		Site
1	3′ - **T***TG CTG CCG GTC ACT TAA GTC AAG AGG AGC T - 5′	-
D6	3′ - **T***TG CTΦ CCG GTC ACT TAA GTC AAG AGG AGC T - 5′	6/G
D11	3′ - **T***TG CTG CCG GΦC ACT TAA GTC AAG AGG AGC T - 5′	11/T
D16	3′ - **T***TG CTG CCG GTC ACT ΦAA GTC AAG AGG AGC T - 5′	16/T
D17	3′ - **T***TG CTG CCG GTC ACT TΦA GTC AAG AGG AGC T - 5′	17/A
D19	3′ - **T***TG CTG CCG GTC ACT TAA ΦTC AAG AGG AGC T - 5′	19/G
D20	3′ - **T***TG CTG CCG GTC ACT TAA GΦC AAG AGG AGC T - 5′	20/T
D21	3′ - **T***TG CTG CCG GTC ACT TAA GTΦ AAG AGG AGC T - 5′	21/C
D26	3′ - **T***TG CTG CCG GTC ACT TAA GTC AAG ΦGG AGC T - 5′	26/A

Figure 5.2: Sequences of oligonucleotides used to study the effect of substituting an abasic residue for natural bases in the incoming strand.

Results and Discussion

Effect of abasic sugar residues in incoming strand

As a starting point for determining the contributions of various functional groups on the target duplex and on the bases on the third strand, we designed an experiment where each base was substituted in turn by an abasic sugar (Figure 5.2). Also, substitutions were made at more than one position for the same base determine any position effect along the length of the filament. The results from this study are shown in figure 5.3. Clearly, in the 31 mer oligonucleotide, the effect of substitution of each base depends on both the identity of the base and its position in the filament. A coarse estimate of the contribution of each putative base-triplet toward the stability of the three stranded complex is in the order C•(CG) > G•(GC)~A•(AT)>>T•(TA). It must be noted that in the absence of a sensitive assay to determine the differential binding of RecA to 31 mers differing only at one base position, one cannot rule out that the observed effects are simply a reflection of the stability of these nucleoprotein filaments.

Figure 5.3 : Storage phosphor autoradiogram of an 8% denaturing polyacrylamide gel containing the products of affinity cleavage reactions from oligonucleotides listed in figure 5.2. All lanes contain the cleavage products from DNA labeled on the 3'-end at the Hind III site of pUCJW . Lane 1 contains the products of adenine-specific reaction (10) on 3'-end labeled duplex.

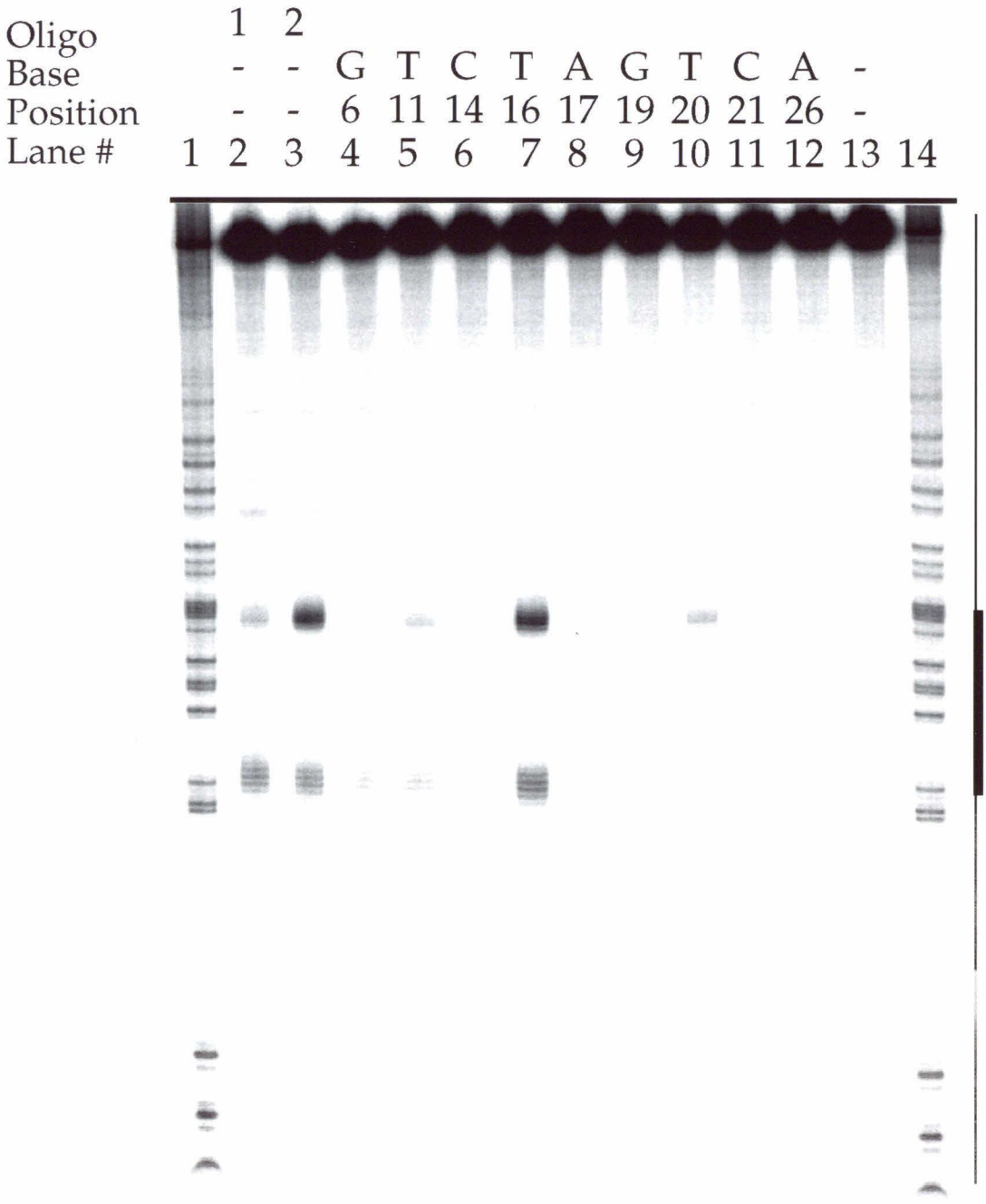
Oligo 1 2
Base - - G T C T A G T C A -
Position - - 6 11 14 16 17 19 20 21 26 -
Lane # 1 2 3 4 5 6 7 8 9 10 11 12 13 14

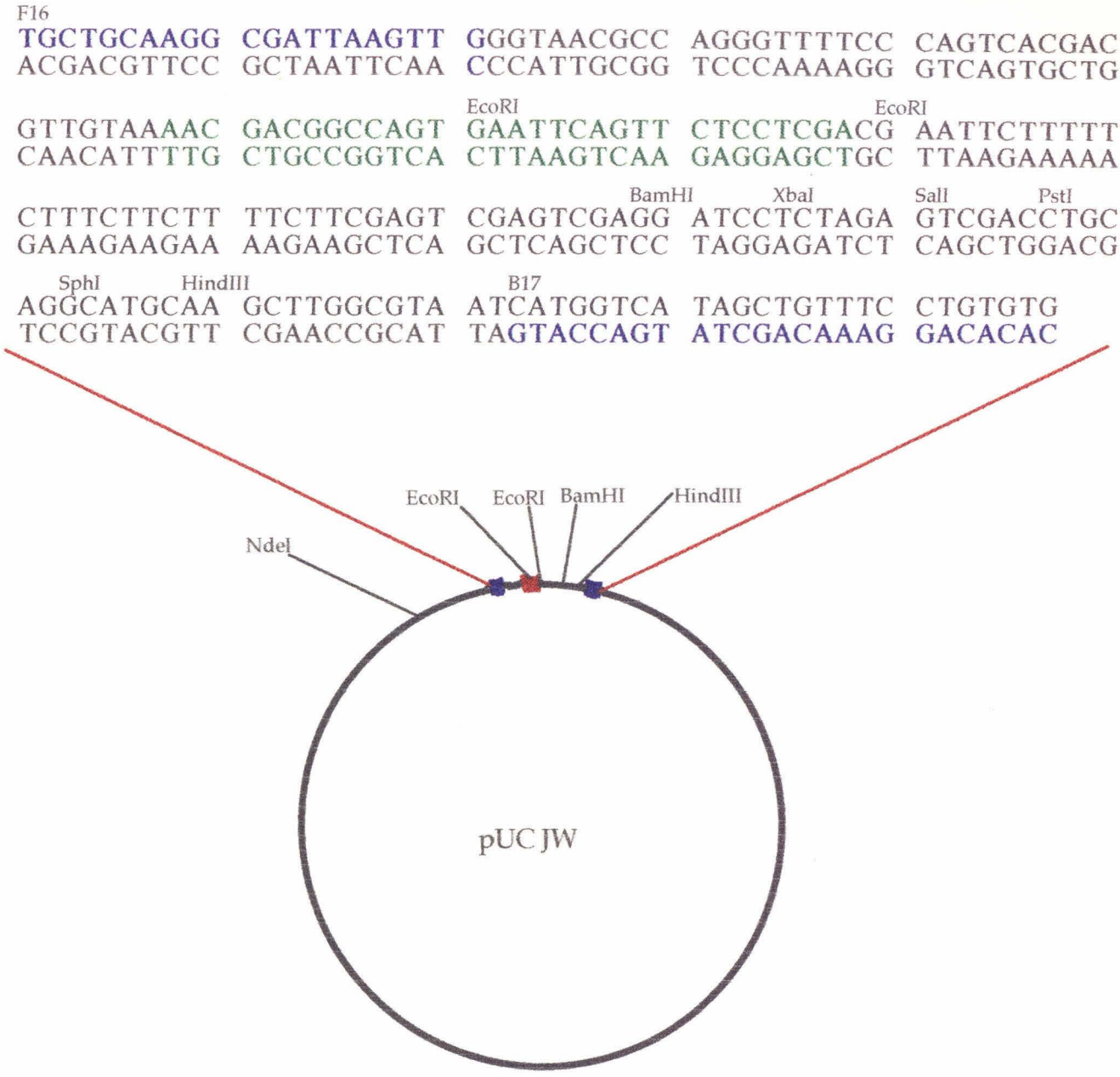

Figure 5.4: Schematic diagram of system used for generation of modified duplexes by PCR. The target site is shown in green and the primer sites are shown in blue.

Functional group substitutions in the duplex

To examine the contribution of functional groups in the duplex toward recognition by small molecules, Waring and coworkers have used the polymerase chain reaction to incorporate analogs of adenine and guanosine bases into duplex DNA (6). Since AT and TA base pairs are essentially degenerate in the manner in which functional groups are presented in the minor groove, one conceivable mode of recognition of the minor groove by RecA nucleoprotein filaments is through "digital recognition" of a pattern of protons on the GC or CG base pairs (7). To investigate this possibility, using the polymerase chain reaction, we generated duplexes that contained inosine instead of guanine bases (Figure 5.4). If recognition of the 2-amino group were critical to homologous alignment, one would expect to see a diminution or even total disappearance of cleavage patterns on inosine duplexes. Also, duplexes with 7-deazaguanosine or 7-deazaadenosine were generated to investigate the effect of these substitutions in the major groove on the efficiency of three-stranded joint molecule formation. Note that these serve as controls for correlating our data with what has been observed in the literature (8).

Functional group substitutions in the incoming strand

An alternate mode of specific recognition in the minor groove could involve recognition of hydrogen bond acceptors in minor groove by the exocyclic amino groups on the bases of the incoming strand. To test this possibility we designed a series of oligonucleotides (Figure 5.5, 5.6) where adenine bases were

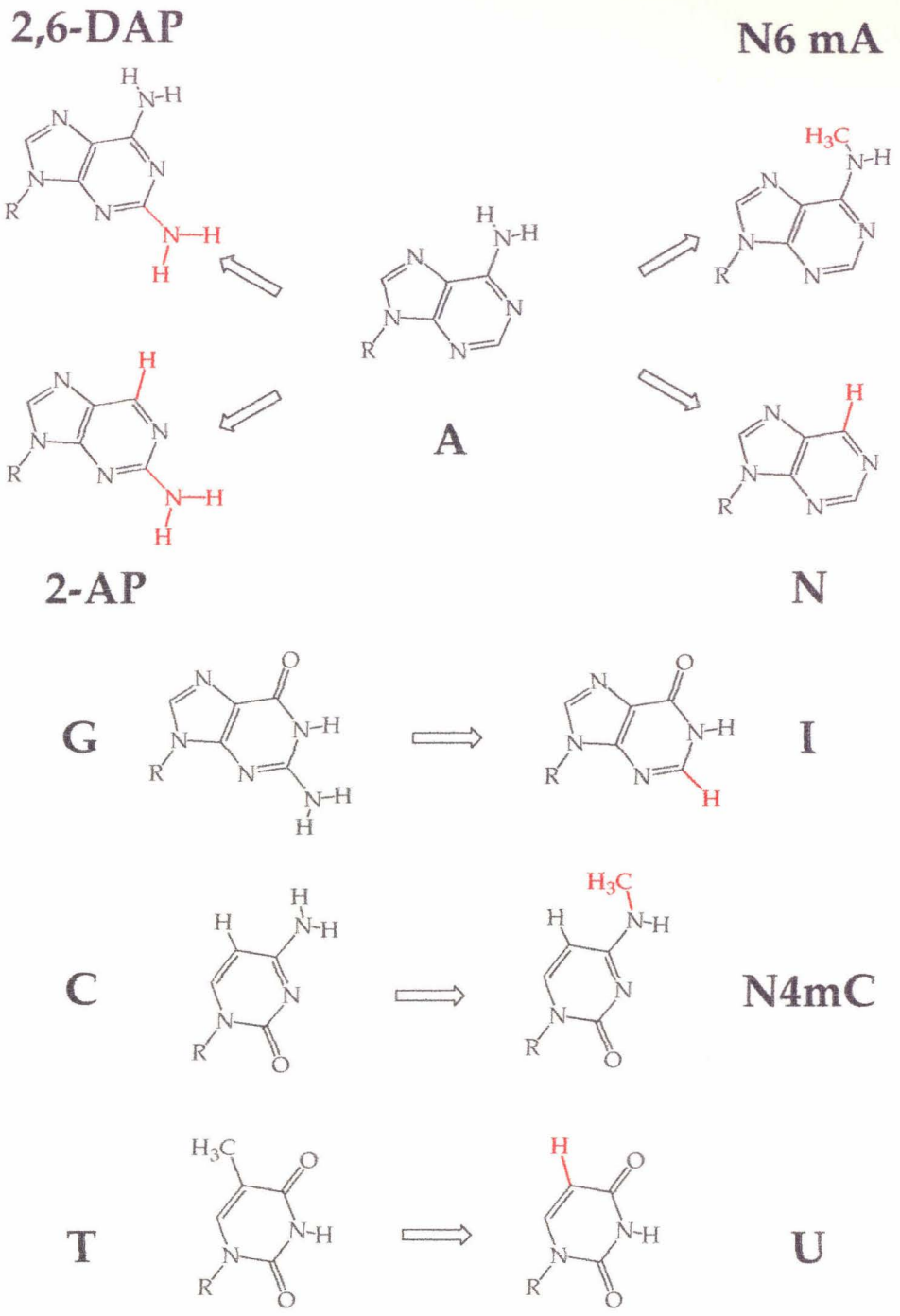

Figure 5.5: Functional group substitutions in the third strand used in this study.

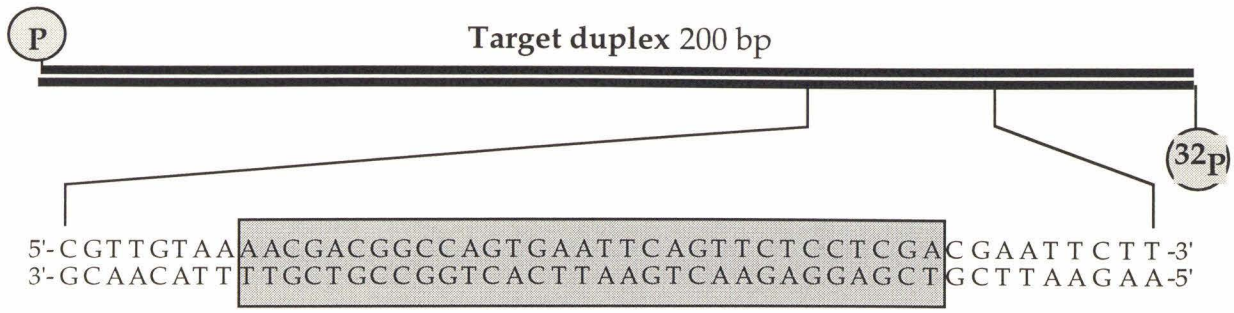

1	3′ - **T*** TG CTG CCG GTC ACT TAA GTC AAG AGG AGC T - 5′
2	3′ - **T*** TG CTG CCG GTC ACT T**P**A GTC AAG AGG AGC T - 5′
3	3′ - **T*** TG CTG CCG GTC **P**CT T**PP** GTC **PP**G **P**GG **P**GC T - 5′
4	3′ - **T*** TG CTG CCG GTC ACT T**D**A GTC AAG AGG AGC T - 5′
5	3′ - **T*** TG CTG CCG GTC **D**CT T**DD** GTC **DD**G **D**GG **D**GC T - 5′
6	3′ - **T*** TG CTG CCG GTC ACT TAA **I**TC AAG AGG AGC T - 5′
7	3′ - **T*T**I CT**I** CC**I** **I**TC ACT TAA **I**TC AA**I** A**II** A**I**C T - 5′
8	3′ - **T*** TG CTG CCG GTC ACT TA**M** GTC AAG AGG AGC T - 5'
9	3′ - **T*** TG CTG CCG GTC **M**CT T**MM** GTC **MM**G **M**GG **M**GC T - 5′
10	3′ - **T*** TG CTG CCG GTC ACT TAA GT**C** AAG AGG AGC T - 5′
11	3′ - **T*** TG **C**TG **CC**G GT**C** A**C**T TAA GT**C** AAG AGG AGC T - 5′
12	3′ - **T*** TG CTG CCG GTC ACT TA**N** GTC AAG AGG AGC T - 5′
13	3′ - **T*** TG CTG CCG GTC **N**CT T**NN** GTC **NN**G **N**GG **N**GC T - 5′
14	3′ - **T*** TG CTG CCG GTC ACT **U**AA GTC AAG AGG AGC T - 5′
15	3′ - **T*U**G C**U**G CCG G**U**C AC**U** **U**AA G**U**C **UU**G **U**GG **U**GC **U** - 5′

Figure 5.6: Sequences of oligonucleotides used to study the effect of substituting bases in the third strand. **P**: 2-Aminopurine, **D**: 2,6-Diaminopurine **I**: Inosine, **M**: N6 Methyl adenosine, **C**: N4 methyl Cytosine **N**: Nebularine, **U:** Uridine.

substituted with 2- amino purine, nebularine, N6-methyl adenine or 2,6 diaminopurine bases. The exocyclic amine of guanosine bases was eliminated by substitution of guanosine with inosine. The 4-amino group of cyosine bases was modified by addition of a methyl group. For comparison each modified oligonucleotide was annealed with the common complementary strand and the melting profile of the heteroduplexes was recorded. While 2-amino purine, 2,6-diaminopurine, N4 methyl cytosine and N methyl adenosine containing oligonucleotides showed melting temperatures that were within 2°C of the parent duplex, nebularine and inosine expectedly caused large decreases in the observed melting temperature (Figure 5.7).

Figure 5.7: Thermal melting profiles of each of the modified oligonucleotides used in this study. Tm's were recorded under the exact buffer conditions of affinity cleavage experiments in the absence of a reducing agent. The values reported are the temperature at which the UV hyperchromicity is half maximal.

2,6-Diaminopurine

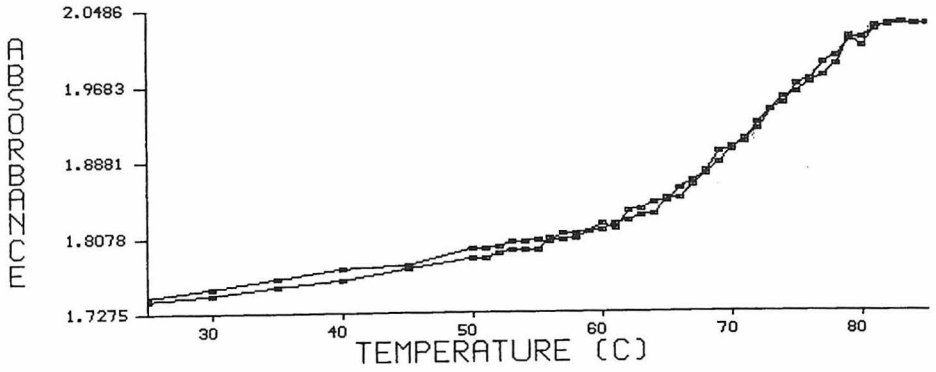

Tm = 68.3 °C

Inosine

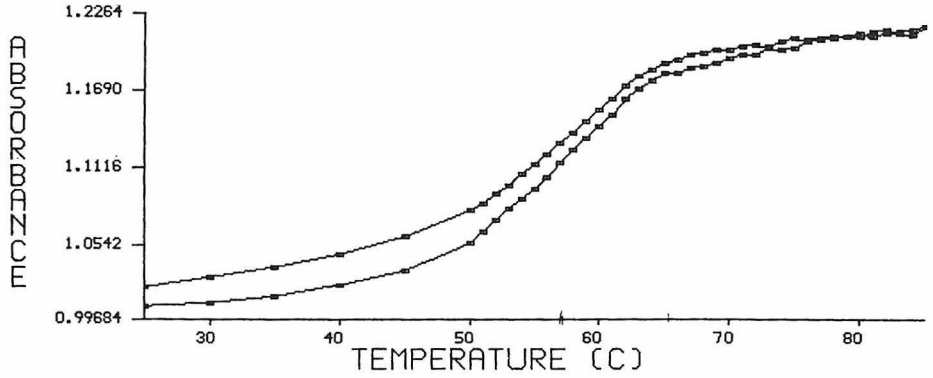

Tm = 57.5 °C

6- Methyl adenine

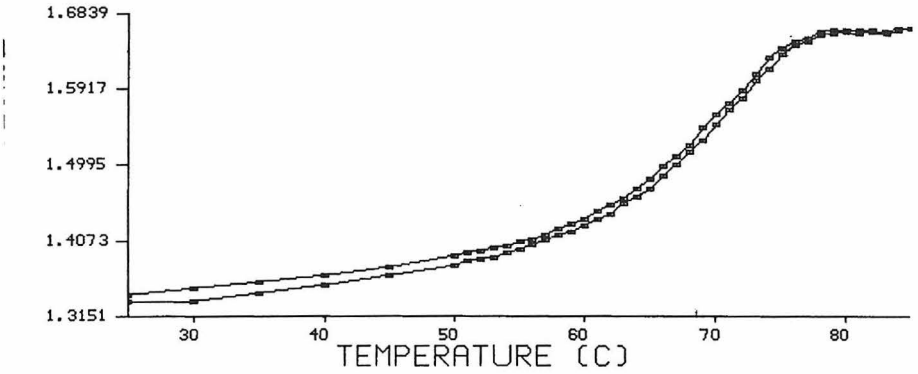

Tm = 67.5 °C

Underivatized

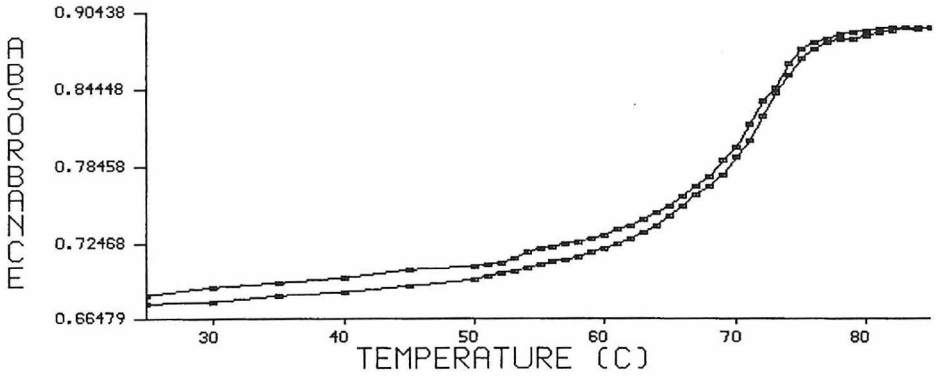

Tm = 76°C

2-Aminopurine

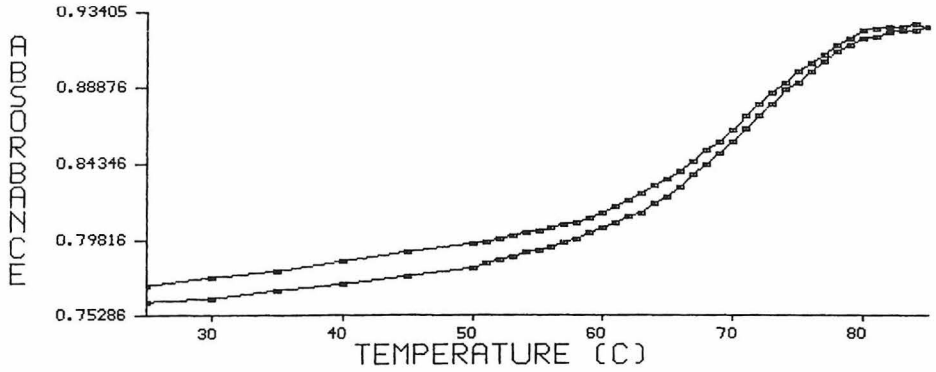

Tm = 68.5°C

Normal duplex

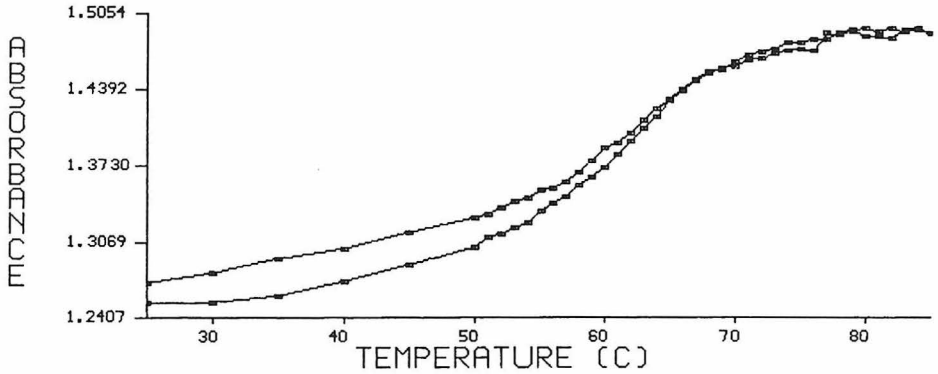

Tm = 69.5 °C

Figure 5.8 : Storage phosphor autoradiogram of an 8% denaturing polyacrylamide gel containing the products of affinity cleavage reactions from oligonucleotides listed in figure 5.6. All lanes contain the cleavage products from PCR generated fragment containing guanosine bases (Normal duplex) labeled on one end using polynucleotide kinase. Lane 1 contains the products of adenine-specific reaction (10) .

Normal duplex

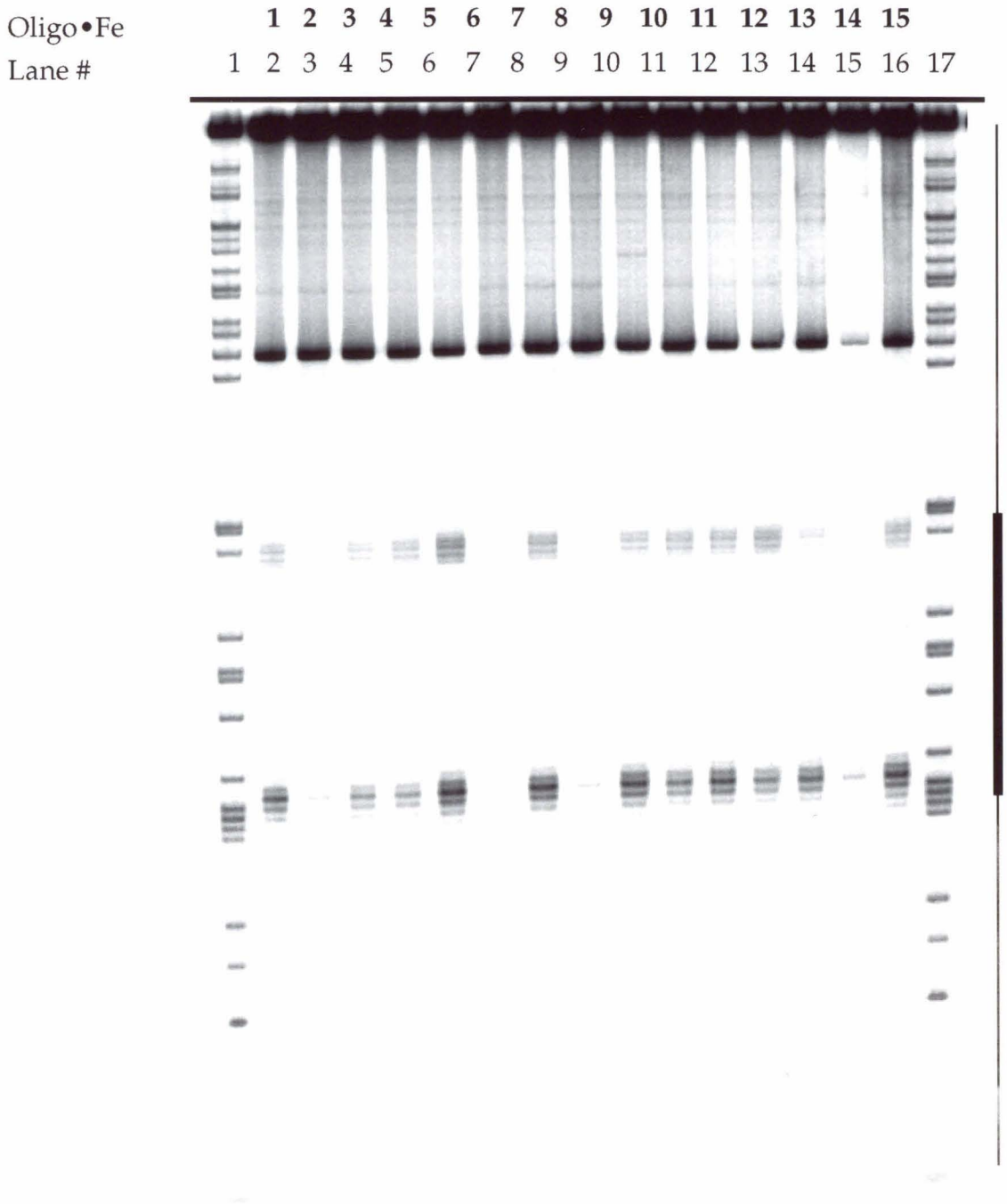

Figure 5.9 : Storage phosphor autoradiogram of an 8% denaturing polyacrylamide gel containing the products of affinity cleavage reactions from oligonucleotides listed in figure 5.6. All lanes contain the cleavage products from PCR generated fragment containing inosine instead of guanosine bases (Inosine duplex) labeled on one end using polynucleotide kinase. Lane 1 contains the products of adenine-specific reaction (10) .

Inosine duplex

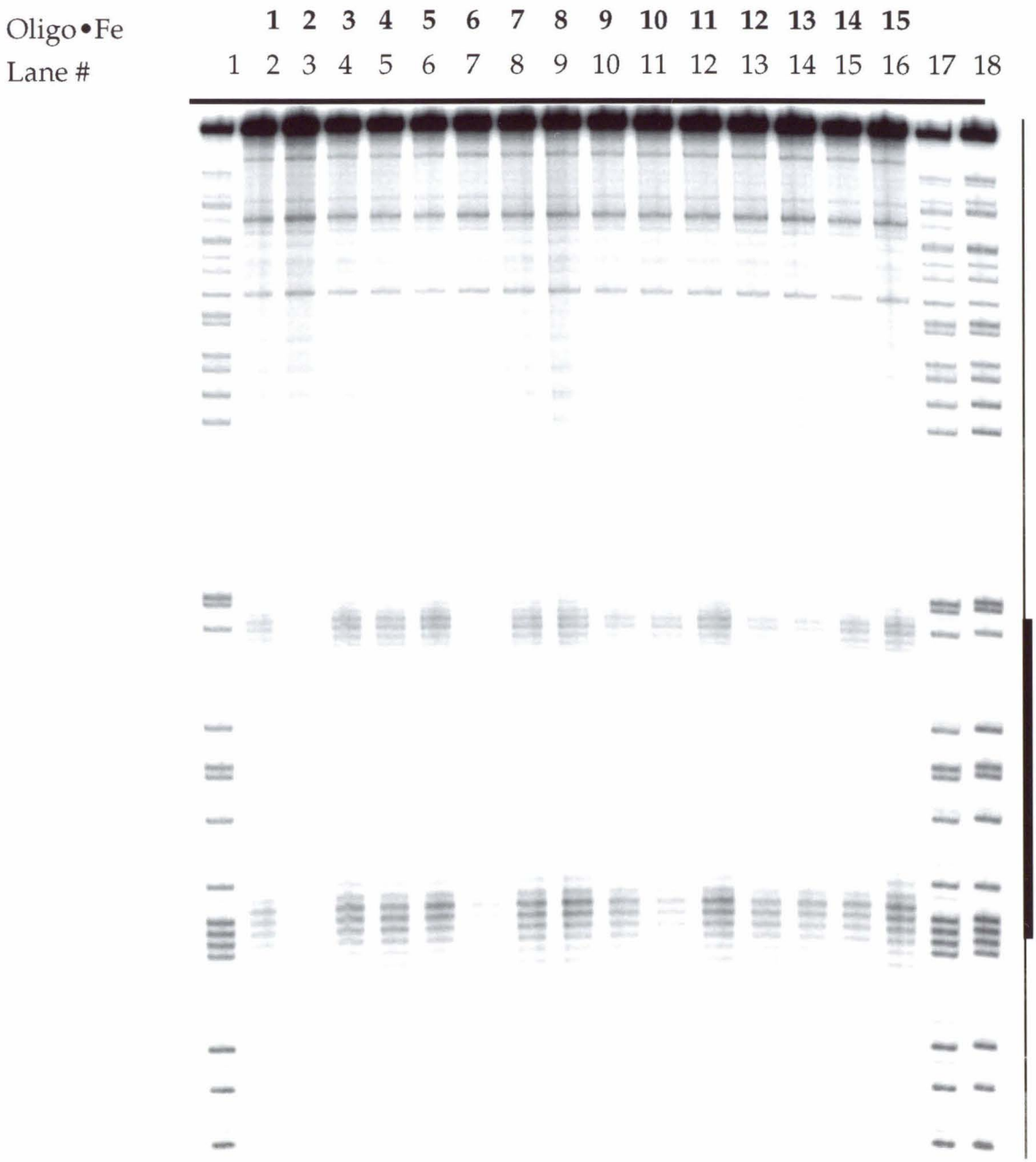

Figure 5.10 : Storage phosphor autoradiogram of an 8% denaturing polyacrylamide gel containing the products of affinity cleavage reactions from oligonucleotides listed in figure 5.6. All lanes contain the cleavage products from PCR generated fragment containing 7-deaza adenosine instead of adenosine bases (7-deaza A duplex) labeled on one end using polynucleotide kinase. Lane 1 contains the products of guanine-specific reaction.

7-deaza Adenosine duplex

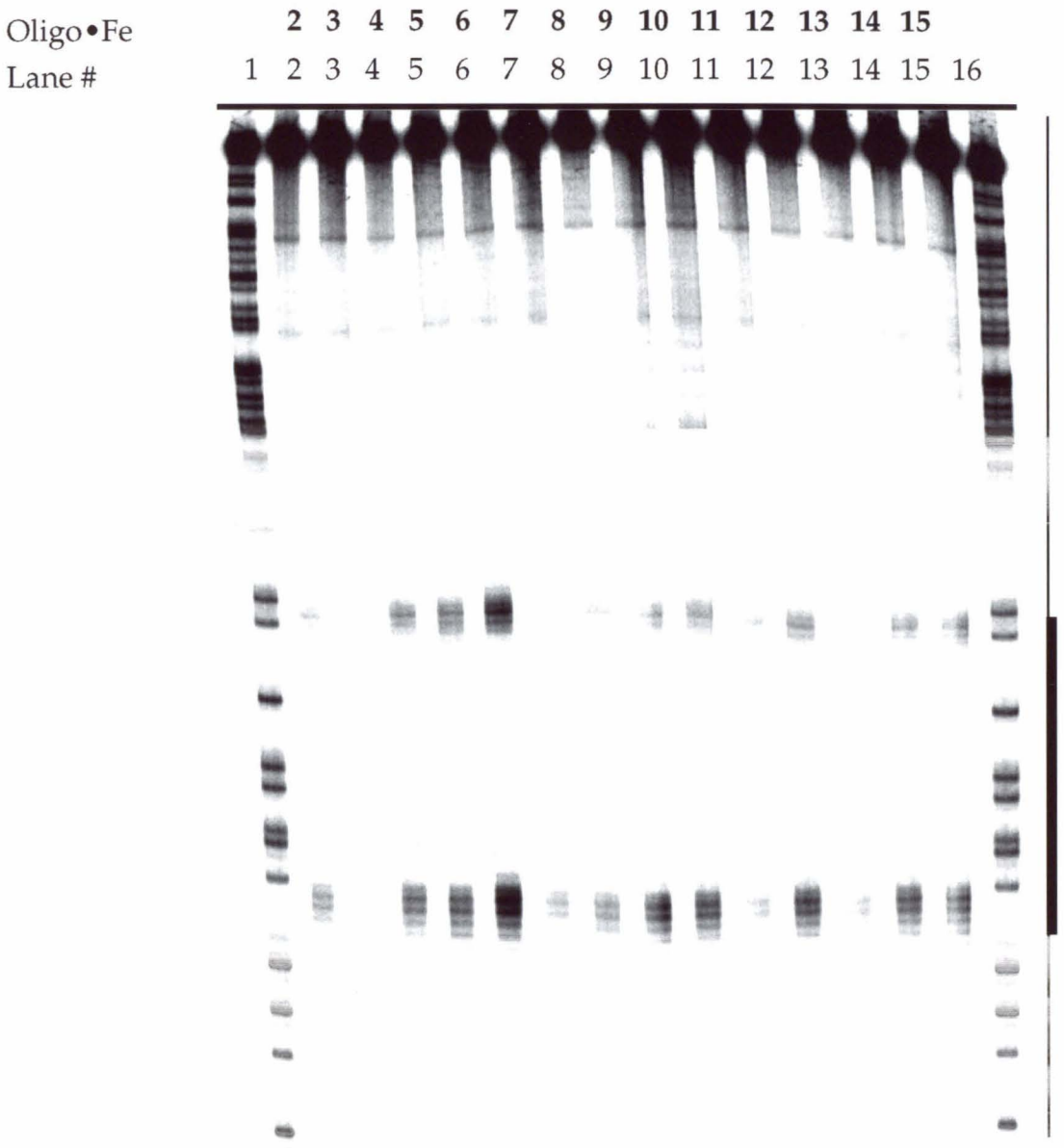

Next, each of the oligonucleotides in the set described above was incubated under the standard reaction conditions with either a duplex containing natural bases or one containing inosine or 7-deaza adenosine bases to determine if any consistent change in cleavage patterns is observed. The results from these two experiments are shown in figures 5.8, 5.9 and 5.10 and summarized in figure 5.11.

Several key observations in this set of experiments are worthy of comment. It is clear that the cleavage pattern generated from inosine duplex is similar in both placement and intensity to that obtained from guanosine containing duplexes. Therefore, the 2-amino group of guanosine bases is dispensable for homologous alignment.

Also, modification of the exocyclic amines of guanosines, cytosines or adenines results in decreased three-stranded complex formation. The fact that oligonucleotides containing multiple 2,6-diaminopurine substituents, which carry a 2-amino group on the purine ring like guanosine, can recognize their targets with equal or greater affinity than oligonucleotides containing adenosine indicates that the 2-amino group of 2,6-diaminopurine is likely not used in intial recognition but stabilizes the putative A•AT triplet or the product triplex or heteroduplex by an additional hydrogen bond. Oligonucleotides containing 6-methyl adenine bases show efficient recognition of inosine duplexes but not the normal duplex. Efficient recognition of the 7-deaza adenosine duplex by 2,6-diaminopurine containing oligonucleotides is further evidence against major groove binding of the third strand (Figure 5.11 B). The expected thermal stability of heteroduplexes formed by recognition of the AT base pair by 2,6 diaminopurine, 2-aminopurine or N6 methyl adenine are quite similar. Stability

of the putative triplets however, will be differentially affected by each of these base substitutions and could be the reason behind the effects observed.

CONCLUSIONS

The base substitution analysis described here, although preliminary, illuminates some aspects of the mechanism of alignment of homologous sequences. First, the contributions of each base triplet to the three stranded structure depends on the nature of the base as well as its position within the filament. Second, the hydrogen bond donors in the floor of the minor groove–the 2-amino groups of guanine bases, and the hydrogen bond acceptors in the major groove–the N-7 atoms of purine bases, are both dispensable for the process of homologous alignment. And lastly, the exocyclic amine groups on the bases in the incoming strand appear to play an important part in the recognition process. Whether this is simply a reflection of the lower stability of the modified heteroduplex products of the strand exchange reaction, destabilization due to disruption of some initial recognition event or destabilization of base *triplets* therefore remains an open question.

Figure 5.11. **A.** A schematic diagram summarizing the observations from functional group mutation analysis of the RecA mediated three-strand reaction.

B. A comparison of experimental outcomes with those expected from major or minor groove binding of modified third strands.

A.

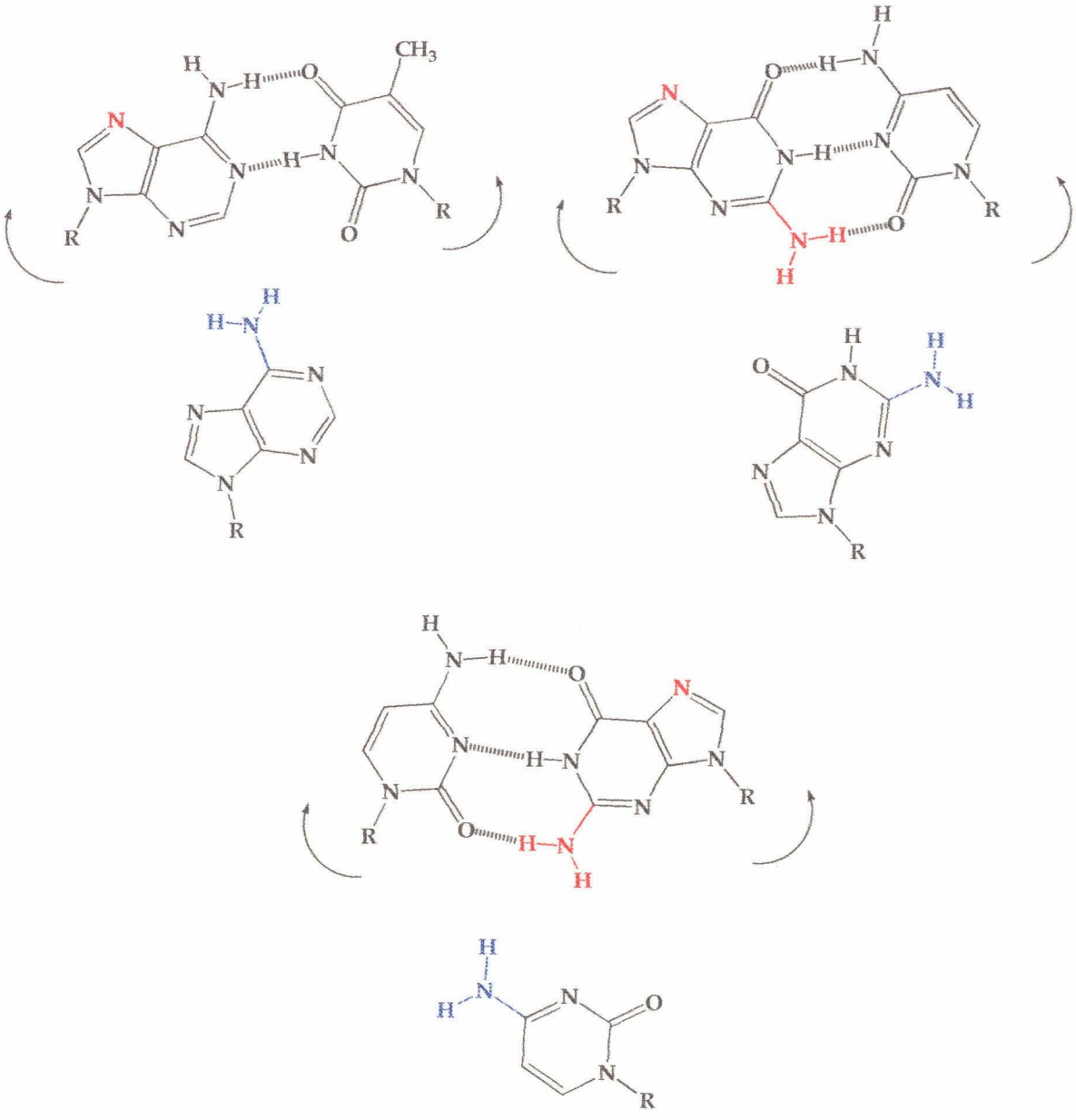

B. **Major** **Minor** **Experiment**

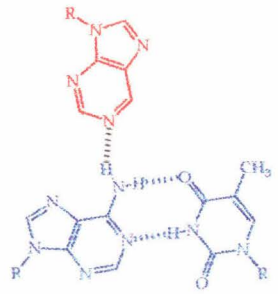

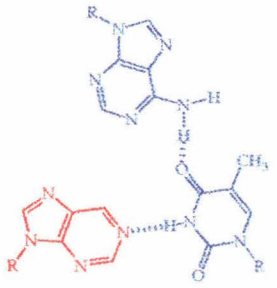

+/-

N•AT

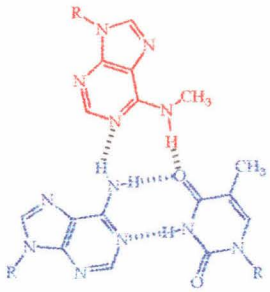

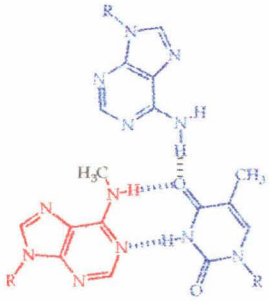

-

mA•AT

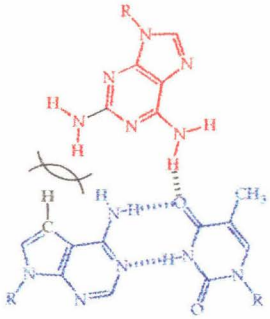

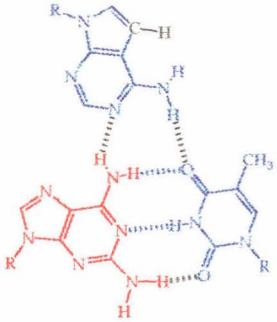

+

2,6 DAP•c7AT

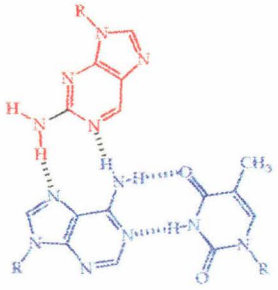

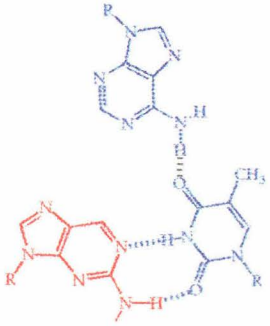

-

2AP•AT

EXPERIMENTAL

General

RecA protein was isolated from the strain JC12772 using published procedures as modified by Kowalcykowski. Sonicated, deproteinized calf thymus DNA (Pharmacia) was dissolved in H_2O to a final concentration of 2.0 mM in base pairs and was stored at 4 °C. Glycogen was obtained from Boehringer-Mannheim as a 20 mg/ml aqueous solution. γ-S-ATP was purchased from Sigma and was stored at -20 °C. Nucleoside triphosphates labeled with ^{32}P were obtained from Amersham or ICN and were used as supplied. Cerenkov radioactivity was measured with a Beckman LS 2801 scintillation counter. Restriction endonucleases were purchased from Boehringer Mannheim or New England Biolabs and were used according to the supplier's recommended protocol in the activity buffer provided. Klenow fragment, calf intestinal alkaline phosphatase and snake venom phosphodiesterase were obtained from Boehringer Mannheim. Phosphoramidites were purchased from Glenn Research.

Synthesis and Purification of Oligodeoxyribonucleotides

All oligodeoxyribonucleotides were synthesized and purified as described before. Special deprotection schemes were used where needed (2-amino purine/2,6-diaminopurine containing oligonucleotides require stronger deprotection in the presence of methylamine in ammonia).

The concentrations of single-stranded oligonucleotides were determined by UV absorbance at 260 nm using extinction coefficients calculated by addition of the monomer nucleoside values (values for T were used in place of T* in the calculation). Oligonucleotide solutions were lyophilized to dryness for storage at -20 °C. Each oligonucleotide was further characterized by digestion with calf intestinal alkaline phosphatase and snake venom phosphodiesterase followed by

analysis of the digested oligos using reversed phase HPLC to confirm complete post-synthetic modification of the primary amine appended to C-5 of the terminal thymidine residues (11). Coinjection with authentic standards and comparison of the UV spectra of relevant peaks was used to confirm the presence of desired analogs. As additional chracterization, each oligonucleotide was radiolabeled and checked for purity on a 15% denaturing polyacrylamide gel.

DNA Manipulations

The 300 bp HindIII/NdeI restriction fragment of the plasmid pUCJWII47 was isolated and labeled at the 3'-end at the HindIII site by standard procedures . Adenine-specific sequencing reactions were carried out as previously described (10) .

Generation of modified duplexes using PCR

Primers to amplify the desired target region were selected using the MacVector program. The sequence of the two primers used were as indicated in figure 5.4. Primer **1** was chemically phosphorylated at its 5'-end to prevent labeling with polynucleotide kinase. To ensure complete phosphorylation, aliquots of phosphorylated primer were further treated with polynucleotide kinase and ATP. The conditions used for PCR amplification for generation of normal or 7-deaza purine duplexes were only slightly modified from published procedures (7). The cycling parameters for generation of inosine duplexes were 30 cycles of 94°C for 1 min., 50°C for 2 min. and 37°C for 10 min., followed by a final cycle of 72°C for 10 min., 55°C for 5 min. and 37°C for 5 min. for complete extension. Generation of inosine containing duplexes was found to be about 10 fold less efficient than the other three duplexes and adequate amounts were generated by pooling several reactions. Duplex containing 7-deaza adenosine shows diminished detectability with ethidium bromide staining, but the

amplification reaction was found to be of efficiency comparable to reactions containing natural dNTP's. Because the duplexes generated are short (> 200 bp) and contain modified bases which are known to destabilize duplex DNA, duplex character of the substrates was verified by elecrophoresis on a 10% non-denaturing gel before setting up affinity cleavage reactions.

Affinity Cleavage Reactions

The protocol used for affinity cleavage was essentially the same asthat described in Chapter 4. A nucleotide to monomer ratio of 3:1 with filament concentration at 3μM was chosen asthe standard set of conditions. Affinity cleavage reactions were in general seen to give higher backgrounds with 7-deaza purine substituted duplexes.

REFERENCES

1. Flory, J., Tsang, S.S. and Muniyappa, K. (1984) *Proc. Natl. Acad. Sci. USA* **81**, 7026-7030.

2. Reddy, G., Jwang, B., Rao, B.J. and Radding, C.M. (1994) *Biochemistry* **33**, 11486-11492.

3. Baliga, R. , Singleton, J.W. and Dervan, P.B. (1995) *Proc. Natl. Acad. Sci. USA* **92**, 10393-10397.

4. Strobel, S.A., *et al.*, (1994) *Biochemistry*, **33**, 13824-13835; Strobel, S.A. and Cech, T.R. (1995) *Science*, **267**, 675-679.

5. Newman, P.C., *et al.*, (1990) Biochemistry, **29**, 9891-9901.

6. Bailly, C., Marchand, C., Waring, M.J., (1993) *J. Am. Chem. Soc.* , **115**, 3784-3785; Bailly, C., Waring, M.J., Travers, A.A. (1995) *J. Mol.Biol.* **253**, 1-7.

7. Bailly, C., Waring, M.J. (1995) *J. Am. Chem.Soc.*, **117**, 7311-7316; Bailly, C., *et al.*, (1995) *EMBO J.*, **14**, 2121-2131.

8. Jain, S., Cox, M. M. & Inman, R. B. (1995) *J. Biol. Chem* **270**, 4943-4949; Kim, M. G., Zhurkin, V. B., Jernigan, R. L. & R. D. Camerini-Otero (1995), *J.Mol.Biol.* **247**, 874-889.

9. Waring, M.J., Bailly, C.B. , (1994) *Gene*, **149**, 69-79.

10. Iverson, B. L. & Dervan, P. B. (1987) *Nucleic Acids Res.* **15**, 7823-7830.

11. Han, H. & Dervan, P. B. (1994) *Nucleic Acids Res*.**22**, 2837-2844.